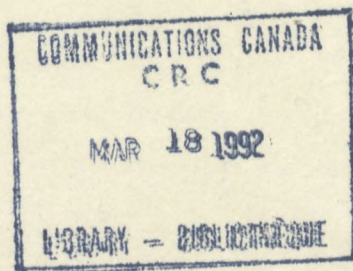


Communications Research Centre

MODAL CONVERSION BY GRATINGS IN OPTICAL FIBRES: THE THEORY AND ITS APPLICATION TO ALL-OPTICAL SWITCHING (U)

by

Dr. Iain M. Skinner
(Optical Communications and Electrophotonics Technologies)



CRC REPORT 91-002

October 1991
Ottawa

This document was prepared for and is the property of the Department of National
Defence, Research and Development Branch under Project No. 041LP.

of Canada
Communications

Gouvernement du Canada
Ministère des Communications

IC

TK
5102.5
C673e
#91-002

Canada

COMMUNICATIONS RESEARCH CENTRE

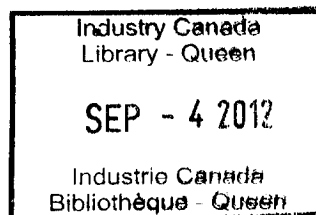
DEPARTMENT OF COMMUNICATIONS
CANADA

**MODAL CONVERSION BY GRATINGS IN OPTICAL FIBRES:
THE THEORY AND ITS APPLICATION TO ALL-OPTICAL SWITCHING (U)**

by

Dr. Iain M. Skinner

(Optical Communications and Electrophotonics Technologies)



CRC REPORT 91-002

**October 1991
Ottawa**

**This document was prepared for and is the property of the Department of National
Defence, Research and Development Branch under Project No. 041LP.**

Faint header text, possibly containing a title or reference number.

Faint text block, possibly a date or a short paragraph.

Faint text block, possibly a name or a specific identifier.

Faint text block, possibly a description or a note.

1007 100700
EYB22

000 00 10000 00000

Faint text block, possibly a footer or a disclaimer.

TK
5102.5
CG73e
#91-002
c.b

DD 11850734
DL 11939822

ABSTRACT

Using the formalism of coupled-mode theory, an improved description — allowing for a lack of axisymmetry in the waveguide — of the resonant transfer of power between modes propagating in a few-mode optical fibre is derived, and applied to both an axisymmetric $LP_{01} \leftrightarrow LP_{02}$ modal conversion grating and a non-axisymmetric $LP_{01} \leftrightarrow LP_{11}$ grating. The theory of the vector form of modes in a periodic, slightly non-axisymmetric structure is obtained, and applied to the $LP_{01} \leftrightarrow LP_{11}$ grating. For the $LP_{01} \leftrightarrow LP_{02}$ grating, the spectral region of appreciable resonant coupling, as measured by a linewidth, was found to be very narrow. The feasibility of exploiting this extreme sensitivity by using the grating as an all-optical switch was demonstrated.

RESUMÉ

On dérive une description améliorée du transfert résonant de puissance entre les modes d'une fibre optique où quelques modes peuvent se propager. Cette amélioration consiste à tenir compte d'une absence de symétrie axiale du guide et est appliquée aux cas d'un réseau de conversion modale $LP_{01} \leftrightarrow LP_{02}$ (symétrique) et $LP_{01} \leftrightarrow LP_{11}$ (non-symétrique). On obtient la théorie des modes vectoriels d'un milieu périodique à symétrie axiale légèrement perturbée, avec laquelle on traite le cas du réseau $LP_{01} \leftrightarrow LP_{11}$. Pour le réseau $LP_{01} \leftrightarrow LP_{02}$, on trouve que la largeur spectrale de la résonance de couplage est très étroite. On démontre ainsi la faisabilité d'utiliser cette sensibilité du réseau pour la fabrication d'un commutateur tout-optique.

EXECUTIVE SUMMARY

The purpose of this work was to better understand the properties of a grating — i.e. a periodic, small variation in refractive index — written in an few-mode, optical fibre, and, having understood them, to better exploit the gratings in the design of all-optical devices for signal and information processing. (Gratings within fibres are fabricated at the Communications Research Centre.)

The important feature of the grating is that it causes a periodic, predictable exchange of power to occur between different modes which propagate in the fibre. As the properties of the modes are slightly different, it is possible to examine the power in each mode separately. Initially, a mathematical description of the power exchanged was obtained. This was in terms of scaled quantities, and, specifically, the operational wavelength was converted to the familiar V -number. The description improved on previous ones by allowing for the possibility that the grating was not rotationally symmetric about the axis of the fibre, which is the direction of the modal propagation.

The utility of the gratings comes about because the fraction of power exchanged is minimal, except in narrow spectral bands around specific resonant wavelengths. The separation of these wavelengths and the width of the associated resonances in the spectrum are important characteristics of the gratings. Analysis showed the theoretical resonances to be very narrow — of the order of 0.1 nm. Comparing the spectral responses obtained from computer solution of the mathematical model of coupling and experimental observations showed the description to be a good approximation of the gratings. The theory predicted that, in forming the grating, the slight changes made to the refractive index are very weakly anisotropic. The relative difference between the variations to the two transverse indices (i.e those sensed by X- or Y-polarized light) is of the order of 0.1%.

Of interest here, is the use of the grating as an all-optical switch, with its implication for optical computing. High power in the fibre causes a slight change to its refractive index; this changes the grating's resonant wavelength, moving it sufficiently to distinguish it from

the original narrow resonant peak. Thus, the power exchange is switched off for the original resonant wavelength. The study determined that it was possible to use the $LP_{01} \leftrightarrow LP_{02}$ grating as a switch, but that this depended critically on the operating conditions. Specifically, with it illuminated by the resonant wavelength in the fundamental (LP_{01}) mode, the value of V must satisfy $4.23 < V < 5.62$. If the light is slightly away from the resonant wavelength, the condition is slightly different. As an optical switch, the grating shows a wide variety of the switching patterns, depending upon whether the illumination is or is not at the resonant wavelength. The conditions for optimal efficiency were found. For example, at resonance, optimal efficiency corresponds to $V = 4.69$. The power needed to observe the significant switching effects was found to be around 1 KW.

TABLE OF CONTENTS

Abstract/Resumé.....	iii
Executive Summary.....	v
Table of Contents.....	vii
List of Figures and Tables.....	ix
1.0 INTRODUCTION.....	1
2.0 THEORY OF MODAL COUPLING BY GRATING IN OPTICAL FIBRE.....	3
2.1 Coupled Mode Equations.....	4
2.2 Approximations.....	5
2.3 Periodic Grating and Resonance.....	7
2.4 Reflections.....	9
2.5 Axisymmetric Grating.....	9
2.6 Anisotropy.....	11
3.0 EXAMPLE: NORMAL INTERFACE, UNIFORM PERTURBATION.....	12
3.1 Geometry.....	12
3.2 Grating for $LP_{01} \leftrightarrow LP_{02}$ Modal Conversion.....	14
3.3 Spectral Response — Step-Fibre.....	18
3.4 Resonant Spectral Linewidth.....	19
3.5 Anisotropy.....	22
3.6 Bragg Grating.....	24
4.0 EXAMPLE: $LP_{01} \leftrightarrow LP_{11}$ GRATING IN STEP-FIBRE.....	29
4.1 Construction and Geometry.....	29
4.2 Preliminary Scalar Observations.....	31
4.3 Modes of Circular Fibre.....	31
4.4 Perturbation and Local Modes.....	34
4.5 Coupling Matrices.....	37
4.6 Fourier Coefficients.....	40

4.7	Coupling Equations and Solution	44
4.8	Results	44
5.0	NONLINEAR SWITCHING IN $LP_{01} \leftrightarrow LP_{02}$ GRATINGS	50
5.1	Structure	51
5.2	Modes	52
5.3	Nonlinear Polarization	53
5.4	From Maxwell Equation to Coupling Equation	54
5.5	Near Resonance	55
5.6	Constant Amplitude Solution	57
5.7	General Solution	58
5.8	Qualitative Results of Linearly Tuned Grating	60
5.9	Parameters of Fibre	62
5.10	Nonlinear Switching of Linearly Tuned Grating	65
5.11	Detuning Parameter	65
5.12	Nonlinear Switching of Detuned Grating	70
6.0	CONCLUSION	71
7.0	ACKNOWLEDGEMENTS AND REFERENCES	73
APPENDICES		76
	Appendix A: Two Coupled Linear Differential Equations	76
	Appendix B: Modes in Periodically, Axi-Asymmetrically Perturbed Fibres	78
	Appendix C: Three Coupled Linear Differential Equations	102
	Appendix D: Zeroes of Polynomial	105
	Appendix E: Solution of Power Equation	118

LIST OF FIGURES AND TABLES

Figure 1: Structure of the $LP_{01} \leftrightarrow LP_{02}$ modal conversion grating	13
Figure 2: Frequency variation of the coupling coefficient	16
Figure 3: Frequency variation of scaled scalar period	17
Figure 4: Frequency variation of properties of an $LP_{01} \leftrightarrow LP_{02}$ grating	19
Figure 5: Frequency variation of output in LP_{01} mode	20
Figure 6: Frequency variation of linewidth parameter	23
Figure 7: Frequency variation of output: input X- or Y-polarized	25
Figure 8: Frequency variation of output: input 50-50 polarized	26
Figure 9: Structure of the $LP_{01} \leftrightarrow LP_{11}$ modal conversion grating	30
Figure 10: Frequency variation of scaled scalar period	32
Figure 11: Frequency variation of output in LP_{01} mode: anisotropy	46
Figure 12: Frequency variation of output in LP_{01} mode: anisotropy	47
Figure 13: Frequency variation of output in LP_{01} mode	49
Figure 14: Frequency variation of competition parameter $q_0(V)$	63
Figure 15: Frequency variation of mismatch parameter $\tau(V)$	64
Figure 16: Frequency variation of power required for switching	66
Figure 17: Frequency variation of fractional efficiency of switch	67
Figure 18: Frequency variation of detuning parameters	69
Figure 19: Modal rotation and limiting forms	87
Figure 20: Frequency variation of interference parameters: step-profile	93
Figure 21: Modal rotation during passage through grating	95
Figure 22: Change in β during passage through grating	96
Figure 23: "Local birefringence" during passage through grating	97
Figure 24: Frequency variation of β averaged over one period	98

Figure 25: Modal rotation during passage through anisotropic grating	101
Figure 26: Graphical solution for critical points	107
Table 1: Solutions for critical points	108
Figure 27: Pattern of zeroes $\bar{\gamma} = 0$	110
Figure 28: Examples of pattern of zeroes $\bar{\gamma} \neq 0$	111-113
Figure 29: Region in which switching is possible	115
Figure 30: μ variation of discontinuity parameters	117

1.0 INTRODUCTION

This report describes work done while the author was a Visiting Fellow within the Communication Research Centre of the Canadian Government's Department of Communications, and under the supervision of Dr Kenneth O. Hill. It was prompted by a desire to better understand devices being made within the laboratories, and explore the possibility of other devices — most notably an optical switch.

Ponder two questions related to experimental observations of the $LP_{01} \leftrightarrow LP_{11}$ modal conversion grating. Why are there four resonant peaks in the curve illustrating the spectral variation of the resonant coupling? What theoretical limitation exists on the linewidth of these peaks?

To answer these questions, it was necessary to improve the theory of power coupling between the modes propagating in a few-mode optical fibre in which a grating is written, to a theory allowing for the possibility that the grating is not axisymmetric about the direction of modal propagation. Such a theory was developed within the well-known formalism of weakly guiding waveguides and using the equally well-known notion of coupled modes. Also, it was necessary to investigate the way the polarization state of a mode evolves in a periodic, non-axisymmetric waveguide, where neither the commonly used approximation of linearly polarized (LP) modes nor the true modes of an axisymmetric fibre are valid. In fact, the polarization of the modes is not well defined. It varies with the periodicity of the waveguide, and oscillates between the two different LP modes, which are limiting cases.

In examining the theoretic linewidth, for reasons of simplicity (two modes propagate instead of four), the $LP_{01} \leftrightarrow LP_{02}$ modal conversion grating was considered. In comparing theoretical predictions with experimental results, some discrepancies were seen. To remove these, the theory of modal conversion was improved to include anisotropic gratings in a fibre. Given this, results for the $LP_{01} \leftrightarrow LP_{11}$ modal conversion grating were seen to be in fair agreement with experiment.

In Chapter 2 is developed the improved theory of coupling between modes on an axi-

asymmetric fibre by a periodic grating. In Chapter 3 this theory is applied to the simple, well known examples of $LP_{01} \leftrightarrow LP_{02}$ modal conversion gratings and Bragg reflection gratings. It contains the theoretic limitation on the linewidth of the peaks in the spectral response curve. Chapter 4 includes the results of modal conversion in the $LP_{01} \leftrightarrow LP_{11}$ grating. The theory of the true modes on a periodic non-axisymmetric fibre is found in Appendix B.

Consider another question. Given that the resonant spectral linewidth is observed to be very narrow, is it possible to use such a modal conversion grating as an optical switch?

Again, for reasons of simplicity, the $LP_{01} \leftrightarrow LP_{02}$ modal conversion grating was considered. Extensive analysis of the mathematical structure of the problem was needed before an affirmative answer was possible, and then it was dependent on suitable operating conditions for the fibre. Fortunately, these were typical, when a power level of around a KWatt destroys the resonant modal conversion. If the grating is operating away from resonance, then less power is needed. Indeed, quite complicated switching patterns are possible. Sufficient power may cause a resonance where none existed previously; increasing the power destroys the new resonance.

Chapter 5 contains the results of nonlinear switching as it occurs in the $LP_{01} \leftrightarrow LP_{02}$ modal conversion grating. The relevant mathematical results are presented in Appendices D and E.

2.0 THEORY OF INTERMODAL POWER COUPLING

To begin, it is necessary to develop the theory of coupling between modes, as caused by a grating in a fibre. The gratings under consideration are, in reality, very small perturbations of the refractive index of an otherwise axisymmetric fibre, and so perturbation methods are applicable. Most quantities are found by perturbing [e.g. 1: ch18] the corresponding values found on the axially invariant fibre.

One conventional — and by far the most frequently used — approach to the problem of modal conversion in a grating in a weakly guiding optical waveguide, uses the notion of coupled modes [e.g. 2]. However, in keeping with other problems in which coupled mode theory is used, the presentations are invariably confusing, partly (I think) because of poorly chosen and defined notation. As in most mathematical arguments, an elegant choice of notation renders analysis almost trivial.

A second point is that, to the best of my knowledge, the formalism pertaining to modal conversion within gratings has been restricted to gratings that are axisymmetric and weakly guiding. The latter means that LP modes have been used; the former cannot model any effects due to the breaking of circular symmetry. It was found necessary to develop an improved theory that recognizes both the true vector form of the modes of the grating and polarization distinguishing corrections to the weak guidance result.

A question frequently pondered (but infrequently answered with rigor) in analysis of gratings concerns back reflections. Once reflections are included, multiple reflections become a possibility. Nevertheless, it is straightforward to extend the analysis to include such possibilities.

The theory of modal conversion by a grating assumes that the grating is a perfectly periodic structure. In practice, this is not the case. Indeed, a specific nonperiodicity can be included in the design of a grating. A theory describing modal conversion by such quasi-periodic gratings is presented.

It is important to note that the problem is developed within the formalism of the theory of weak guidance [e.g. 1: ch13]. Corrections to the initial approximation of weak guidance are obtained from the initial approximation, as they are shown to be necessary in describing the observed phenomena.

The following analysis ignores any losses from the system, i.e. any coupling into the continuum of radiation modes. Again, the condition of extremely small perturbation to the refractive index in making the grating validates this assumption.

2.1 COUPLED MODE EQUATIONS

To see how power is exchanged between modes on a waveguide with a slow z -variation, it is first necessary to construct a form of coupled mode system. Suppose that, with the summation convention on Latin subscripts but not on Greek ones, the exact travelling electric field is written in the form

$$\mathcal{E} = \frac{1}{\langle \beta_n \rangle^{\frac{1}{2}} \|E_n\|} a_n(z) \mathbf{E}_n(r, \theta, z) e^{i\langle \beta_n \rangle z} \quad (2.1)$$

where $\langle \beta_n \rangle$ is the average propagation constant of the mode and shows the way the phase of the mode accumulates as it travels along the varying waveguide, $a_n(z)$ is the slowly varying amplitude of this mode, $\mathbf{E}_n(r, \theta, z)/\|E_n\|$ is the n th normalized local mode at position z along fibre and co-ordinate (r, θ) in the cross-section, and this local mode has propagation constant $\beta_n(z)$. The power in the α th local mode is given by

$$P_\alpha(z) = \frac{\epsilon_0 c^2 \rho \langle \beta_\alpha \rangle}{2\omega} |\mathcal{E}|^2 = \frac{\epsilon_0 c^2 \rho}{2\omega} |a_\alpha(z)|^2.$$

Also, it is possible to write an approximate expansion for \mathcal{E} in terms of the modes of the unperturbed fibre.

$$\mathcal{E} = \frac{1}{\bar{\beta}_n^{\frac{1}{2}} \|\bar{E}_n\|} p_n(z) \bar{\mathbf{E}}_n(r, \theta) e^{i\bar{\beta}_n z} \quad (2.2)$$

where $\bar{\mathbf{E}}_n(r, \theta)$ is the n th mode of the unperturbed waveguide with propagation constant $\bar{\beta}_n$, and $p_n(z)$ is a slowly varying coefficient. This gives power in the α th mode of the unperturbed waveguide to be

$$\bar{P}_\alpha(z) = \frac{\epsilon_0 c^2 \rho}{2\omega} |p_\alpha(z)|^2.$$

The solutions for the local modes are readily obtained. Define the matrix $D(z)$ by

$$\mathbf{E}_\alpha(r, \theta, z) = d_{\alpha n}(z) \bar{\mathbf{E}}_n(r, \theta) \|E_\alpha\| / \|\bar{\mathbf{E}}_n\|. \quad (2.3)$$

It is trivially obvious that $D(z)$, so defined, is orthogonal. Thus, from (2.1), (2.2) and (2.3), it follows that

$$p_\alpha(z) = \frac{\bar{\beta}_\alpha^{\frac{1}{2}}}{\langle \beta_n \rangle^{\frac{1}{2}}} d_{n\alpha}(z) a_n(z) e^{i(\langle \beta_n \rangle - \bar{\beta}_\alpha)z} \quad (2.4)$$

which gives

$$p'_\alpha(z) = \frac{\bar{\beta}_\alpha^{\frac{1}{2}}}{\langle \beta_n \rangle^{\frac{1}{2}}} \left(d_{n\alpha}(z) a'_n(z) + d'_{n\alpha}(z) a_n(z) + i(\langle \beta_n \rangle - \bar{\beta}_\alpha) d_{n\alpha}(z) a_n(z) \right) e^{i(\langle \beta_n \rangle - \bar{\beta}_\alpha)z} \quad (2.5a)$$

$$p''_\alpha(z) = \frac{\bar{\beta}_\alpha^{\frac{1}{2}}}{\langle \beta_n \rangle^{\frac{1}{2}}} \left(d_{n\alpha}(z) a''_n(z) + 2d'_{n\alpha}(z) a'_n(z) + d''_{n\alpha}(z) a_n(z) + 2i(\langle \beta_n \rangle - \bar{\beta}_\alpha) d_{n\alpha}(z) a'_n(z) \right. \\ \left. + 2i(\langle \beta_n \rangle - \bar{\beta}_\alpha) d'_{n\alpha}(z) a_n(z) - (\langle \beta_n \rangle - \bar{\beta}_\alpha)^2 d_{n\alpha}(z) a_n(z) \right) e^{i(\langle \beta_n \rangle - \bar{\beta}_\alpha)z} \quad (2.5b)$$

Thus, to see how $p_\alpha(z)$ evolves and power is exchanged between the modes of the unperturbed fibre, it suffices to know how the grating influences the evolution of the $a_\alpha(z)$ and the exchange of power between the pseudo-modes of the grating. This is the essence of coupled mode theory.

2.2 APPROXIMATIONS

The full, exact solution of the second-order system given at (2.5) is generally not possible. Thus, it becomes necessary to obtain some approximations to allow simplification of the equations.

Firstly, the adiabatic approximation shows that for a grating that is truly a perturbation, the exchange of power is very slow, so the slowly varying coefficients $a_\alpha(z)$ are such that it can be assumed $a''_\alpha(z) \equiv 0$.

Secondly, it is known [e.g. 1] that \mathcal{E} satisfies

$$[\nabla^2 + \frac{\partial^2}{\partial z^2} + k^2 n_0^2 + V^2 g(r, \theta, z)] \mathcal{E} = -2\Delta \nabla [\mathcal{E} \cdot \nabla g(r, \theta, z)] \quad (2.6)$$

correct to order Δ . Here, $g(r, \theta, z)$ is the z -dependent perturbed index on the fibre. It is known also that the unperturbed index gives the equation

$$[\nabla^2 - \bar{\beta}_\alpha^2 + k^2 n_0^2 + V^2 \bar{g}(r)] \bar{\mathbf{E}}_\alpha(r, \theta) = -2\Delta \nabla [\bar{\mathbf{E}}_\alpha(r, \theta) \cdot \nabla \bar{g}(r)]$$

for the α th mode of the unperturbed circular fibre. If this and (2.2) are substituted into (2.6), then it follows

$$\begin{aligned} p''_{\alpha}(z) + 2i\bar{\beta}_{\alpha}p'_{\alpha}(z) + G_{\alpha n}(z)\frac{\bar{\beta}_{\alpha}^{\frac{1}{2}}}{\bar{\beta}_n^{\frac{1}{2}}}p_n(z)e^{i(\bar{\beta}_n - \bar{\beta}_{\alpha})z} \\ = -2\Delta p_n(z)\frac{\bar{\beta}_{\alpha}^{\frac{1}{2}}}{\bar{\beta}_n^{\frac{1}{2}}}\frac{\langle \bar{\mathbf{E}}_{\alpha}(r, \theta), \nabla[\bar{\mathbf{E}}_n(r, \theta) \cdot \nabla[g(r, \theta, z) - \bar{g}(r)]] \rangle}{\|\bar{\mathbf{E}}_{\alpha}\| \|\bar{\mathbf{E}}_n\|}e^{i(\bar{\beta}_n - \bar{\beta}_{\alpha})z} \end{aligned} \quad (2.7)$$

since the unperturbed modes are orthogonal, i.e. $\langle \bar{\mathbf{E}}_{\alpha}(r, \theta), \bar{\mathbf{E}}_{\beta}(r, \theta) \rangle$ vanishes unless $\alpha = \beta$. Also, the matrix $G(z)$ is defined by

$$G_{\alpha\gamma}(z) = V^2 \frac{\langle \bar{\mathbf{E}}_{\alpha}(r, \theta), (g(r, \theta, z) - \bar{g}(r))\bar{\mathbf{E}}_{\gamma}(r, \theta) \rangle}{\|\bar{\mathbf{E}}_{\alpha}\| \|\bar{\mathbf{E}}_{\gamma}\|} \quad (2.8)$$

These elements are of the order $\frac{\delta}{\Delta} \sim (g(r, \theta, z) - \bar{g}(r))$. Consideration of the right-hand side of (2.7) shows it to be of order $\Delta \frac{\delta}{\Delta}$, and thus it will be ignored in the following analysis.

To change from this simply coupled equation for the $p_{\alpha}(z)$ s, to one for the $a_{\alpha}(z)$ s, substitute (2.4) and (2.5) into (2.7). Making the above two approximations, one obtains

$$\begin{aligned} (\langle \beta_n \rangle d_{n\alpha}(z) - i d'_{n\alpha}(z)) \frac{1}{\langle \beta_n \rangle^{\frac{1}{2}}} a'_n(z) e^{i\langle \beta_n \rangle z} \\ = \frac{1}{2} i \left(d''_{n\alpha}(z) + 2i \langle \beta_n \rangle d'_{n\alpha}(z) + (\bar{\beta}_{\alpha}^2 - \langle \beta_n \rangle^2) d_{n\alpha} + G_{\alpha l}(z) d_{nl}(z) \right) \frac{1}{\langle \beta_n \rangle^{\frac{1}{2}}} a_n(z) e^{i\langle \beta_n \rangle z}. \end{aligned}$$

Further, take advantage of $D(z)$ being an orthogonal matrix, so that the approximate coupled amplitude equations are

$$\begin{aligned} (\delta_{\alpha n} - i \frac{d_{\alpha p}(z) d'_{np}(z)}{\langle \beta_{\alpha} \rangle^{\frac{1}{2}} \langle \beta_n \rangle^{\frac{1}{2}}}) a'_n(z) e^{i\langle \beta_n \rangle z} = \frac{1}{2} i \left(\frac{d_{\alpha p}(z) d''_{np}(z)}{\langle \beta_{\alpha} \rangle^{\frac{1}{2}} \langle \beta_n \rangle^{\frac{1}{2}}} \right. \\ \left. + 2i \frac{\langle \beta_n \rangle^{\frac{1}{2}}}{\langle \beta_{\alpha} \rangle^{\frac{1}{2}}} d_{\alpha p}(z) d'_{np}(z) + (\bar{\beta}_p^2 - \langle \beta_n \rangle^2) \frac{d_{\alpha p}(z) d_{np}(z)}{\langle \beta_{\alpha} \rangle^{\frac{1}{2}} \langle \beta_n \rangle^{\frac{1}{2}}} + G_{pl}(z) \frac{d_{\alpha p}(z) d_{nl}(z)}{\langle \beta_{\alpha} \rangle^{\frac{1}{2}} \langle \beta_n \rangle^{\frac{1}{2}}} \right) a_n(z) e^{i\langle \beta_n \rangle z} \end{aligned} \quad (2.9)$$

where $\delta_{\alpha n}$ is the Krönecker delta.

Now all is readied for the third approximation. Since $\beta_j \sim \Delta^{-1/2}$, a little thought shows that the matrix on the left-hand side of (2.9) can be inverted approximately; namely

$$(\delta_{\alpha\gamma} - i \frac{d_{\alpha p}(z) d'_{\gamma p}(z)}{\langle \beta_{\alpha} \rangle^{\frac{1}{2}} \langle \beta_{\gamma} \rangle^{\frac{1}{2}}})^{-1} \approx (\delta_{\alpha\gamma} + i \frac{d_{\alpha p}(z) d'_{\gamma p}(z)}{\langle \beta_{\alpha} \rangle^{\frac{1}{2}} \langle \beta_{\gamma} \rangle^{\frac{1}{2}}}).$$

The variation of $d_{\alpha\gamma}(z)$ with z is also slow, so that the derivative $d_{\alpha\gamma}(z)$ with respect to z is small, making this approximation even better. Using this approximate inverse, the left-hand side of (2.9) is simplified, and the coupling equation becomes

$$d'_{\alpha}(z)e^{i(\beta_{\alpha})z} = \frac{1}{2}i\left(\frac{d_{\alpha p}(z)d''_{np}(z)}{\langle\beta_{\alpha}\rangle^{\frac{1}{2}}\langle\beta_n\rangle^{\frac{1}{2}}} - 2\frac{\langle\beta_n\rangle^{\frac{1}{2}}}{\langle\beta_{\alpha}\rangle^{\frac{1}{2}}\langle\beta_q\rangle}d_{\alpha r}(z)d'_{qr}(z)d_{qp}(z)d'_{np}(z)\right. \\ \left.+ 2i\frac{\langle\beta_n\rangle^{\frac{1}{2}}}{\langle\beta_{\alpha}\rangle^{\frac{1}{2}}}d_{\alpha p}(z)d'_{np}(z) + (\bar{\beta}_p^2 - \langle\beta_n\rangle^2)\frac{d_{\alpha p}(z)d_{np}(z)}{\langle\beta_{\alpha}\rangle^{\frac{1}{2}}\langle\beta_n\rangle^{\frac{1}{2}}} + G_{pl}(z)\frac{d_{\alpha p}(z)d_{nl}(z)}{\langle\beta_{\alpha}\rangle^{\frac{1}{2}}\langle\beta_n\rangle^{\frac{1}{2}}}\right)a_n(z)e^{i(\beta_n)z}, \quad (2.10a)$$

where further approximations are made by ignoring terms with factors of order $\beta_j^2 \sim \Delta^{-2}$ in their denominators. Thus, we obtain the matrix equation — coupled first order linear differential equations:

$$a'_{\alpha}(z)e^{i(\beta_{\alpha})z} = iM_{\alpha n}(z)a_n(z)e^{i(\beta_n)z}, \quad (2.10b)$$

with matrix $M_{\alpha\gamma}(z)$ defined in the obvious way from comparison of the two parts of (2.10). It is stressed that this is obtained by retaining terms to dominant order in Δ .

2.3 PERIODIC GRATING AND RESONANCE

Since the grating is periodic with spatial period Λ , it follows that so is matrix $M(z)$. Hence, define

$$M_{\alpha\gamma}(z) = m_{\alpha\gamma j}e^{ij2\pi z/\Lambda},$$

with

$$m_{\alpha\gamma\epsilon} = \frac{1}{\Lambda} \int_0^{\Lambda} dz M_{\alpha\gamma}(z)e^{-i\epsilon 2\pi z/\Lambda} \quad (2.11)$$

so that (2.10b) becomes

$$a'_{\alpha}(z) = im_{\alpha n j}a_n(z)e^{i(\langle\beta_n\rangle - \langle\beta_{\alpha}\rangle + j\frac{2\pi}{\Lambda})z}. \quad (2.12)$$

There are two aspects to the solution of (2.12). Far away from any resonance, i.e. when $(\langle\beta_n\rangle - \langle\beta_{\alpha}\rangle + j\frac{2\pi}{\Lambda})$ is away from 0 (when it also happens to be large) for all n, α, j , then the solution gives only small variations in the $a_{\alpha}(z)$ s. Explicitly, these are

$$a_{\alpha}(z) = a_{\alpha}(0) + m_{\alpha n j}a_n(0)\frac{(e^{i(\langle\beta_n\rangle - \langle\beta_{\alpha}\rangle + j\frac{2\pi}{\Lambda})z} - 1)}{(\langle\beta_n\rangle - \langle\beta_{\alpha}\rangle + j\frac{2\pi}{\Lambda})}. \quad (2.13)$$

Two observations are in order. The magnitude of the $m_{\alpha n j}$, depending on the coupling matrix $G(z)$, is small. Resonance occurs when the denominator of a term in the sum on the right-hand side of (2.13) vanishes. When it does, a different solution is needed.

Resonance between two modes, indexed by α, γ , exists when there is an integer value j such that

$$\langle \beta_\gamma \rangle - \langle \beta_\alpha \rangle = j \frac{2\pi}{\Lambda}. \quad (2.14)$$

It is worth stressing that there is always self-coupling, which occurs for $\alpha = \gamma$ and $j = 0$. Suppose instead that the modes indexed by α, γ belong to the same family of modes, i.e. they have the same scalar value of β . Then the average propagation constants are almost degenerate, i.e. $\langle \beta_\alpha \rangle \approx \langle \beta_\gamma \rangle$, so that resonance almost occurs for $j = 0$. This is a birefringent coupling. On a fibre operating so that modes of two different families of modes propagate, we find a j th-order, mode-converting, resonant coupling when the period of the grating is tuned so that it approximately satisfies (2.14), for some non-zero value of j . This is a very specific condition.

For the case of such mode conversion with a j th order ($j \neq 0$) resonance, suppose the first family of modes is indexed by $\alpha \in \mathcal{I}_I$ and the second family by $\alpha \in \mathcal{I}_{II}$. From (2.12), the system of coupled equations then becomes, for $\alpha \in \mathcal{I}_{\{I, II\}}$,

$$\begin{aligned} a'_\alpha(z) = & i m_{\alpha\alpha 0} a_\alpha(z) + i \sum_{\substack{n \in \mathcal{I}_{\{I, II\}} \\ n \neq \alpha}} m_{\alpha n 0} a_n(z) e^{i(\langle \beta_n \rangle - \langle \beta_\alpha \rangle)z} \\ & + i \sum_{n \in \mathcal{I}_{\{I, II\}}} m_{\alpha n J(\alpha, n)} a_n(z) e^{i(\langle \beta_n \rangle - \langle \beta_\alpha \rangle + J(\alpha, n) \frac{2\pi}{\Lambda})z}, \end{aligned} \quad (2.15)$$

where it is defined that

$$J(\alpha, \gamma) = \begin{cases} 0 & , \text{ if } \alpha, \gamma \text{ in same family} \\ j & , \text{ if } \alpha \in \mathcal{I}_{II}, \gamma \in \mathcal{I}_I \\ -j & , \text{ if } \alpha \in \mathcal{I}_I, \gamma \in \mathcal{I}_{II} . \end{cases}$$

In (2.15), the first term is the self coupling, the second term is the birefringent coupling, and the third term is the mode-converting coupling. The complicated treatment of the sign given in $J(\alpha, n)$ in the exponent takes account of whether $\langle \beta_n \rangle$ is greater or less than $\langle \beta_\alpha \rangle$. This forms a set of coupled, first-order, linear differential equations with periodic coefficients.

With the value of Λ and j fixed, a matrix $m_{\alpha n} J(\alpha, n) e^{i(\langle\beta_n\rangle - \langle\beta_\alpha\rangle + J(\alpha, n) \frac{2\pi}{\Lambda})z}$ is fixed, as detailed at (2.15). Simplification of (2.15) leads to a system with constant complex coefficients. Without any loss of generality, we can assume that the values of $\langle\beta_j\rangle$ are greater for family *I* than family *II*. With C an arbitrary constant to make matters as “nice” as possible, defining

$$\begin{aligned}\phi_\alpha &= \langle\beta_\alpha\rangle - C + J(\alpha, 1) \frac{2\pi}{\Lambda} \\ a_\alpha(z) &= A_{\alpha m} e^{i(\mu_m - \phi_\alpha)z},\end{aligned}$$

and noting that $J(\alpha, \gamma) = J(\alpha, 1) - J(\gamma, 1)$, yields the system of matrix equations

$$((\mu_\gamma - \phi_\alpha)\delta_{\alpha n} - m_{\alpha n} J(\alpha, n)) A_{n\gamma} = 0.$$

Now $\mu_\gamma, A_{\alpha\gamma}$ are fixed by standard eigenvalue methods. When the matrix on the left-hand side is Hermitian — which it is when all modes are propagating forward — theory tells that there exists a periodic solution for $a_\alpha(z)$ [3]. When the matrix is anti-Hermitian, the solution involves exponential functions. Knowing there is a solution, even its form, is a long way from actually having the solution; finding it can be a lot more work.

2.4 REFLECTIONS

To include the possibility of reflections in the grating it is straightforward. Reflections are modes propagating towards z negative, and these are described by values of $\langle\beta_\alpha\rangle < 0$. Such modes, and values of $\langle\beta_\alpha\rangle$, can be included in expansions (2.1) and (2.2). The local transverse modal field is still given by $\mathbf{E}_\alpha(r, \theta, z)$. However, when $\langle\beta_\alpha\rangle < 0$, then $\langle\beta_\alpha\rangle^{\frac{1}{2}}$ is imaginary, and account must be taken of this in the evaluations proceeding from (2.10). That these extra imaginary numbers appear is not surprising, as there are phase shifts of π at reflections. The resonance condition for a strong conversion to reflection remains (2.13). Thus, reflections present no difficulty.

2.5 AXISYMMETRIC GRATING

If the grating is axisymmetric, two further simplifications exist. Firstly, the vector direction of the modes of the grating remains that of the modes found on the unperturbed circular fibre, and the matrix $D(z)$ is the identity matrix. This means that the matrix $M(z)$,

found at (2.10), is simply

$$M_{\alpha\gamma}(z) = \frac{1}{2} \left(\frac{\bar{\beta}_\alpha^2 - \langle \beta_\alpha \rangle^2}{\langle \beta_\alpha \rangle} \delta_{\alpha\gamma} + \frac{G_{\alpha\gamma}(z)}{\langle \beta_\alpha \rangle^{\frac{1}{2}} \langle \beta_\gamma \rangle^{\frac{1}{2}}} \right). \quad (2.16)$$

Secondly, the grating is formed of a perturbation which factors as

$$g(r, \theta, z) - \bar{g}(r) = \frac{\delta}{\Delta} g_r(r) g_z(z).$$

On this axisymmetric structure, within the approximation worked here, the radial dependence and vector form of a mode is everywhere identical to those of the unperturbed fibre. A little thought about the effect of an axisymmetric perturbation and the angular dependence of circularly polarized electric fields simplifies the coupling coefficients. With the radial dependence of $\bar{\mathbf{E}}_\alpha(r, \theta)$ given by $F_\alpha(r)$, the integrals in (2.8) become

$$G_{\alpha\gamma}(z) = \frac{\delta}{\Delta} g_z(z) V C_{\alpha\gamma}(V), \quad (2.17a)$$

together with the definition

$$C_{\alpha\gamma}(V) = \frac{V}{\|F_\alpha\| \|F_\gamma\|} \int_0^\infty dr r g_r(r) F_\alpha(r) F_\gamma(r), \quad (2.17b)$$

which are generalized coupling coefficients, involving the radial dependence of the modes and including all the frequency dependence of the coupling matrix $M(z)$. The extra V appearing in (2.17a) disappears when it is inserted in (2.16) because $|\langle \beta_\alpha \rangle| \approx V/\sqrt{2\Delta}$.

It is worthy of note that the self-coupling term vanishes. The self-coupling term comes about from

$$\begin{aligned} m_{\alpha\alpha 0} &= \frac{1}{2\langle \beta_\alpha \rangle} (\bar{\beta}_\alpha^2 - \langle \beta_\alpha \rangle^2) + \frac{1}{\Lambda} \int_0^\Lambda dz G_{\alpha\alpha}(z) \\ &= 0, \end{aligned} \quad (2.18)$$

because we know, from standard perturbation theory [e.g. 1], that the average propagation constant is defined by

$$\begin{aligned} \langle \beta_\alpha \rangle^2 &= \bar{\beta}_\alpha^2 + \frac{1}{\Lambda} \int_0^\Lambda dz \frac{\delta}{\Delta} \frac{V^2}{\|\bar{\mathbf{E}}_\alpha\|^2} \langle \bar{\mathbf{E}}_\alpha(r, \theta), (g(r, \theta, z) - \bar{g}(r)) \bar{\mathbf{E}}_\alpha(r, \theta) \rangle \\ &= \bar{\beta}_\alpha^2 + \frac{1}{\Lambda} \int_0^\Lambda dz \frac{\delta}{\Delta} \frac{V^2}{\|\bar{\mathbf{E}}_\alpha\|^2} \int_C dS (g(r, \theta, z) - \bar{g}(r)) |\bar{\mathbf{E}}_\alpha(r, \theta)|^2 \\ &= \bar{\beta}_\alpha^2 + \frac{1}{\Lambda} \int_0^\Lambda dz G_{\alpha\alpha}(z) \end{aligned}$$

from the definition of $G(z)$ at (2.8) and noting that the domain \mathcal{C} is the portion of the cross-section in which $g(r, \theta, z) \neq \bar{g}(r)$. In the conventional approach to coupling in gratings, the average value of the propagation constants is not inserted, and the self-coupling term remains. Its removal in solving the ensuing coupled equations has the same mathematical effect as using the average constant in the first place.

The other elements in the Fourier decomposition of the coupling matrix follow. If $g_z(z)$ has the Fourier expansion

$$g_z(z) = g_j e^{i2\pi jz/\Lambda}, \quad (2.19)$$

then, from (2.11), (2.16) and (2.17) and recalling how $\epsilon = J(\alpha, \gamma)$, there is the coupling matrix

$$m_{\alpha\gamma\epsilon} = \frac{\delta}{\sqrt{2\Delta}} B_{\alpha\gamma} C_{\alpha\gamma}(V) g_\epsilon, \quad (2.20)$$

where $B_{\alpha\gamma} = V/\sqrt{2\Delta} \langle \beta_\alpha \rangle^{\frac{1}{2}} \langle \beta_\gamma \rangle^{\frac{1}{2}}$, which has value 1 when the signs of $\langle \beta_\alpha \rangle$ and $\langle \beta_\gamma \rangle$ are the same and value i when their signs differ. This follows since $|\langle \beta_\alpha \rangle| \approx V/\sqrt{2\Delta}$, to the accuracy required here.

2.6 ANISOTROPY

Suppose that the grating is formed by a perturbation that is anisotropic. The effect is twofold. Firstly, and obviously, it has an influence in the values of $\langle \beta_\alpha \rangle$ and the matrix $D_{\alpha\gamma}(z)$. This is as given by standard theories.

Secondly, the coupling matrix given at (2.8) is more complex. It is assumed that the axes of anisotropy align with the Cartesian axes, so the scalar value $g(r, \theta, z) - \bar{g}(r)$ is replaced by a diagonal matrix. (General theory shows how such Cartesian axes can be defined; finding them will complicate the form of (r, θ) dependence of grating, if they do not match the symmetry axes of the grating.) This means

$$G_{\alpha\gamma}(z) = \frac{V^2}{\|\bar{E}_\alpha\| \|\bar{E}_\gamma\|} \langle \bar{E}_\alpha(r, \theta), \begin{pmatrix} g_x(r, \theta, z) - \bar{g}(r) & 0 \\ 0 & g_y(r, \theta, z) - \bar{g}(r) \end{pmatrix} \bar{E}_\gamma(r, \theta) \rangle. \quad (2.21)$$

where $g_j(r, \theta, z) - \bar{g}(r)$ defines the perturbation sensed by j -polarized light.

3.0 EXAMPLE: NORMAL INTERFACES, UNIFORM PERTURBATION

3.1 GEOMETRY

The study of such a grating is motivated by realized structures [e.g. 4, 5]; it is the simplest case. The structure, seen in Fig. 1, is of period Λ and consists of N elements of length $\ell < \Lambda$. These regions have a higher refractive index in the core: $\Delta + \delta$ instead of Δ . However, it is only slightly higher so $\delta \ll \Delta$, thereby making it possible to treat these elements as perturbations of an otherwise axially invariant waveguide, and use the theory derived previously. The constant ζ is fixed by

$$\zeta = \frac{\ell}{\Lambda},$$

and all lengths have been normalized by the radius of the fibre. Obviously, for a grating to exist, $\zeta < 1$.

The interfaces separating the elements of the grating are normal to the axis of the grating, which is the axis of propagation of modes. Hence, the grating is axisymmetric, so we use the simplified results based on (2.16). The radial dependence of the modes, and their vector forms are always as on axisymmetric, unperturbed fibre, and the radial and periodic longitudinal perturbations of the refractive index factor independently. Further, the perturbation is not only axisymmetric, but constant, in the core. Hence, the coupling coefficients given at (2.17b) follow as

$$C_{\alpha\gamma}(V) = \frac{V}{\|F_\alpha\| \|F_\gamma\|} \int_0^1 dr r F_\alpha(r) F_\gamma(r). \quad (3.1)$$

With the z -variation of the grating given as

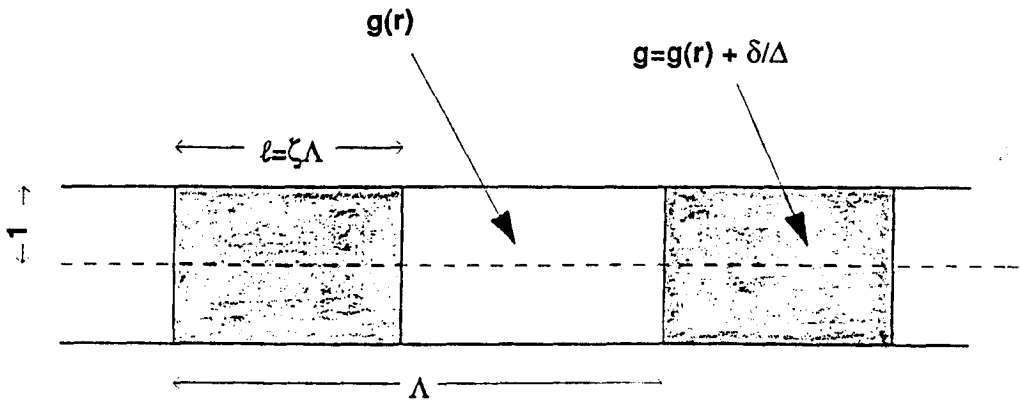
$$g_z(z) = \sum_n \hat{g}\left(\frac{z}{\Lambda} - n + \frac{1}{2}\right);$$

$$\hat{g}(x) = \begin{cases} 1 & , \text{ if } x \in \left(-\frac{1}{2}, \zeta - \frac{1}{2}\right) \\ 0 & , \text{ if } x \in \left(\zeta - \frac{1}{2}, \frac{1}{2}\right), \end{cases}$$

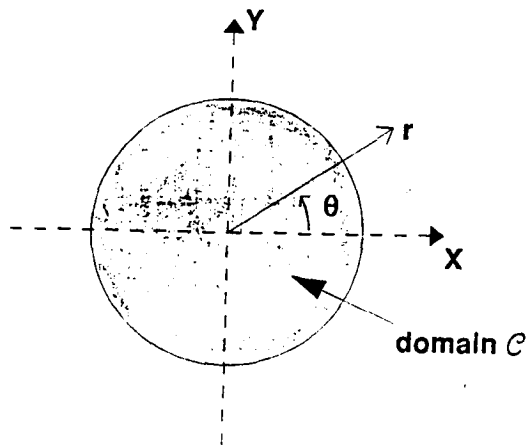
it follows that

$$g_\alpha = e^{i\alpha\pi(1-\zeta)} \frac{\sin(\alpha\pi\zeta)}{\alpha\pi} \quad (3.2)$$

for use in (2.20).



(a) fibre seen from the side



(b) fibre seen in cross-section

Figure 1: Structure of the $LP_{01} \leftrightarrow LP_{02}$ modal conversion grating

The shaded regions represent those of perturbed refractive index, characterized by $\Delta + \delta$; the unperturbed index is measured by Δ .

3.2 GRATING FOR LP₀₁ ↔ LP₀₂ MODAL CONVERSION

This grating is designed to give a first-order resonance between two forward propagating modes. Denote either the X- or Y-polarized fundamental (or HE₁₁) and HE₁₂ modes as modes 1 and 2, respectively. Since these polarizations are degenerate with respect to propagation and form, it does not matter which polarization is selected. Further, they are axisymmetric, and are the only ones connected by the axisymmetric grating considered. The families of LP₁₁ and LP₂₁ modes will be ignored.

Since both modes travel forward, the $B_{\alpha\gamma}$ are all 1. Clearly $\langle\beta_1\rangle > \langle\beta_2\rangle$. Define the real values

$$\Gamma = \frac{1}{2}(\langle\beta_2\rangle - \langle\beta_1\rangle + \frac{2\pi}{\Lambda}); \quad (3.3)$$

$$M(V) = \frac{\delta}{\sqrt{2\Delta}} C_{12}(V) \frac{\sin(\pi\zeta)}{\pi}; \quad (3.4a)$$

so that, with C_{12} coming from (3.1), g_1 from (3.2), and m_{121} from (2.20),

$$\begin{aligned} C_{12}(V) &= \frac{V}{\|F_1\| \|F_0\|} \int_0^1 dr r F_0(r) F_1(r); \\ m_{121} &= -M e^{-i\pi\zeta}. \end{aligned} \quad (3.4b)$$

It follows that $m_{21-1} = m_{121}^*$. Hence, from (2.15) and (2.18), the pertinent set of coupled equations is

$$\begin{pmatrix} a_1'(z) \\ a_2'(z) \end{pmatrix} = i \begin{pmatrix} 0 & -M e^{-i\pi\zeta} e^{i2\Gamma z} \\ -M e^{i\pi\zeta} e^{-i2\Gamma z} & 0 \end{pmatrix} \begin{pmatrix} a_1(z) \\ a_2(z) \end{pmatrix}.$$

The solution of this system is easy (see Appendix A). With the boundary conditions $a_1(0) = 1, a_2(0) = 0$ imposed, i.e. all the power initially enters the grating in mode 1, it follows that

$$a_1(z) = e^{i\Gamma z} \left(\cos(\mu z) - \frac{i\Gamma}{\mu} \sin(\mu z) \right) \quad (3.5a)$$

$$a_2(z) = e^{-i\Gamma z} \frac{-iM e^{i\pi\zeta}}{\mu} \sin(\mu z) \quad (3.5b)$$

where it is defined that

$$\mu^2(V) = M^2(V) + \Gamma^2(V); \quad (3.6)$$

$$\eta(V) = 1 / \left(1 + \frac{\Gamma^2(V)}{M^2(V)} \right). \quad (3.7)$$

The latter is useful in the expression for power:

$$|a_1(z)|^2 = 1 - \eta \sin^2(\mu z). \quad (3.8)$$

Maximum power exchange occurs if $\eta = 1$, or equivalently if $\Gamma = 0$, exactly the well-known conditions. The coupling length, after which the maximum possible fraction of power η has transferred to mode 2, is $\pi/2M(V)$.

For the step profile fibre [1: ch14], we find that

$$C_{12}(V) = \frac{2W_1W_2U_1U_2(\chi_1 - \chi_2)}{V(U_1^2 - U_2^2)\chi_1\chi_2}$$

where U_1, W_1 and U_2, W_2 are the conventional pairs of normalized propagation constants of the LP_{01} and LP_{02} modes, respectively, and $\chi_j = U_j J_1(U_j)/J_0(U_j)$. This function of frequency is illustrated in Fig. 2. The average values of the propagation constants are (refer below (2.18))

$$\langle \beta_j \rangle^2 = \tilde{\beta}_j^2 - \Delta \frac{\chi_j}{\|F_j\|^2} + \frac{\delta}{\Delta} \xi V^2 \eta_j$$

correct to order δ and Δ^2 . Here, η_j is the customary modal efficiency and $\|F_j\|$ the customary modal normalization [e.g. 1: ch14]. The interpretation of this expression is easy. The tilded value is the scalar propagation constant of the LP_{0j} mode, the second term is the polarization correction to this, and the final term is average correction due to the presence of the grating.

At times it is desirable to find the period of a grating that would achieve complete modal conversion at a nominated wavelength. This comes about by satisfying (2.14), as mentioned previously. An easier expression that is approximately satisfied can be found. Instead of using the averaged propagation constants, use the scalar approximations to the propagation constants. Then we find

$$\Lambda \sqrt{\Delta} \approx 2\sqrt{2}\pi \frac{V}{\tilde{\beta}_1^2 - \tilde{\beta}_2^2} = 2\sqrt{2}\pi \frac{V}{W_1^2 - W_2^2}. \quad (3.9)$$

This estimate for $\Lambda(\omega)$ is correct to order $\Delta, \frac{\delta}{\Delta}$. The characteristic behaviour of this solution is well defined, and can be seen in Fig. 3. The period decreases as V moves above 3.832, the cut-off value of the LP_{02} mode, attains a minimum at $V = 4.448$, and thereafter increases without limit. Alternately, a given periodicity Λ of the grating may fail to achieve full modal conversion, may achieve conversion at two frequencies, or perhaps only one.

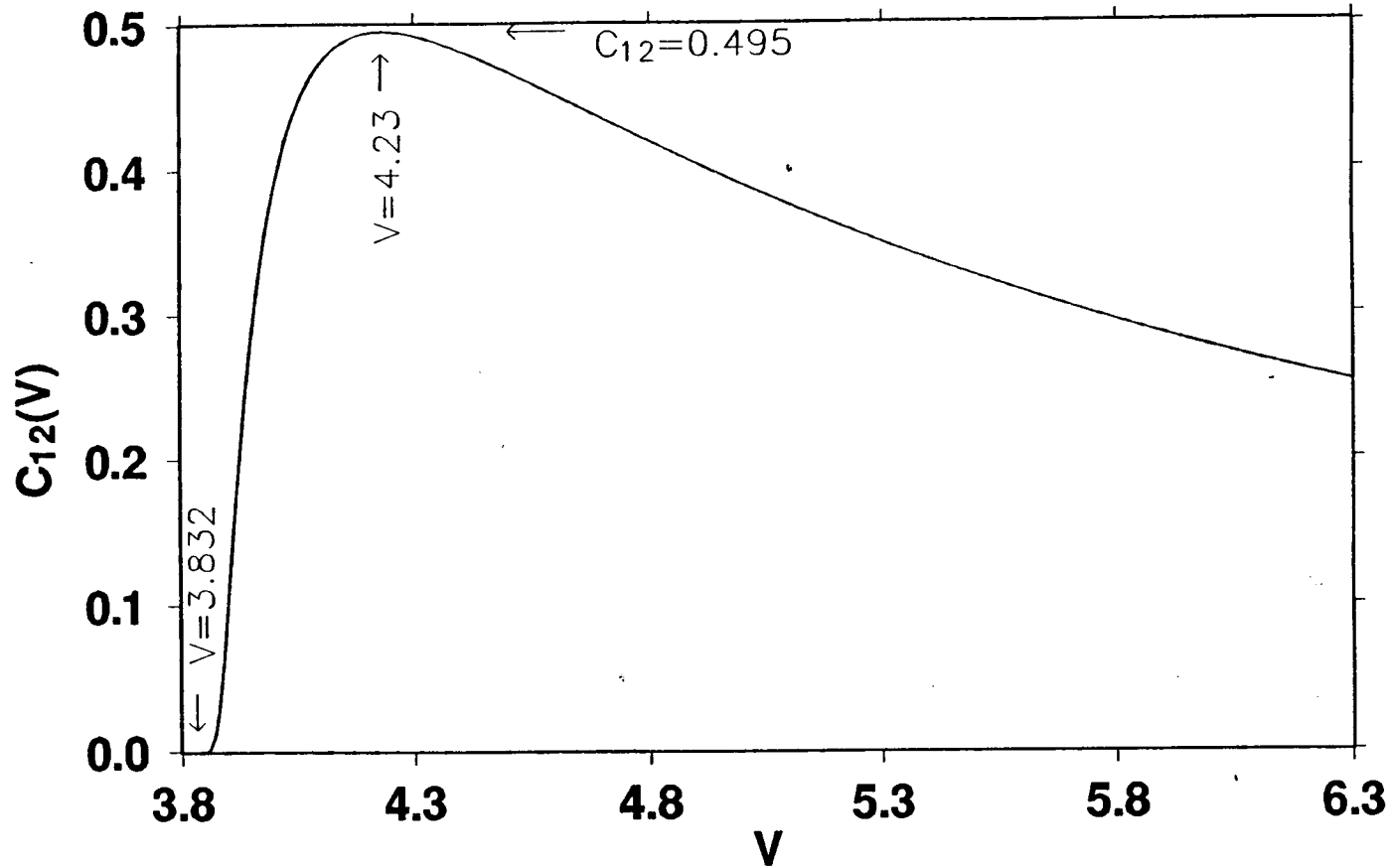


Figure 2: Frequency variation of the coupling coefficient

For the $LP_{01} \leftrightarrow LP_{02}$ grating, the coupling coefficient, defined by Eq. (3.1), is shown as a function of normalized frequency.

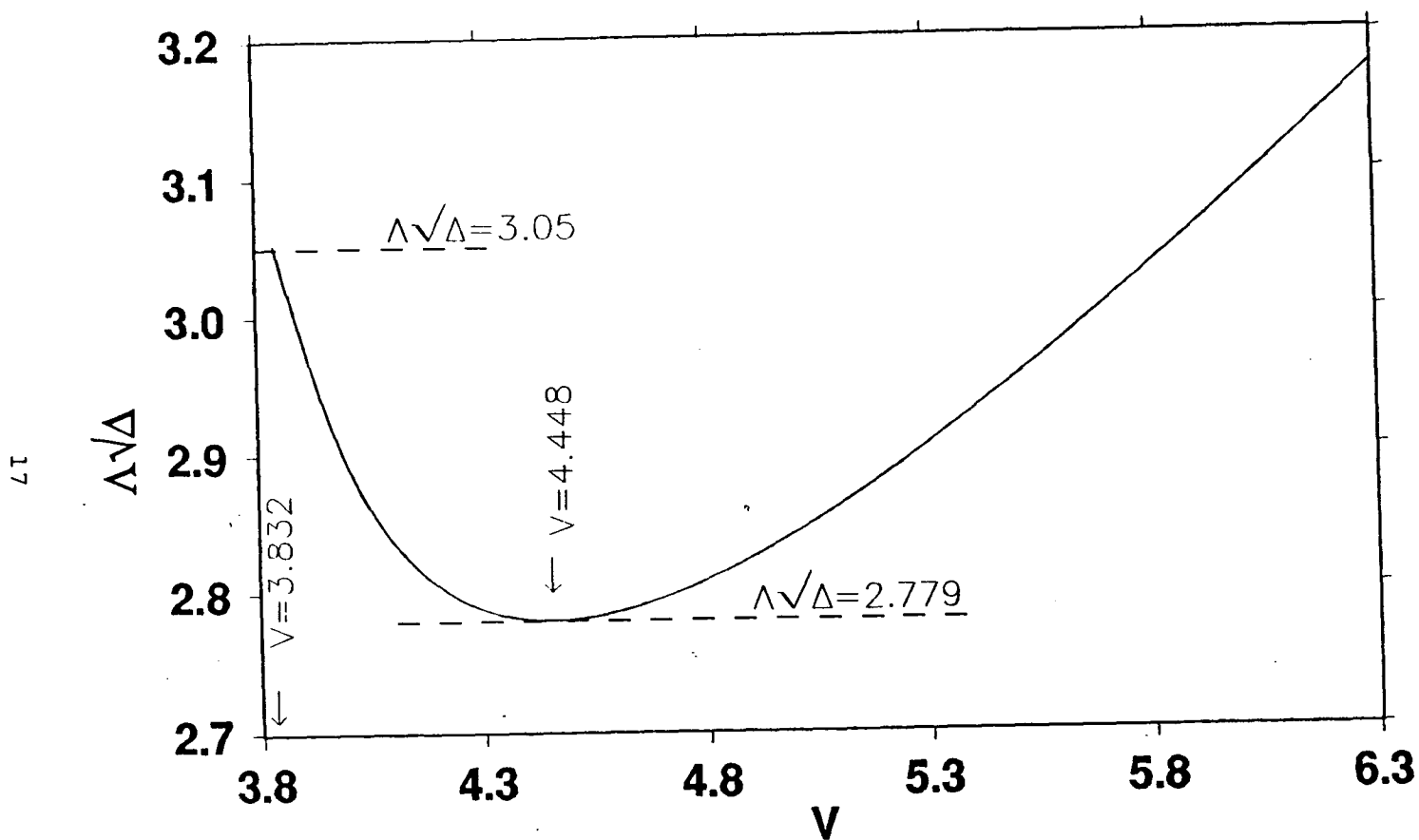


Figure 3: Frequency variation of scaled scalar period

For the $LP_{01} \leftrightarrow LP_{02}$ grating, the scaled scalar period, given in Eq. (3.9), for complete coupling between modes is shown as a function of normalized frequency.

3.3 SPECTRAL RESPONSE — STEP FIBRE

Consider a step fibre with radius $\rho = 4.198 \mu\text{m}$ and first higher-mode cut-off wavelength at $\lambda = 1.286 \mu\text{m}$. Consider a grating made of 2000 elements, for which $\zeta = \frac{1}{2}$, and $\delta = 4 \times 10^{-6}$. These correspond to the magnitudes of parameters in gratings of interest [5]. The maximum amount of power that can be exchanged between the LP_{01} and LP_{02} modes $\eta(V)$ and the length of grating $\pi/2M$ needed to exchange this maximum power are shown in Fig. 4, for periodicity $\Lambda = 207.3 \mu\text{m}$. In both cases, the functions are very sharply spiked about the resonant frequencies. Of course, if the grating is not of the correct total length, which is frequency dependent, then less than complete transfer of power from the LP_{01} mode is observed.

Once a grating of nominated periodicity and length is fabricated, the amount of conversion at a continuum of frequencies is easily established. In Fig. 5 are shown a sampling of such response curves, for different periodicities Λ of the grating. They agree favourably with the spectral response curves found experimentally. The fraction of power remaining in the LP_{01} mode is shown:

$$1 - \eta(V) \sin^2(\mu(V)N\Lambda).$$

Complete power transfer is not achieved because the length of the grating $N\Lambda$ is less than the coupling length $\frac{\pi}{2M}$. For the periodicities selected and combination of fibre parameters, two resonant frequencies exist. Observe that the peak of the conversion decreases with increasing distance from $V = 4.23$ — the location of the peak value of $C_{12}(V)$ (see Fig. 2) — which corresponds to the shortest coupling length. Observe that the spectral response is narrower, further from $V = 4.448$. It is useful to quantify how narrow the response is.

Results were generated also with $\delta = 5 \times 10^{-6}$. They were virtually identical to those presented.

3.4 RESONANT SPECTRAL LINEWIDTH

Suppose we have a grating arranged at resonance. Further, suppose that this grating has a very narrow linewidth in its response, as frequency varies. It follows that M changes very little in the narrow neighbourhood of this resonance. Thus, in this region, set $M \equiv M_0$,

Figure 4(b)

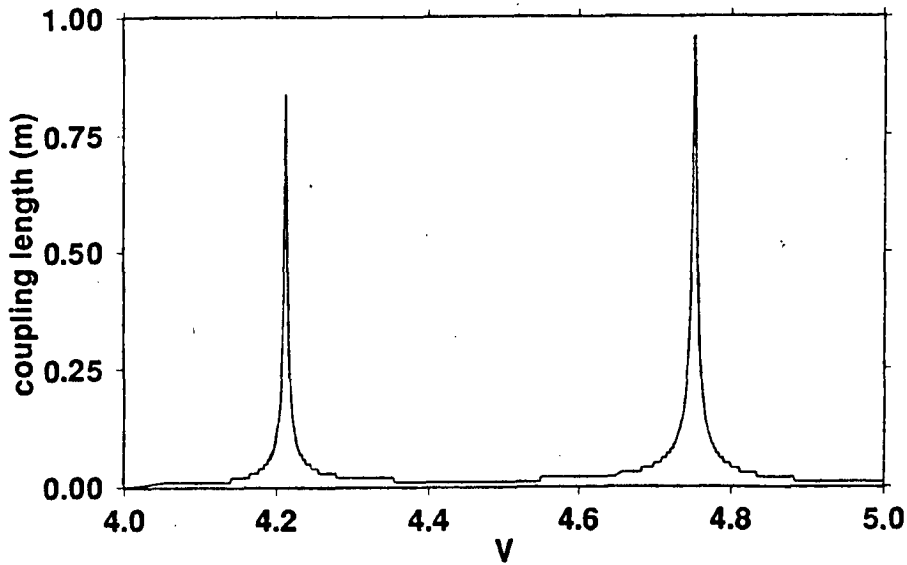


Figure 4(a)

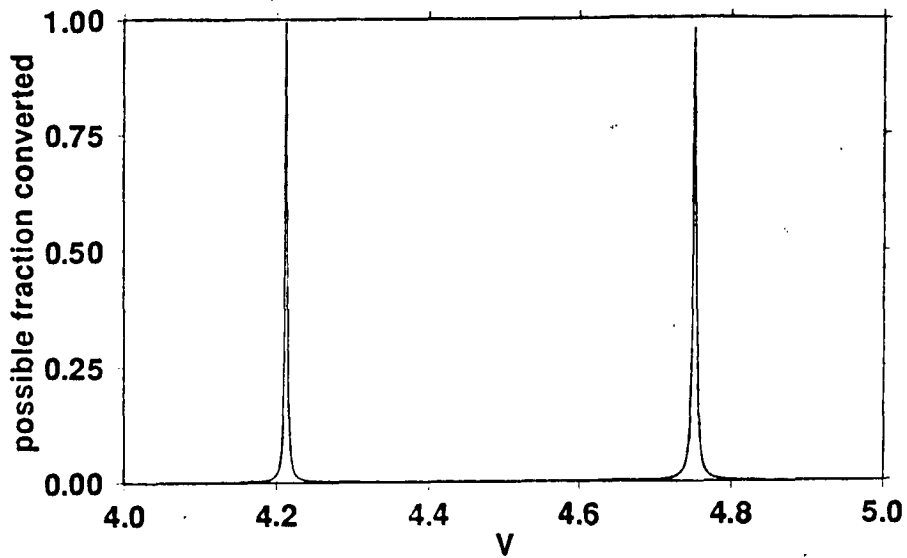


Figure 4: Frequency variation of properties of an $LP_{01} \leftrightarrow LP_{02}$ grating

An example of an $LP_{01} \leftrightarrow LP_{02}$ grating: $\Lambda = 203.7 \mu\text{m}$, with $\delta = 4 \times 10^{-6}$ and $\zeta = \frac{1}{2}$. The fibre has $\rho = 4.198 \mu\text{m}$ and a cutoff wavelength of $1.286 \mu\text{m}$. In (a) the efficiency, as given by Eq. (3.7), and in (b) the coupling length, as given by Eq. (3.4a), are shown as functions of normalized frequency. Notice the coupling length is minute except where the efficiency is large.

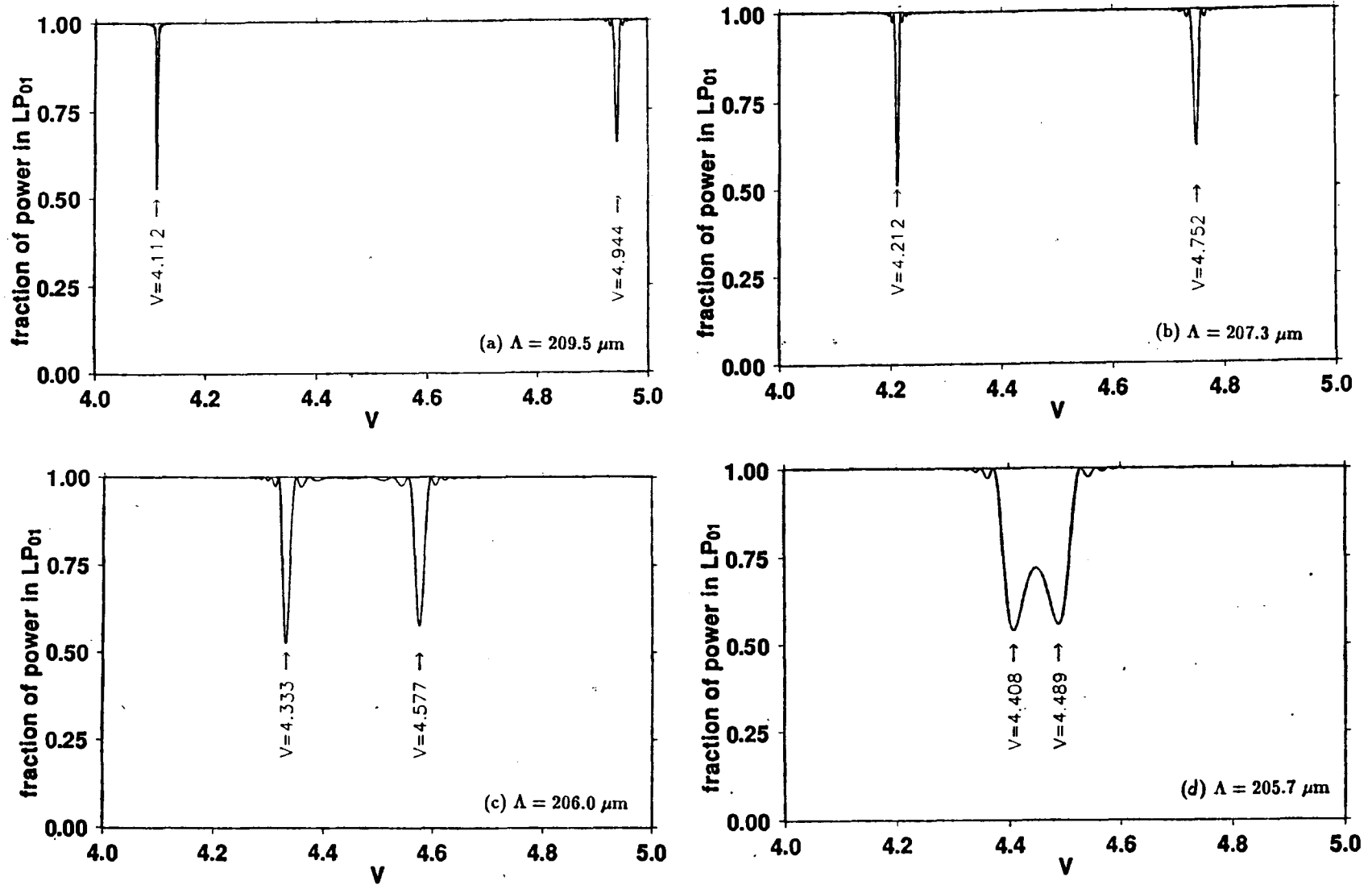


Figure 5: Frequency variation of output in LP₀₁ mode

The amount of power remaining in the LP₀₁ mode after passage through 2000 elements of an LP₀₁ ↔ LP₀₂ grating with $\delta = 4 \times 10^{-6}$ and $\zeta = \frac{1}{2}$. The fibre has $\rho = 4.198 \mu\text{m}$ and a cutoff wavelength of $1.286 \mu\text{m}$.

a constant. Further, if we put $s = V - V_r$, then we assume the Taylor expansion

$$\Gamma(s) \approx \Gamma(0) + s\Gamma'(0)$$

to be valid and note that resonance means $\Gamma(0) = 0$. Thus we get from (3.6) and (3.7) that

$$\mu^2(s) \approx M_0^2 + s^2\Gamma'^2(0) \quad (3.10a)$$

$$\eta \approx 1/(1 + s^2 \left(\frac{\Gamma'(0)}{M_0}\right)^2). \quad (3.10b)$$

This approximation can be improved if operation is in a region where M does change significantly. Assume that the total length of the grating is $\pi/2\mu(0) = \pi/2M_0$, which is the length for complete power transfer at resonance. The problem can be worked for the spectral linewidth at other lengths, but this is more complicated and not done here. The solution presented gives the features of interest.

With (3.10) and from (3.8), it follows that the power in the LP₀₁ mode is approximately

$$|a_1(z; s)|^2 = 1 - \frac{1}{1 + s^2\gamma^2} \sin^2\left(\frac{\pi}{2}\sqrt{1 + s^2\gamma^2}\right), \quad (3.11)$$

after defining

$$\gamma = |\Gamma'(0)/M_0|.$$

To find the linewidth, note the numerically determined fact that, with the expression (3.11), the power is at a half when $s\gamma = 0.7988$. Thus, the variation in V to give the FWHM of the resonance is defined by

$$V - V_r = s = 2 \times 0.7988 \left| \frac{M_0}{\Gamma'(0)} \right|.$$

The value of M_0 comes from (3.4a), namely

$$M_0 = \frac{\delta}{\sqrt{2\Delta}} \frac{\sin(\pi\zeta)}{\pi} C_{12}(V_r).$$

The value of $\Gamma'(0)$ is found as follows. It is known [1: ch14] that

$$\frac{dW_j}{dV} = \frac{W_j}{V} \left(1 + \frac{U_j^2}{\chi_j^2}\right),$$

so that, to dominant order, from (3.3) the expression

$$\Gamma' = \frac{1}{2}(\tilde{\beta}'_2 - \tilde{\beta}'_1) = \frac{\sqrt{2}\sqrt{\Delta}}{2V^2} \left(W_2^2 \left(1 + \frac{2U_2^2}{\chi_2^2}\right) - W_1^2 \left(1 + \frac{2U_1^2}{\chi_1^2}\right) \right)$$

is obtained. To evaluate $\Gamma'(0)$, specifically take the values of W_j and U_j corresponding to V_r .

Hence, the linewidth is given by

$$\bar{V} \equiv |V_{HM} - V_r| = 1.598\Delta \frac{\delta}{\Delta^2} \frac{\sin(\pi\zeta)}{\pi} D(V_r) \quad (3.12)$$

with V_{HM} being the value when intensity is half, and

$$D(V) = \left| \frac{V^2 C_{12}(V)}{W_2^2(1 + \frac{2U_2^2}{x_2^2}) - W_1^2(1 + \frac{2U_1^2}{x_1^2})} \right|.$$

It follows that \bar{V} is small, because Δ is very small, except when $D(V)$ is big. The form of $D(V)$ is seen in Fig. 6. For $V > 4.8$, it is clear that $D \sim 1$. The resonance in $D(V)$ occurs where the group velocities of the LP_{01} and LP_{02} modes are equal. Within the scalar approximation, this occurs at $V = 4.448$. Here, the linear Taylor approximation, combined with using the scalar values for the propagation constants, is inadequate, and the determination of the linewidth is more difficult. However, the domain needing this correction is small, and the problem will not be examined here.

Instead of V , we can fix a linewidth in terms of wavelength or frequency. If the higher mode cut-off is given by $\lambda_{co}, \omega_{co}$, then the linewidth is given from

$$\begin{aligned} |\lambda_{HM} - \lambda_r| &\approx \lambda_r \frac{\bar{V}}{V_r} = \lambda_{co} 2.405 \frac{\bar{V}}{V_r^2}; \\ \bar{\nu}_r \equiv |\omega_{HM} - \omega_r| &= \omega_r \frac{\bar{V}}{V_r} = \frac{\omega_{co}}{2.405} \bar{V}. \end{aligned} \quad (3.13)$$

The former is valid providing the value of \bar{V} is small; the latter defines $\bar{\nu}_r$ which will be used below.

3.5 ANISOTROPY

The spectral response curves generated above do not agree in every detail with the experimental results. For example, the response peaks at lower frequencies are predicted to be narrower and the peak values to decrease as the frequency decreases. However, this is not observed.

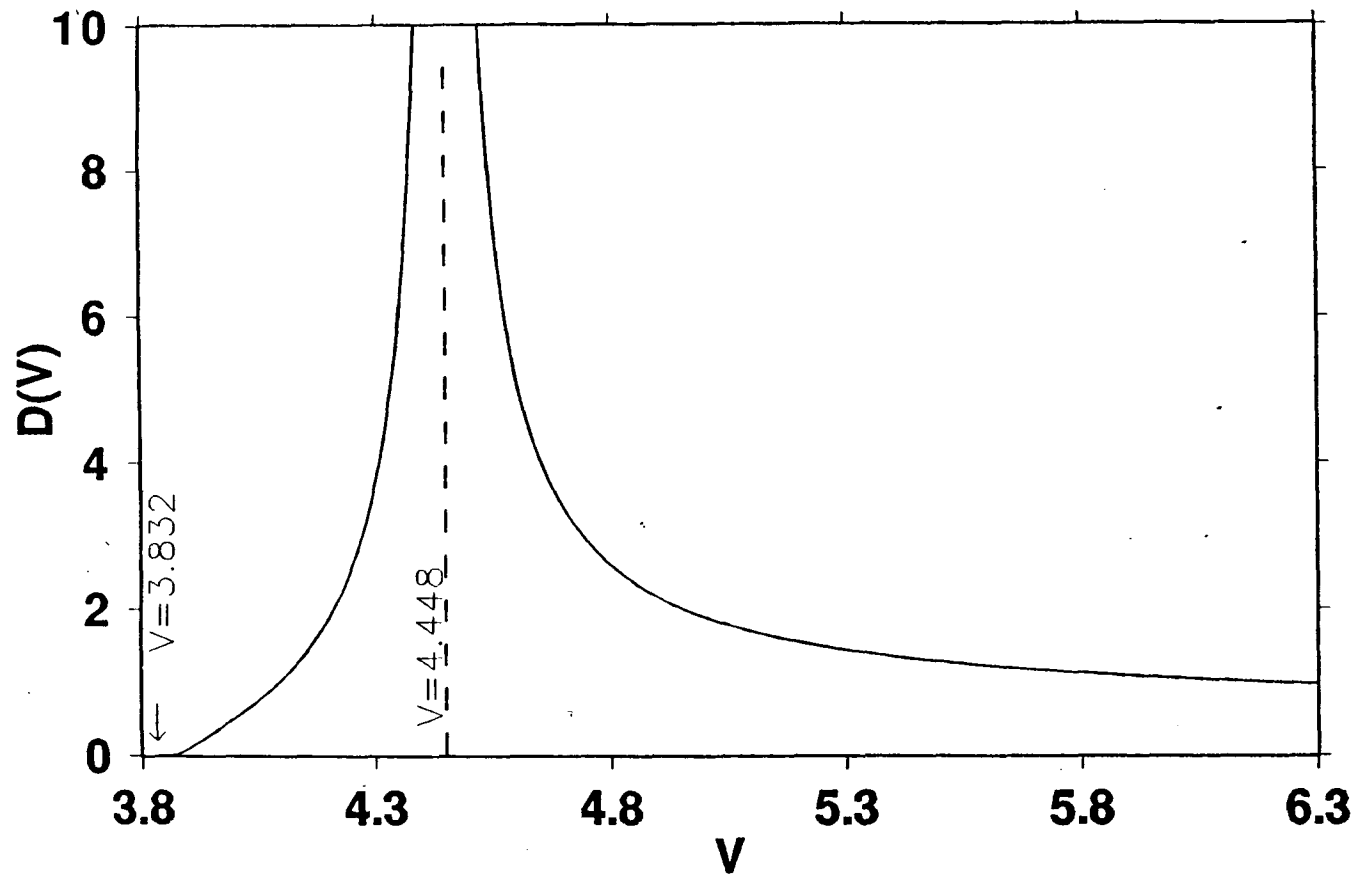


Figure 6: Frequency variation of linewidth parameter

For the $LP_{01} \leftrightarrow LP_{02}$ grating, the linewidth parameter, given below Eq. (3.12), is shown as a function of normalized frequency.

If the grating is anisotropic, then X- and Y-polarized modes will give slightly different responses. Suppose that the respective perturbations are given by $\delta_x = \delta$ and $\delta_y = (1 + \Xi)\delta$. The solution for P-polarized modes can be generated with the formulae above, with δ_P substituted for δ . In Fig. 7 is shown a pair of spectral response curves for an anisotropic grating, into which an X- or Y-polarized LP_{01} mode is launched. In Fig. 8 we see the response if light that consists of equal amounts of each polarization is used. In this latter example, the spectral linewidth at lower frequencies is “smeared out”, when compared with the corresponding result in an isotropic fibre (see Fig. 5). Nor does the peak value of the conversion decrease with V , as it did for the isotropic case.

3.6 BRAGG GRATING

In this case, the fibre supports one mode. It couples to the “same” mode, travelling in the opposite direction. Denote the mode propagating forward as mode 1, and that backward as mode 2. Their modal fields and related properties are identical, and $\langle\beta_1\rangle = -\langle\beta_2\rangle$. Thus, from (2.14) the resonance condition $\langle\beta_1\rangle = \frac{\pi}{\Lambda}$ defines a Bragg grating.

The negative sign on $\langle\beta_2\rangle$ means that $[B_{\alpha\gamma}] = \begin{pmatrix} 1 & i \\ i & 1 \end{pmatrix}$. With the definitions

$$\Gamma = \frac{\pi}{\Lambda} - \langle\beta_1\rangle; \quad (3.14)$$

$$M(V) = \frac{\delta}{\sqrt{2\Delta}} C_{12}(V) \frac{\sin(\pi\zeta)}{\pi}, \quad (3.15a)$$

it follows that

$$m_{121} = -m_{21-1}^* = -iM(V)e^{-i\pi\zeta}, \quad (3.15b)$$

from (2.20), (3.2) and the observations above about $B_{\alpha\gamma}$. Since the two modes have the same radial variation for the electric field, from (3.1)

$$C_{12}(V) = V\eta(V)$$

where $\eta = \frac{1}{\|F\|^2} \int_0^1 dr r F^2(r)$ is the usual modal efficiency. Thus, (2.15), (3.14) and (3.15) show that to describe a Bragg grating, which is both a first-order resonance and axisymmetric, the set of coupled modes equations is

$$\begin{pmatrix} a_1'(z) \\ a_2'(z) \end{pmatrix} = i \begin{pmatrix} 0 & -iM e^{-i\pi\zeta} e^{i2\Gamma z} \\ -iM e^{i\pi\zeta} e^{-i2\Gamma z} & 0 \end{pmatrix} \begin{pmatrix} a_1(z) \\ a_2(z) \end{pmatrix}.$$

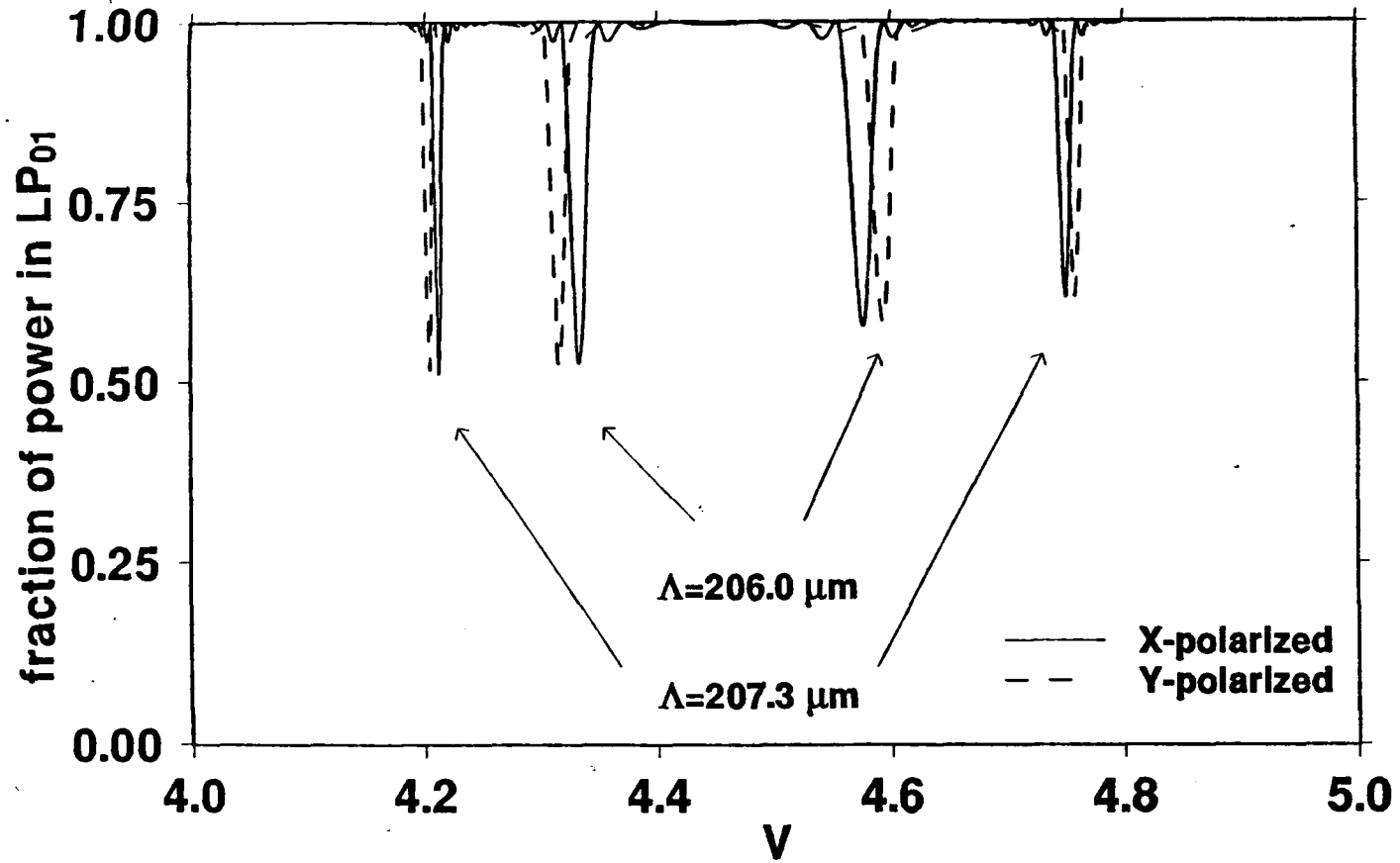


Figure 7: Frequency variation of output: input X- or Y-polarized

The amount of power remaining in the LP_{01} mode after passage through 2000 elements of an anisotropic $LP_{01} \leftrightarrow LP_{02}$ grating with $\Xi = 0.001$, $\delta = 4 \times 10^{-6}$ and $\zeta = \frac{1}{2}$. The fibre has $\rho = 4.198 \mu\text{m}$ and a cutoff wavelength of $1.286 \mu\text{m}$. Input power is polarized along the optical axes, which coincide with the Cartesian axes.

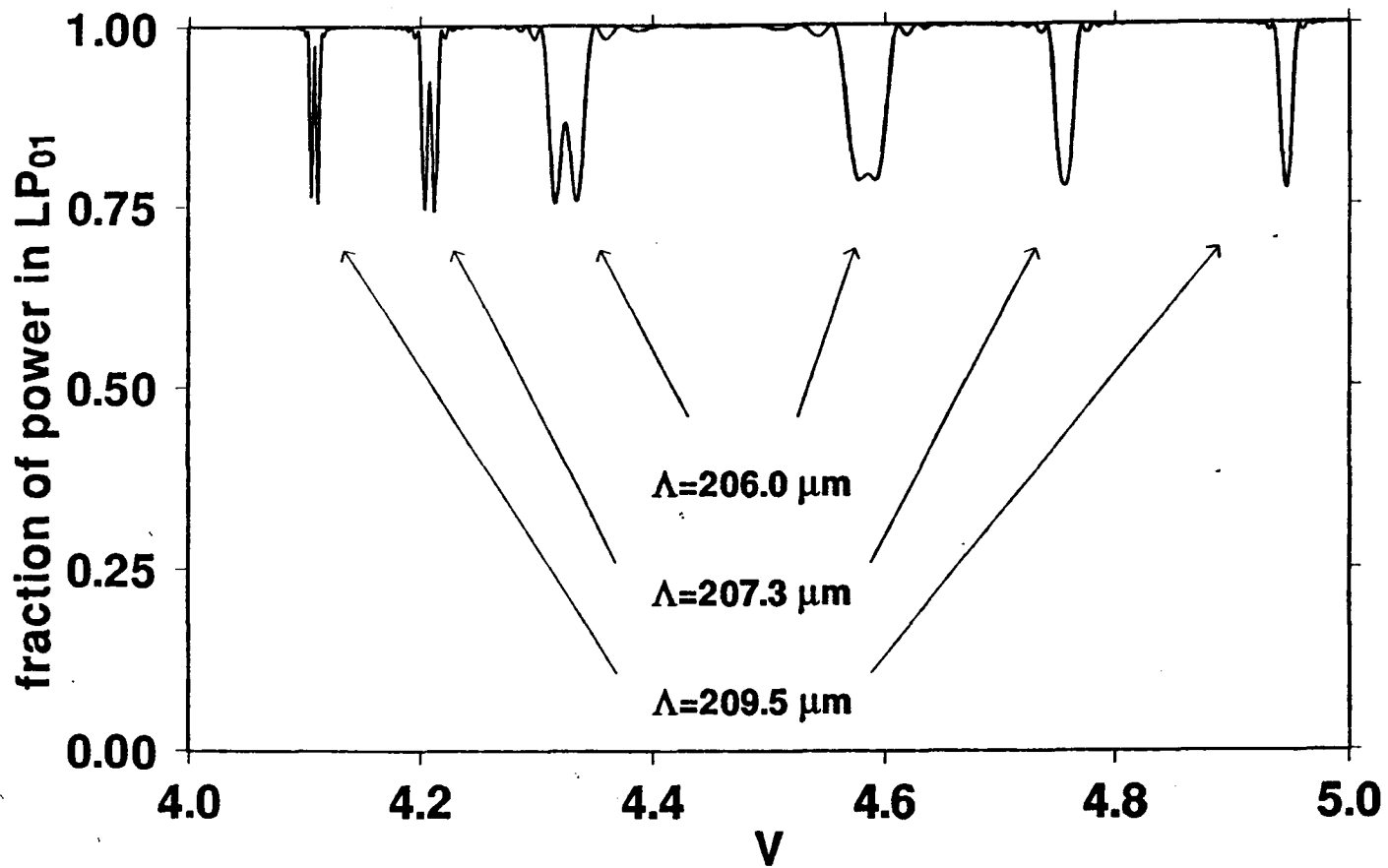


Figure 8: Frequency variation of output: input 50-50 polarized

The amount of power remaining in the LP₀₁ mode after passage through 2000 elements of an anisotropic LP₀₁ ↔ LP₀₂ grating with $\Xi = 0.001$, $\delta = 4 \times 10^{-6}$ and $\zeta = \frac{1}{2}$. The fibre has $\rho = 4.198 \mu\text{m}$ and a cutoff wavelength of $1.286 \mu\text{m}$. Input power is polarized at 45° to the optical (Cartesian) axes.

For the boundary conditions, a little thought is necessary. At $z = 0$, entering the grating, there is unit amplitude in mode 1, i.e. $a_1(0) = 1$, and, at the other end $z = N\Lambda$, there is no power entering the grating in mode 2, i.e. $a_2(N\Lambda) = 0$. Given these, the above system of equations has the easy solution (see Appendix A, seen previously [6]:

$$a_1(z) = e^{i\Gamma z} (\cosh(\mu z) - A \sinh(\mu z)) \quad (3.16a)$$

$$a_2(z) = -e^{i\pi\zeta} e^{-i\Gamma z} \left(\frac{i\Gamma - A\mu}{M} \cosh(\mu z) + \frac{\mu - iA\Gamma}{M} \sinh(\mu z) \right), \quad (3.16b)$$

where

$$A = \frac{\mu \tanh(\mu N\Lambda) + i\Gamma}{\mu + i\Gamma \tanh(\mu N\Lambda)}$$

$$\mu^2 = M^2 - \Gamma^2. \quad (3.17)$$

Recall that interest is primarily with behaviour around resonance, i.e. when $\Gamma \approx 0$. Under this condition μ is real. Obviously, as $|\Gamma|$ increases, then eventually μ becomes imaginary, the hyperbolic functions become trigonometric functions and the behaviour of the solution changes.

Recovering the expression for the reflected power leaving the grating gives

$$|a_2(0)|^2 = \frac{1}{M^2} \frac{|\mu^2 \tanh(\mu N\Lambda) + i\mu\Gamma - i\Gamma\mu + \Gamma^2 \tanh(\mu N\Lambda)|^2}{\mu^2 + \Gamma^2 \tanh^2(\mu N\Lambda)}$$

$$= \frac{\sinh^2(\mu N\Lambda)}{\cosh^2(\mu N\Lambda) - \frac{\Gamma^2}{M^2}}. \quad (3.18)$$

This is the efficiency of conversion, since unit power was launched as $a_1(0)$. As expected, the maximum value occurs when $\Gamma = 0$, where

$$|a_2(0)|^2 = \tanh^2(|M|N\Lambda) < 1.$$

Thus, as the number of elements in the grating increases, the efficiency of the Bragg reflection grating increases. Obviously increasing the value of $|M|$, i.e. the strength of coupling, given at (3.15a), also improves efficiency. To achieve 90% efficiency at resonance, it is found [7: table4, p216] that the need is

$$1.82 < |M|N\Lambda \approx 2\delta\eta(V_r)N \sin(\pi\zeta),$$

using (3.15a) and approximating $\Lambda = \frac{\pi\sqrt{2\Delta}}{V_r}$ for resonance. The resonant frequency is made explicit as the argument of η . For $\delta \sim 10^{-5}$, this means $N \sim 10^5$. For only 50% efficiency, the need is

$$0.88 < 2\delta\eta(V_r)N \sin(\pi\zeta).$$

4.0 EXAMPLE: $LP_{01} \leftrightarrow LP_{11}$ GRATING

4.1 CONSTRUCTION AND GEOMETRY

Consider as an example a grating constructed to convert power in the fundamental (LP_{01}) mode into power in first higher-order (LP_{11}) mode [8]. In this case, the grating is not axisymmetric, but rather is as shown in Fig. 9. Hence, the modes of the grating are not circularly symmetric, the modes of the unperturbed fibre are inadequate to describe the modes of the grating, and the analysis developed above is necessary. Before venturing further with the analysis, it is again important to remember that all lengths are scaled with the fibre's radius.

In the construction process, the angle of the blaze Θ is prescribed, as is the period of the grating Λ , and the width of the exposed region σ . Also, of course, it is known exactly the number of elements N written in the fibre. Thus, other quantities follow.

It is trivial that the total length L of the grating is

$$L = N\Lambda.$$

Other lengths follow equally easily. The axial lengths of the grating element (perturbed region) and the unperturbed region, respectively, are

$$\ell_1 = \sigma / \sin \Theta \quad \text{and} \quad \ell_0 = \Lambda - \sigma / \sin \Theta.$$

The length over which the interface operates is

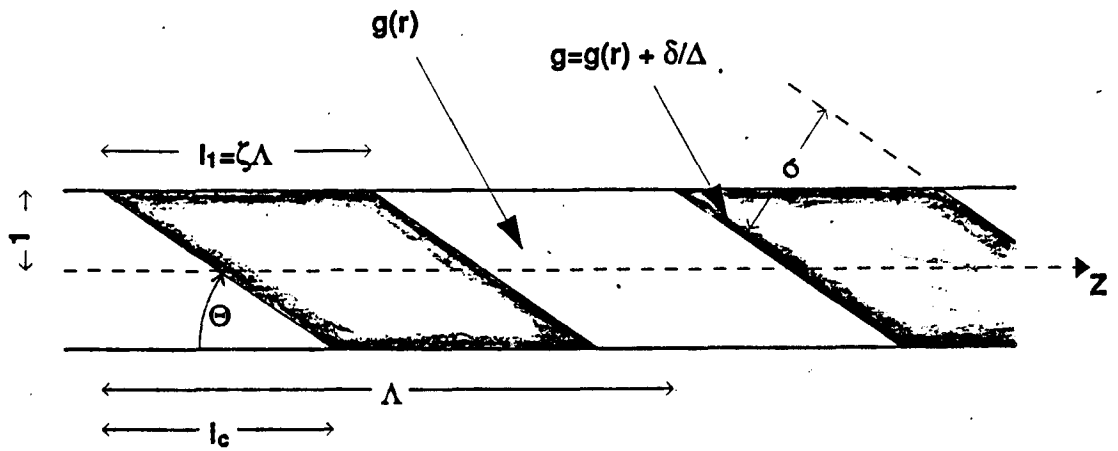
$$\ell_c = 2 / \tan \Theta.$$

Thus, the fraction of axial length exposed and half the fraction of axial length devoted to the interfaces are, respectively,

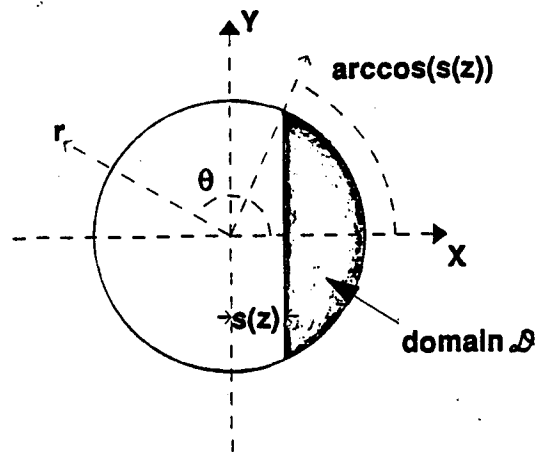
$$\zeta = \frac{\ell_1}{\Lambda} = \frac{\sigma}{\Lambda \sin \Theta} \quad \text{and} \quad \xi = \frac{\ell_c}{\Lambda} = \frac{2}{\Lambda \tan \Theta}. \quad (4.1)$$

Of course, for this grating to be meaningful, the constraint is that

$$\ell_0 \geq \ell_c \leq \ell_1 \quad \text{or} \quad \Lambda \sin \Theta - \sigma \geq 2 \cos \Theta \leq \sigma.$$



(a) fibre seen from the side



(b) fibre seen in cross-section

Figure 9: Structure of the $LP_{01} \leftrightarrow LP_{11}$ modal conversion grating

The shaded regions represent those of perturbed refractive index, characterized by $\Delta + \delta$; the unperturbed index is measured by Δ .

It is useful to explicitly write the equations that define the interfaces where the grating's refractive index changes. These give

$$s(z) = \begin{cases} 1 - 2z/\ell_c & , \text{ if } z \in (0, \ell_c) \\ -1 & , \text{ if } z \in (\ell_c, \ell_1) \\ -1 + 2(z - \ell_1)/\ell_c & , \text{ if } z \in (\ell_1, \ell_1 + \ell_c) \\ 1 & , \text{ if } z \in (\ell_1 + \ell_c, \Lambda) \end{cases} \quad (4.2)$$

so that the interface is given by the function $s(z)$ over one period $(0, \Lambda)$, and this is easily made into a periodic function.

Finally, the size of the perturbation to the refractive index, used to define the grating, is known. The perturbation is anisotropic. The J-polarized light senses the index to change from $n_0^2(1 + 2\Delta g(r))$ to $n_0^2(1 + 2\Delta g(r) + 2\delta_j)$. For convenience define

$$\delta_x = \delta \quad \text{and} \quad \delta_y = \delta(1 + \Xi).$$

Since the grating is very weak, it follows that $\frac{\delta}{\Delta} \ll 1$. This condition is the requirement to allow determination of modal properties using perturbation analysis of an axisymmetric waveguide.

4.2 PRELIMINARY SCALAR OBSERVATIONS

As with the $LP_{01} \leftrightarrow LP_{02}$ grating, a scaled scalar resonant period can be evaluated. Analogously to (3.9), this is prescribed by

$$\Lambda\sqrt{\Delta} \approx 2\sqrt{2} \pi \frac{V}{W_1^2 - W_2^2}.$$

This is shown, as a function of frequency, in Fig. 10.

However, as with the previous problem, the scalar theory is unable to fully describe the output of the grating. In particular, experimental observations [8] show four distinct peaks of spectral response, not one. Hence, the vector nature of the modes within the $LP_{01} \leftrightarrow LP_{11}$ grating must be considered.

4.3 MODES OF CIRCULAR FIBRE

Start by defining

$$V^2 = k^2 \rho^2 n_0^2 2\Delta.$$

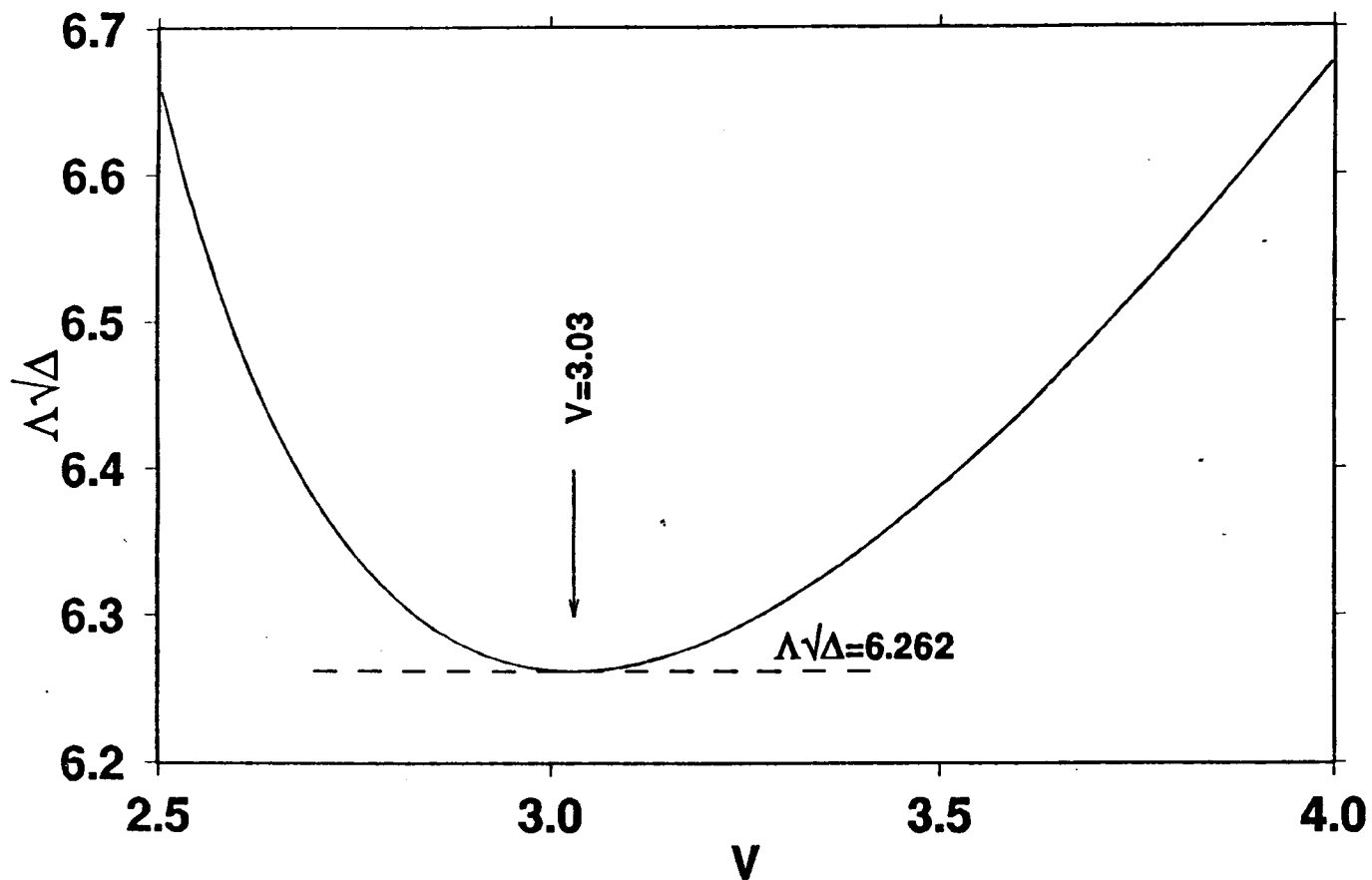


Figure 10: Frequency variation of scaled scalar period

For the $LP_{01} \leftrightarrow LP_{11}$ grating, the scaled scalar period, as given in §4.2, for complete coupling between modes is shown as a function of normalized frequency.

In this problem, we are concerned with operating at values of V such that 6 modes propagate in the fibre. On the unperturbed fibre, these are the two polarization states of the fundamental mode, which are the LP_{01} modes, and the odd and even forms of the HE_{11} mode, the TE_{01} mode, and the TM_{01} mode, which are all LP_{11} modes. Thus, the vector modes on the unperturbed fibre are indexed by the convention

$$\begin{aligned}\bar{\mathbf{E}}_1 &= F_0(r) \hat{\mathbf{x}} \quad ; \quad \bar{\mathbf{E}}_2 = F_0(r) \hat{\mathbf{y}} \\ \bar{\mathbf{E}}_3 &= F_1(r)(\cos \theta \hat{\mathbf{x}} - \sin \theta \hat{\mathbf{y}}) \quad ; \quad \bar{\mathbf{E}}_4 = F_1(r)(\cos \theta \hat{\mathbf{x}} + \sin \theta \hat{\mathbf{y}}) \\ \bar{\mathbf{E}}_5 &= F_1(r)(\sin \theta \hat{\mathbf{x}} + \cos \theta \hat{\mathbf{y}}) \quad ; \quad \bar{\mathbf{E}}_6 = F_1(r)(-\sin \theta \hat{\mathbf{x}} + \cos \theta \hat{\mathbf{y}}).\end{aligned}\tag{4.3}$$

Notice that there is a change in the customary convention, by reversing the sign of the TE_{01} mode. When the local modes in the grating are examined, they, too, are enumerated by this system so that the index j will be on the mode which corresponds to $\bar{\mathbf{E}}_j$ on the unperturbed fibre. The corresponding index is meaningful on the local propagation constants $\beta_j(z)$, which include the polarization corrections.

With $\tilde{\beta}_f$ and $\tilde{\beta}_h$ the scalar propagation constants (as determined by the weak guidance theory) and $F_0(r)$ and $F_1(r)$ the modal fields' radial dependences of the LP_{01} and LP_{11} modes, respectively, on the unperturbed portions of the fibre, the modal propagation constants, corrected for polarization effects, are

$$\begin{aligned}\bar{\beta}_1^2 &= \bar{\beta}_2^2 = \tilde{\beta}_f^2 - \Delta I_0 \\ \bar{\beta}_3^2 &= \bar{\beta}_4^2 = \tilde{\beta}_h^2 - \Delta(I_1 - I_2) \\ \bar{\beta}_5^2 &= \tilde{\beta}_h^2 - \Delta 2(I_1 + I_2) \\ \bar{\beta}_6^2 &= \tilde{\beta}_h^2,\end{aligned}$$

where

$$\begin{aligned}I_0 &= \frac{1}{\|F_0\|^2} \int_0^\infty dr r F_0(r) F_0'(r) g'(r); \\ I_1 &= \frac{1}{\|F_1\|^2} \int_0^\infty dr r F_1(r) F_1'(r) g'(r); \\ I_2 &= \frac{1}{\|F_1\|^2} \int_0^\infty dr F_1^2(r) g'(r).\end{aligned}$$

These are known, at least numerically. Define the scalar modal efficiencies as η_f, η_h for the LP_{01} and LP_{11} families of modes, respectively, as the integrals

$$\eta_h^f = \frac{\int_0^\infty dr r F_0^2(r)}{\|F_0\|_1^2}.$$

For a circular step fibre, the actual expressions for all these quantities can be extracted from standard references [e.g. 1: ch14]. Namely, with the definitions,

$$\chi_j = -\frac{F_j'(1)}{F_j(1)},$$

for $j = 0, 1$, they follow as

$$F_0(r) = \begin{cases} \frac{J_0(U_0 r)}{J_0(U_0)} & , r < 1 \\ \frac{K_0(W_0 r)}{K_0(W_0)} & , 1 < r \end{cases} ; \quad F_1(r) = \begin{cases} \frac{J_1(U_1 r)}{J_1(U_1)} & , r < 1 \\ \frac{K_1(W_1 r)}{K_1(W_1)} & , 1 < r \end{cases}$$

$$\chi_0 = U_0 \frac{J_1(U_0)}{J_0(U_0)} ; \quad \chi_1 = 1 - U_1 \frac{J_0(U_1)}{J_1(U_1)}$$

$$\eta_f = \frac{W_0^2(U_0^2 + \chi_0^2)}{V^2 \chi_0^2} ; \quad \eta_h = \frac{W_1^2(U_1^2 + \chi_1^2 - 1)}{V^2(\chi_1^2 - 1)}$$

$$\|F_0\|^2 = \frac{V^2 \chi_0^2}{2U_0^2 W_0^2} ; \quad \|F_1\|^2 = \frac{V^2(\chi_1^2 - 1)}{2U_1^2 W_1^2}$$

$$I_0 = \chi_0 / \|F_0\|^2 ; \quad I_1 = \chi_1 / \|F_1\|^2 ; \quad I_2 = -1 / \|F_1\|^2.$$

4.4 PERTURBATION AND LOCAL MODES

Using perturbation analysis, the properties of the local modes were found very easily from those of the modes on the unperturbed fibre.

In describing the coupling caused by the grating, we are not interested in the local propagation constants, but their averages over the period of the grating. These are

$$\langle \beta_j \rangle^2 \approx \langle \beta_j^2 \rangle = \frac{1}{\Lambda} \int_0^\Lambda dz \beta_j^2(z)$$

$$= (1 - \zeta - \xi) \beta_j^2(s=1) + (\zeta - \xi) \beta_j^2(s=-1) + \xi \int_{-1}^1 ds \beta_j^2(s)$$

by changing the variable of integration from z to s using (4.2). Previously, it was shown for the fundamental modes

$$\langle \beta_1 \rangle^2 = \bar{\beta}_1^2 + \frac{\delta}{\Delta} \zeta V^2 \eta_f = \tilde{\beta}_f^2 + \frac{\delta}{\Delta} \zeta V^2 \eta_f - \Delta I_0$$

$$\langle \beta_2 \rangle^2 = \bar{\beta}_2^2 + \frac{\delta}{\Delta} (1 + \Xi) \zeta V^2 \eta_f \tag{4.4}$$

Define the constants

$$\alpha_x = \frac{\pi \Delta^2 (3 - \chi_1)}{2\delta V^2 \|F_1\|^2} ; \quad \alpha_y = \frac{\pi \Delta^2 (1 + \chi_1)}{2\delta V^2 \|F_1\|^2}. \tag{4.5}$$

It is worth noting that $\text{sgn}(\alpha_y) = 1$ and that $\alpha_y > \alpha_x$ (both known numerically). Define also the functions

$$\begin{aligned} Q_+(z) &= \frac{1}{2\|F_1\|^2} \int_{\mathcal{D}(s(z))} dS F_1^2(r) \\ &= \begin{cases} \frac{1}{\|F_1\|^2} \int_s^1 dr r F_1^2(r) \arccos(s/r) & , \text{ if } s > 0 \\ \pi\eta_h - Q_+(-s) & , \text{ if } s < 0 \end{cases} \end{aligned} \quad (4.6a)$$

$$\begin{aligned} Q_-(z) &= \frac{1}{2\|F_1\|^2} \int_{\mathcal{D}(s(z))} dS F_1^2(r) \cos 2\theta \\ &= \begin{cases} \frac{s}{\|F_1\|^2} \int_s^1 dr F_1^2(r) \sqrt{1 - \frac{s^2}{r^2}} & , \text{ if } s > 0 \\ -Q_-(-s) & , \text{ if } s < 0 \end{cases} \end{aligned} \quad (4.6b)$$

after inserting the specific description of $\mathcal{D}(s(z))$. These are combined to give

$$Q_x(z) = (1 + \frac{\Xi}{2})Q_-(z) \mp \frac{\Xi}{2}Q_+(z). \quad (4.7)$$

The complete set of average propagation constants for the higher-order modes follows:

$$\langle \beta_3 \rangle^2 = \tilde{\beta}_h^2 + \frac{\delta}{\Delta} (1 + \frac{\Xi}{2}) \zeta V^2 \eta_h - \Delta \frac{(\chi_1 + 1)}{\|F_1\|^2} - \Delta \frac{\delta}{\pi \Delta^2} \text{sgn}(\alpha_x) V^2 L_x \quad (4.8a)$$

$$\langle \beta_4 \rangle^2 = \tilde{\beta}_h^2 + \frac{\delta}{\Delta} (1 + \frac{\Xi}{2}) \zeta V^2 \eta_h - \Delta \frac{2(\chi_1 - 1)}{\|F_1\|^2} + \Delta \frac{\delta}{\pi \Delta^2} \text{sgn}(\alpha_x) V^2 L_x \quad (4.8b)$$

$$\langle \beta_5 \rangle^2 = \tilde{\beta}_h^2 + \frac{\delta}{\Delta} (1 + \frac{\Xi}{2}) \zeta V^2 \eta_h - \Delta \frac{(\chi_1 + 1)}{\|F_1\|^2} - \Delta \frac{\delta}{\pi \Delta^2} V^2 L_y \quad (4.8c)$$

$$\langle \beta_6 \rangle^2 = \tilde{\beta}_h^2 + \frac{\delta}{\Delta} (1 + \frac{\Xi}{2}) \zeta V^2 \eta_h + 0 + \Delta \frac{\delta}{\pi \Delta^2} V^2 L_y. \quad (4.8d)$$

with the definition, for $j = x, y$,

$$\begin{aligned} L_j &= \frac{1}{\Lambda} \int_0^\Lambda dz (|\alpha_j^2 + Q_j^2(z)|^{\frac{1}{2}} - |\alpha_j|) \\ &= (\zeta - \xi) (|\alpha_j^2 + Q_j^2(-1)|^{\frac{1}{2}} - |\alpha_j|) + \xi \int_{-1}^1 ds (|\alpha_j^2 + Q_j^2(s)|^{\frac{1}{2}} - |\alpha_j|) \\ &= (\zeta - \xi) (|\alpha_j^2 + \frac{\pi^2 \Xi^2}{4} \eta_h^2|^{\frac{1}{2}} - |\alpha_j|) \\ &\quad + \xi \left(-2|\alpha_j| + \int_0^1 ds (|\alpha_j^2 + Q_j^2(s)|^{\frac{1}{2}} + |\alpha_j^2 + (Q_j(s) \pm \frac{\pi \Xi}{2} \eta_h)^2|^{\frac{1}{2}}) \right), \end{aligned}$$

where the upper and lower signs correspond to x and y , respectively. The important finding is that there are four distinct values of $\langle \beta_j \rangle$, instead of the three seen on an unperturbed waveguide. Considering these, we observe $\text{sgn}(\alpha_x)$ matches $\text{sgn}(3.794 - V)$ (known numerically). Also, it requires some ingenuity, but it is possible to show that $L_x > L_y$ everywhere.

This inequality shows how the degeneracy between the even and odd HE₁₁ modes is broken, i.e. we see that $\langle \beta_5 \rangle \neq \langle \beta_3 \rangle$, even in the isotropic case when $\Xi = 0$.

Define the two angles $\phi_x(s)$ and $\phi_y(s)$ such that

$$\phi_j(s) = -\frac{1}{2} \arctan(Q_j/\alpha_j). \quad (4.9)$$

The local vector direction of the electric field can be easily written, as is given in Appendix B. Observe from (4.6), (4.7) and (4.9) that, while $\phi_j(s = 1) = 0$, i.e. the angles vanish where there is no perturbation, in the uniformly perturbed region

$$\phi_{\mathbf{y}}(s = -1) = \pm \frac{1}{2} \arctan\left(\frac{\Xi \pi \eta h}{2\alpha_{\mathbf{y}}}\right).$$

This only vanishes when the anisotropy vanishes. It is useful at this juncture to list some expressions containing ϕ_x and ϕ_y .

$$\sin \phi_j(s) = \frac{-\text{sgn}(\alpha_j)Q_j(s)}{\sqrt{2} |\alpha_j^2 + Q_j^2(s)|^{\frac{1}{4}} (|\alpha_j^2 + Q_j^2(s)|^{\frac{1}{2}} + |\alpha_j|)^{\frac{1}{2}}}. \quad (4.10a)$$

$$\cos \phi_j(s) = \frac{(|\alpha_j^2 + Q_j^2(s)|^{\frac{1}{2}} + |\alpha_j|)^{\frac{1}{2}}}{\sqrt{2} |\alpha_j^2 + Q_j^2(s)|^{\frac{1}{4}}}. \quad (4.10b)$$

$$\sin 2\phi_j(s) = \frac{-\text{sgn}(\alpha_j)Q_j(s)}{|\alpha_j^2 + Q_j^2(s)|^{\frac{1}{2}}}. \quad (4.10c)$$

$$\cos 2\phi_j(s) = \frac{|\alpha_j|}{|\alpha_j^2 + Q_j^2(s)|^{\frac{1}{2}}}. \quad (4.10d)$$

Further, using (4.9), we can find the derivative of $\phi_j(s)$:

$$\dot{\phi}_j(s) = \frac{-\alpha_j \dot{Q}_j(s)}{2|\alpha_j^2 + Q_j^2(s)|} \quad (4.11)$$

$$\dot{Q}_{\mathbf{y}}(s) = (1 + \frac{\Xi}{2})\dot{Q}_-(s) \mp \frac{\Xi}{2}\dot{Q}_+(s)$$

Examination of (4.6) and (4.7) shows that $\dot{Q}_j(s)$ is symmetric. To complete these results, we write, for $s > 0$,

$$\begin{aligned} \dot{Q}_+(s) &= \frac{1}{\|F_1\|^2} \int_s^1 dr \frac{-1}{\sqrt{1 - \frac{s^2}{r^2}}} F_1^2(r) \\ \dot{Q}_-(s) &= \frac{1}{\|F_1\|^2} \int_s^1 dr \frac{1 - 2\frac{s^2}{r^2}}{\sqrt{1 - \frac{s^2}{r^2}}} F_1^2(r). \end{aligned} \quad (4.12)$$

These definitions contain integrable singularities in the integrands. For numerical purposes it is preferable to reformulate them as

$$\begin{aligned}
\dot{Q}_+(s) &= \frac{-2}{\|F_1\|^2} \sqrt{\frac{1-s}{1+s}} + \frac{2}{\|F_1\|^2} \int_s^1 dr \sqrt{r-s} \frac{d}{dr} \left(\frac{rF_1^2(r)}{\sqrt{s+r}} \right) \\
&= \frac{-2}{\|F_1\|^2} \sqrt{\frac{1-s}{1+s}} + \frac{2}{\|F_1\|^2} \int_s^1 dr \sqrt{\frac{r-s}{r+s}} \frac{(s+\frac{r}{2})F_1^2(r) + 2r(r+s)F_1(r)F_1'(r)}{s+r} \\
\dot{Q}_-(s) &= \frac{2(1-2s^2)}{\|F_1\|^2} \sqrt{\frac{1-s}{1+s}} - \frac{2}{\|F_1\|^2} \int_s^1 dr \sqrt{r-s} \frac{d}{dr} \left(F_1^2(r) \frac{r^2-2s^2}{r\sqrt{s+r}} \right) \\
&= \frac{2(1-2s^2)}{\|F_1\|^2} \sqrt{\frac{1-s}{1+s}} \\
&\quad - \frac{2}{\|F_1\|^2} \int_s^1 dr \sqrt{\frac{r-s}{r+s}} \frac{(r^3 + r^2s + rs^2 + 2s^3)F_1^2 + 2r(r+s)(r^2-2s^2)F_1F_1'}{r^2(s+r)}.
\end{aligned}$$

From (4.12), there is one further result that will prove useful: $\dot{Q}_j(s = \pm 1) = 0$.

4.5 COUPLING MATRICES

Now that the modal properties of the grating are determined, we turn our attention to the matrices which couple the modes together. Evaluating the symmetric matrix G , defined at (2.9), is straightforward. Note from (4.3) that, for all α , $\|\bar{E}_\alpha\|^2 = 2\pi\|F_\gamma\|^2$, where γ is the appropriate value.

First, examine the coupling between the different polarization states of the fundamental mode, i.e. modes 1 and 2. By defining $g_1(s)$ as

$$\begin{aligned}
g_1(s) &= \frac{1}{2\pi\|F_0\|^2} \int_{\mathcal{D}(s(z))} dS F_0^2(r) \\
&= \frac{1}{\pi\|F_0\|^2} \int_s^1 dr r F_0^2(r) \arccos(s/r) \\
&= \frac{1}{2}(\eta_f + q_f(s)),
\end{aligned} \tag{4.13}$$

which also defines the antisymmetric function $q_f(s)$. A little thought quickly reveals that

$$G_{11}(s) = \frac{\delta}{\Delta} V^2 g_1(s) \quad ; \quad G_{22}(s) = (1 + \Xi) \frac{\delta}{\Delta} V^2 g_1(s).$$

A similar amount of thought shows that $G_{12} = 0$.

Now move to the coupling coefficients connecting the fundamental and higher-order modes. Examination of the cross-section of the perturbed fibre shows that domain $\mathcal{D}(s(z))$

is symmetric about the X-axis. Thus, when mixed with the P-polarized fundamental mode, a higher order mode only produces a non-zero element for G if the P-component of the higher order mode has a scalar field that has an angular variation that is symmetric about the X-axis. Hence, from examination of (4.3), it follows that $G_{15} = 0 = G_{16}$ and $G_{23} = 0 = G_{24}$. Thus, we see why the pairs of higher-order modes were denoted as the X-pair and the Y-pair — they couple only to the respective state of polarization of the fundamental mode. Further, defining $g_3(s)$ by

$$\begin{aligned} g_3(s) &= \frac{1}{2\pi \|F_0\| \|F_1\|} \int_{\mathcal{D}(s(z))} dS F_0(r) F_1(r) \cos \theta \\ &= \frac{1}{\pi} P(s), \end{aligned} \quad (4.14)$$

where

$$P(s) = \frac{1}{\|F_0\| \|F_1\|} \int_{|s|}^1 dr F_0(r) F_1(r) \sqrt{r^2 - s^2}, \quad (4.15)$$

which is a symmetric function that requires numerical evaluation ($F_1(r)$, $F_0(r)$ involve Bessel functions.), we get

$$G_{13}(s) = G_{14}(s) = \frac{\delta}{\Delta} V^2 g_3(s) \quad ; \quad G_{25}(s) = G_{26}(s) = (1 + \Xi) \frac{\delta}{\Delta} V^2 g_3(s).$$

In considering the coupling between the various forms of the higher order modes, i.e. modes 3, 4, 5, and 6, a little more thought shows that, by defining $g_2^{(j)}(s)$, for $j = x, y$, to be

$$g_2^{(X)}(s) = \frac{1}{\pi} \left((1 + \frac{\Xi}{2}) Q_+(s) \mp \frac{\Xi}{2} Q_-(s) \right) \quad (4.16)$$

it follows from (4.6) that

$$\begin{aligned} G_{33}(s) = G_{44}(s) &= \frac{\delta}{\Delta} V^2 \frac{1}{2\pi \|F_1\|^2} \int_{\mathcal{D}(s(z))} dS F_1^2(r) (\cos^2 \theta + (1 + \Xi) \sin^2 \theta) \\ &= \frac{\delta}{\Delta} V^2 g_2^{(X)} \\ G_{55}(s) = G_{66}(s) &= \frac{\delta}{\Delta} V^2 \frac{1}{2\pi \|F_1\|^2} \int_{\mathcal{D}(s(z))} dS F_1^2(r) (\sin^2 \theta + (1 + \Xi) \cos^2 \theta) \\ &= \frac{\delta}{\Delta} V^2 g_2^{(Y)}. \end{aligned}$$

Finally, we are concerned with the overlap integral between the various higher-order modes. Once again, we find the separation of the modes into the X-pair and Y-pair: $G_{35} = 0 = G_{36}$

and $G_{45} = 0 = G_{46}$. By defining $g_4^{(j)}(s)$,

$$g_4^{(j)}(s) = \frac{1}{\pi} Q_j(s), \quad (4.17)$$

where $Q_j(s)$ was defined at (4.6) and (4.7), it follows that

$$\begin{aligned} G_{34}(s) &= \frac{\delta}{\Delta} V^2 \frac{1}{2\pi \|F_1\|^2} \int_{\mathcal{D}(s(z))} dS F_1^2(r) (\cos^2 \theta - (1 + \Xi) \sin^2 \theta) \\ &= \frac{\delta}{\Delta} V^2 g_4^{(X)}(s) \\ G_{56}(s) &= \frac{\delta}{\Delta} V^2 \frac{1}{2\pi \|F_1\|^2} \int_{\mathcal{D}(s(z))} dS F_1^2(r) (-\sin^2 \theta + (1 + \Xi) \cos^2 \theta) \\ &= \frac{\delta}{\Delta} V^2 g_4^{(Y)}(s). \end{aligned}$$

Thus, it is now possible to write the matrix $G(s)$:

$$G(s) = \frac{\delta}{\Delta} V^2 \begin{pmatrix} g_1(s) & 0 & g_3(s) & g_3(s) & 0 & 0 \\ 0 & (1 + \Xi)g_1(s) & 0 & 0 & (1 + \Xi)g_3(s) & (1 + \Xi)g_3(s) \\ g_3(s) & 0 & g_2^{(X)}(s) & g_4^{(X)}(s) & 0 & 0 \\ g_3(s) & 0 & g_4^{(X)}(s) & g_2^{(X)}(s) & 0 & 0 \\ 0 & (1 + \Xi)g_3(s) & 0 & 0 & g_2^{(Y)}(s) & g_4^{(Y)}(s) \\ 0 & (1 + \Xi)g_3(s) & 0 & 0 & g_4^{(Y)}(s) & g_2^{(Y)}(s) \end{pmatrix}.$$

From (B.18) and since the normalization of the modes is invariant along the grating, it follows that the matrix D , defined at (2.3), is

$$D = \begin{pmatrix} 1 & 0 & 0 & 0 & 0 & 0 \\ 0 & 1 & 0 & 0 & 0 & 0 \\ 0 & 0 & \cos \phi_x & \sin \phi_x & 0 & 0 \\ 0 & 0 & -\sin \phi_x & \cos \phi_x & 0 & 0 \\ 0 & 0 & 0 & 0 & \cos \phi_y & \sin \phi_y \\ 0 & 0 & 0 & 0 & -\sin \phi_y & \cos \phi_y \end{pmatrix}.$$

This matrix (and consequently all its derivatives) also decouples the two groups of modes — $\{E_1, E_3, E_4\}$ and $\{E_2, E_5, E_6\}$. This leads, in the ensuing analysis, to treating the two groups of modes separately.

For derivatives of the matrix D , instead of variation with z , consider variation with s , and use the chain rule to relate them. By convention, while the dashes denote differentiation

with respect to z , dots will be used to show differentiation with respect to s . Thus, from (4.2), can be obtained the identity

$$f'(z) = \frac{-2}{\ell_c} \dot{f}(s)$$

where $f(z)$ is any function of z .

Now we simplify the derivatives of matrix D . Firstly, we find for the X-family

$$D'_x(z) = \frac{-2}{\ell_c} \dot{\phi}_x(s) \begin{pmatrix} 0 & 0 & 0 \\ 0 & -\sin \phi_x & \cos \phi_x \\ 0 & -\cos \phi_x & -\sin \phi_x \end{pmatrix}.$$

For the Y-family, simply replace x with y , and take the transpose. In either case,

$$D_\alpha(z) D_\alpha'^{\dagger}(z) = \frac{-2}{\ell_c} \dot{\phi}_\alpha(s) \begin{pmatrix} 0 & 0 & 0 \\ 0 & 0 & -1 \\ 0 & +1 & 0 \end{pmatrix}$$

with \dagger denoting matrix transpose. Continuing,

$$D_\alpha(z) D_\alpha''^{\dagger}(z) = \frac{4}{\ell_c^2} (\dot{\phi}_\alpha^2(s) \begin{pmatrix} 0 & 0 & 0 \\ 0 & -1 & 0 \\ 0 & 0 & -1 \end{pmatrix} + \ddot{\phi}_\alpha(s) \begin{pmatrix} 0 & 0 & 0 \\ 0 & 0 & -1 \\ 0 & +1 & 0 \end{pmatrix}).$$

Thus, all the coupling matrices are listed.

Examination of (2.9) shows a further useful matrix to be

$$D_\alpha G D_\alpha^\dagger = \frac{\delta}{\Delta} V^2 \begin{pmatrix} g_1 & g_3(\cos \phi_\alpha + \sin \phi_\alpha) & g_3(\cos \phi_\alpha - \sin \phi_\alpha) \\ g_3(\cos \phi_\alpha + \sin \phi_\alpha) & g_2 + g_4 \sin 2\phi_\alpha & g_4 \cos 2\phi_\alpha \\ g_3(\cos \phi_\alpha - \sin \phi_\alpha) & g_4 \cos 2\phi_\alpha & g_2 - g_4 \sin 2\phi_\alpha \end{pmatrix},$$

defined for either the X- or Y-family of modes.

4.6 FOURIER COEFFICIENTS

Recall resonant, mode-converting coupling occurs as described by (2.16). Note that the grating of interest is a 1st order resonance. We can now explicitly write down the matrices associated with this coupling. Of course, for simplicity, the coupling equations for the X-family and the Y-family will be dealt with separately, as they decouple. (This was shown above.) We will proceed in the case of the X-family. For the Y-family, replace subscripts 1, 3, 4, x and superscript X with 2, 5, 6, y , and Y , respectively, to get the analogous results to those obtained below.

The general expression for the Fourier components, given at (2.11), as it applies to the grating, is

$$m_{\alpha\gamma\epsilon} = \frac{i}{2\pi\epsilon}(e^{-i\epsilon 2\pi} - e^{-i\epsilon 2\pi(\zeta+\xi)})M_{\alpha\gamma}(s=1) + \frac{i}{2\pi\epsilon}(e^{-i\epsilon 2\pi\zeta} - e^{-i\epsilon 2\pi\xi})M_{\alpha\gamma}(s=-1) \\ + \xi e^{-i\epsilon\pi(\zeta+\xi)} \int_{-1}^1 ds M_{\alpha\gamma}(s) \cos \epsilon\pi(s\xi + \zeta), \quad (4.18)$$

where $s = 1$ indicates the value on the unperturbed fibre, $s = -1$ indicates the value on the portion of the grating perturbed uniformly over the cross-section, and the variable of integration has been changed from z to s using (4.2). Obviously, for $\epsilon = 0$, take the limit, and obtain

$$m_{\alpha\gamma 0} = (\zeta - \xi)M_{\alpha\gamma}(s=-1) + (1 - \zeta - \xi)M_{\alpha\gamma}(s=1) + \xi \int_{-1}^1 ds M_{\alpha\gamma}(s). \quad (4.19)$$

Now the Fourier coefficients are ready to be worked explicitly.

Finding them is easy, once the elements of $M(z)$ are written down explicitly. The matrix of interest for the right-hand side of (2.10) is

$$M_{11}(z) = \frac{1}{2} \left(\frac{\delta V^2}{\Delta} \frac{1}{\langle \beta_1 \rangle} g_1(s(z)) + \frac{\bar{\beta}_1^2 - \langle \beta_1 \rangle^2}{\langle \beta_1 \rangle} \right) \quad (4.20)$$

$$M_{13}(z) = M_{31}(z) = \frac{1}{2} \frac{\delta V^2}{\Delta} \frac{1}{\langle \beta_1 \rangle^{\frac{1}{2}} \langle \beta_3 \rangle^{\frac{1}{2}}} g_3(s(z)) (\cos \phi_x + \sin \phi_x) \quad (4.21a)$$

$$M_{14}(z) = M_{41}(z) = \frac{1}{2} \frac{\delta V^2}{\Delta} \frac{1}{\langle \beta_1 \rangle^{\frac{1}{2}} \langle \beta_4 \rangle^{\frac{1}{2}}} g_3(s(z)) (\cos \phi_x - \sin \phi_x) \quad (4.21b)$$

$$M_{33}(z) = \frac{1}{2} \left(\frac{\delta V^2}{\Delta} \frac{1}{\langle \beta_3 \rangle} (g_2^{(X)}(s(z)) + g_4^{(X)}(s(z)) \sin 2\phi_x) + \frac{\bar{\beta}_4^2 - \bar{\beta}_3^2}{\langle \beta_3 \rangle} \sin^2 \phi_x \right. \\ \left. + \frac{\bar{\beta}_3^2 - \langle \beta_3 \rangle^2}{\langle \beta_3 \rangle} + \frac{4}{\ell_c^2} \left(\frac{2}{\langle \beta_4 \rangle} - \frac{1}{\langle \beta_3 \rangle} \right) \dot{\phi}_x^2(s(z)) \right) \quad (4.22a)$$

$$M_{44}(z) = \frac{1}{2} \left(\frac{\delta V^2}{\Delta} \frac{1}{\langle \beta_3 \rangle} (g_2^{(X)}(s(z)) - g_4^{(X)}(s(z)) \sin 2\phi_x) + \frac{\bar{\beta}_3^2 - \bar{\beta}_4^2}{\langle \beta_4 \rangle} \sin^2 \phi_x \right. \\ \left. + \frac{\bar{\beta}_4^2 - \langle \beta_4 \rangle^2}{\langle \beta_4 \rangle} + \frac{4}{\ell_c^2} \left(\frac{2}{\langle \beta_3 \rangle} - \frac{1}{\langle \beta_4 \rangle} \right) \dot{\phi}_x^2(s(z)) \right) \quad (4.22b)$$

$$M_{34}(z) = \frac{1}{2} \left(\frac{\delta V^2}{\Delta} \frac{1}{\langle \beta_3 \rangle^{\frac{1}{2}} \langle \beta_4 \rangle^{\frac{1}{2}}} g_4^{(X)}(s(z)) \cos 2\phi_x + \frac{\bar{\beta}_4^2 - \bar{\beta}_3^2}{2\langle \beta_3 \rangle^{\frac{1}{2}} \langle \beta_4 \rangle^{\frac{1}{2}}} \sin 2\phi_x \right. \\ \left. + \frac{-4}{\ell_c^2 \langle \beta_3 \rangle^{\frac{1}{2}} \langle \beta_4 \rangle^{\frac{1}{2}}} \ddot{\phi}_x(s(z)) - i \frac{4\langle \beta_4 \rangle^{\frac{1}{2}}}{\ell_c \langle \beta_3 \rangle^{\frac{1}{2}}} \dot{\phi}_x(s(z)) \right) \quad (4.23a)$$

$$\begin{aligned}
M_{43}(z) = & \frac{1}{2} \left(\frac{\delta V^2}{\Delta} \frac{1}{\langle \beta_3 \rangle^{\frac{1}{2}} \langle \beta_4 \rangle^{\frac{1}{2}}} g_4^{(X)}(s(z)) \cos 2\phi_x + \frac{\bar{\beta}_4^2 - \bar{\beta}_3^2}{2 \langle \beta_3 \rangle^{\frac{1}{2}} \langle \beta_4 \rangle^{\frac{1}{2}}} \sin 2\phi_x \right. \\
& \left. + \frac{4}{\ell_c^2 \langle \beta_3 \rangle^{\frac{1}{2}} \langle \beta_4 \rangle^{\frac{1}{2}}} \ddot{\phi}_x(s(z)) + i \frac{4 \langle \beta_3 \rangle^{\frac{1}{2}}}{\ell_c \langle \beta_4 \rangle^{\frac{1}{2}}} \dot{\phi}_x(s(z)) \right) \quad (4.23b)
\end{aligned}$$

To dominant order, it is clear that all the $\langle \beta_\alpha \rangle$ in the denominators can be replaced by $\sqrt{2\Delta}/V$.

From (4.12), (4.19) and (4.20), it follows that

$$\begin{aligned}
m_{110} = & \frac{1}{2} \frac{\sqrt{2\Delta}}{V} \left((\zeta - \xi) \frac{\delta V^2}{\Delta} \eta_f + \xi \frac{1}{2} \frac{\delta V^2}{\Delta} \int_{-1}^1 ds (\eta_f + q_f(s)) + (\bar{\beta}_1^2 - \langle \beta_1 \rangle^2) \right) \\
= & 0, \quad (4.24)
\end{aligned}$$

since $q_f(s)$ is antisymmetric, and recalling $\langle \beta_1 \rangle$ as found at (4.4a).

Note from (4.5), (4.8a) and (4.8b) that $\bar{\beta}_4 - \bar{\beta}_3 = \frac{2\delta}{\pi\Delta} V^2 \alpha_x$, and thus

$$\begin{aligned}
& \pm \frac{1}{\Lambda} \int_0^\Lambda dz \left(\frac{\delta V^2}{\Delta} g_4^{(X)}(z) \sin 2\phi_x(z) + (\bar{\beta}_4 - \bar{\beta}_3) \sin^2 \phi_x(z) \right) \\
= & \pm \frac{\delta V^2}{\Delta} \frac{1}{\Lambda} \int_0^\Lambda dz \left(\frac{1}{\pi} Q_x \frac{-\text{sgn}(\alpha_x) Q_x}{|\alpha_x^2 + Q_x^2|^{\frac{1}{2}}} + \frac{2}{\pi} \alpha_x \frac{1}{2} \left(1 - \frac{|\alpha_x|}{|\alpha_x^2 + Q_x^2|^{\frac{1}{2}}} \right) \right) \\
= & \mp \frac{\delta V^2}{\pi\Delta} \text{sgn}(\alpha_x) \frac{1}{\Lambda} \int_0^\Lambda dz \left(\frac{Q_x^2}{|\alpha_x^2 + Q_x^2|^{\frac{1}{2}}} - |\alpha_x| + \frac{\alpha_x^2}{|\alpha_x^2 + Q_x^2|^{\frac{1}{2}}} \right)
\end{aligned}$$

using (4.10c), (4.10d), and (4.17). Also, observe from (4.16), that

$$\frac{1}{\Lambda} \int_0^\Lambda dz \frac{\delta V^2}{\Delta} g_2^{(j)}(z) = \frac{\delta(1 + \frac{\Xi}{2}) V^2}{\pi\Delta} \frac{1}{\Lambda} \int_0^\Lambda dz Q_+(z) = \frac{\delta(1 + \frac{\Xi}{2}) V^2}{\Delta} \zeta \eta_h.$$

Recall from (4.8a) and (4.8b) that

$$\langle \beta_3 \rangle^2 - \bar{\beta}_3^2 = \frac{\delta\zeta(1 + \frac{\Xi}{2})}{\Delta} V^2 \eta_h \mp \frac{\delta V^2}{\pi\Delta} \text{sgn}(\alpha_x) \frac{1}{\Lambda} \int_0^\Lambda dz (|\alpha_x^2 + Q_x^2(z)|^{\frac{1}{2}} - |\alpha_x|).$$

Thus, the first three terms in (4.22) cancel each other out. The approximation for $\langle \beta_\alpha \rangle$ means that the final term becomes one, instead of two parts. Thus, from (4.11), (4.19) and (4.22), it follows that

$$\begin{aligned}
m_{440} = m_{330} = & \frac{1}{2} \frac{4\sqrt{2\Delta}}{\ell_c^2 V} \xi \int_{-1}^1 ds \frac{\alpha_x^2}{4} \frac{\dot{Q}_x^2(s)}{|\alpha_x^2 + Q_x^2(s)|^2} \\
= & \frac{\Delta^{\frac{1}{2}} \xi}{\sqrt{2}} \frac{\alpha_x^2}{\ell_c^2 V} \int_0^1 ds \dot{Q}_x^2(s) \left(\frac{1}{|\alpha_x^2 + Q_x^2(s)|^2} + \frac{1}{|\alpha_x^2 + (Q_x(s) + \frac{\Xi\pi\eta_h}{2})^2|^2} \right). \quad (4.25)
\end{aligned}$$

Considering $M_{34}(z)$, a simplification is immediate. From (4.5), (4.10c), (4.10d) and (4.17),

$$\begin{aligned} & \frac{\delta V^2}{\Delta} g_4^{(X)} \cos 2\phi_x + \frac{1}{2}(\bar{\beta}_4^2 - \bar{\beta}_3^2) \sin 2\phi_x \\ &= \frac{\delta V^2}{\Delta} \frac{1}{\pi} \left(1 + \frac{\Xi}{2}\right) Q_x \frac{|\alpha_x|}{|\alpha_x^2 + Q_x^2|^{\frac{1}{2}}} + \frac{1}{2} \frac{2\delta V^2}{\pi\Delta} \alpha_x \frac{-\text{sgn}(\alpha_x)(1 + \frac{\Xi}{2})Q_x}{|\alpha_x^2 + Q_x^2|^{\frac{1}{2}}} = 0, \end{aligned}$$

so that M_{34}, M_{43} only contain the derivatives of the angle ϕ_x . These vanish at $s = \pm 1$.

Hence, from (4.19) and (4.24), it follows

$$\begin{aligned} -m_{430} = m_{340} &= \frac{1-4\xi}{2} \frac{\xi}{\ell_c^2} \int_{-1}^1 ds \left(\frac{1}{\langle\beta_3\rangle^{\frac{1}{2}}\langle\beta_4\rangle^{\frac{1}{2}}} \ddot{\phi}_x(s) + i\ell_c \langle\beta_4\rangle \dot{\phi}_x(s) \right) \\ &= \frac{-2\xi}{\ell_c^2} \frac{\sqrt{2\Delta}}{V} (\dot{\phi}_x(1) - \dot{\phi}_x(-1) + i\ell_c(\phi_x(1) - \phi_x(-1))) \\ &= \frac{i2\xi}{\ell_c} \phi_x(-1) \\ &= \frac{i\xi}{\ell_c} \arctan\left(\frac{\Xi\pi\eta h}{2\alpha_x}\right), \end{aligned} \quad (4.26)$$

since $\dot{\phi}_x(\pm 1) = 0 = \phi_x(1)$. Hence, it is clear that the coupling between modes 3 and 4 vanishes only in the case when the perturbation is isotropic.

Turning now to m_{131} , it follows from (4.18), with $k = 3, 4$,

$$\begin{aligned} m_{1k1} &= \xi e^{-i\pi(\xi+\zeta)} \int_{-1}^1 ds M_{1k}(s) \cos(\pi(\zeta + \xi s)) \\ &= \xi e^{-i\pi(\xi+\zeta)} \int_0^1 ds (M_{1k}(s) \cos(\pi(\xi s + \zeta)) + M_{1k}(-s) \cos(\pi(\xi s - \zeta))). \end{aligned}$$

because, from (4.14), (4.15) and (4.21), it follows that $M_{1k}(\pm 1) = 0$. Also, it follows from Fourier theory that $m_{1k(-1)} = m_{1k1}^*$, the complex conjugate. Further simplification comes from (4.14):

$$\begin{aligned} M_{1_4^3}(s) &= \frac{\delta V}{2\Delta^{\frac{1}{2}}\pi} P(s) \sqrt{2} (\cos \phi_x(s) \pm \sin \phi_x(s)) \\ &= \frac{\delta V}{2\Delta^{\frac{1}{2}}\pi} P(s) \frac{|\alpha_x^2 + Q_x^2|^{\frac{1}{2}} + |\alpha_x| \mp \text{sgn}(\alpha_x) Q_x}{|\alpha_x^2 + Q_x^2|^{\frac{1}{4}} (|\alpha_x^2 + Q_x^2|^{\frac{1}{2}} + |\alpha_x|)}, \end{aligned}$$

where (4.10a) and (4.10b) give the trigonometric functions. Finally, this means that

$$\begin{aligned} m_{1_4^3 1} &= \frac{\delta \xi V}{2\pi\Delta^{\frac{1}{2}}} e^{-i\pi(\xi+\zeta)} \int_0^1 ds P(s) \times \\ &\sqrt{2} ((\cos \phi_x \pm \sin \phi_x(s)) \cos(\pi(\xi s + \zeta)) + (\cos \phi_x(-s) \pm \sin \phi_x(-s)) \cos(\pi(\xi s - \zeta))) \end{aligned} \quad (4.27)$$

From (4.24) to (4.27), the coefficients for the Y-family are obtained by the replacement detailed previously.

$$\begin{aligned}
m_{220} &= 0. \\
m_{\left\{ \begin{smallmatrix} 55 \\ 66 \end{smallmatrix} \right\} 0} &= \frac{\Delta^{\frac{1}{2}} \xi \alpha_y^2}{\sqrt{2} \ell_c^2 V} \int_0^1 ds \dot{Q}_y^2(s) \left(\frac{1}{|\alpha_y^2 + Q_y^2(s)|^2} + \frac{1}{|\alpha_y^2 + (Q_y(s) + \frac{\Xi \pi \eta h}{2})^2|^2} \right). \\
m_{2\left\{ \begin{smallmatrix} 5 \\ 6 \end{smallmatrix} \right\} 1} &= m_{2\left\{ \begin{smallmatrix} 5 \\ 6 \end{smallmatrix} \right\} (-1)}^* = \frac{\delta(1 + \Xi) \xi V}{2\pi \Delta^{\frac{1}{2}}} e^{-i\pi(\xi + \zeta)} \int_0^1 ds P(s) \times \\
&\quad \sqrt{2} \left((\cos \phi_y \pm \sin \phi_y(s)) \cos(\pi(\xi s + \zeta)) + (\cos \phi_y(-s) \pm \sin \phi_y(-s)) \cos(\pi(\xi s - \zeta)) \right). \\
m_{560} &= -m_{650} = \frac{i2}{\ell_c} \phi_y(-1).
\end{aligned}$$

4.7 COUPLING EQUATIONS AND SOLUTIONS

Thus, after all the effort, the coupling equations describing modal conversion within the $LP_{01} \leftrightarrow LP_{11}$ are obtained. For the X-family, they are

$$\begin{pmatrix} a_1'(x) \\ a_3'(x) \\ a_4'(x) \end{pmatrix} = i \begin{pmatrix} 0 & m_{131} & m_{141} \\ m_{131}^* & m_{330} & m_{340} \\ m_{141}^* & -m_{340} & m_{440} \end{pmatrix} \begin{pmatrix} a_1(x) \\ a_3(x) \\ a_4(x) \end{pmatrix}$$

where $m_{1\alpha 1}$ and $m_{\alpha\gamma 0}$ are given at the appropriate one of (4.25), (4.26) and (4.27). Interest is in the case when the X-polarized fundamental mode initially carries all the power; equivalently, the boundary conditions are $a_1(0) = 1$ and $a_3(0) = 0 = a_4(0)$. For the Y-family, i.e. modes 2, 5, and 6, with all initial power in the Y-polarized fundamental mode, the obvious replacements give a similar set of equations.

Both families give a system of three coupled, first-order, linear, ordinary differential equations. Its solution is discussed in Appendix C.

4.8 RESULTS

The refractive index of silica was assumed to be 1.46. Gratings were considered to be of $N = 1000$ elements in length, each element being at an angle $\Theta = 0.0401$ radians = 2.30° to the axis of the fibre. The periodicity was $\Lambda = 590 \mu\text{m}$, and the width of the elements was $\sigma = 12 \mu\text{m}$ [8].

Two cases were examined. Firstly, the fibre was presumed to have a radius of $\rho =$

4.380 μm and a profile height of $\Delta = 2.190 \times 10^{-3}$. This corresponds to a higher-mode cut-off wavelength of 1.106 μm . The accompanying results are seen in Fig. 11, where resonance is around $V = 3.25$. Secondly, the fibre was given a radius of $\rho = 4.576 \mu\text{m}$ and a profile height of $\Delta = 2.500 \times 10^{-3}$. This corresponds to a higher-mode cut-off wavelength of 1.235 μm . The accompanying results are seen in Fig. 12, where resonance is around $V = 3.60$. These combinations of parameters approximate those of actual fibres used.

In general, as the resonant frequency increases, the peaks corresponding to the four modes within the grating become narrower, and closer together. The important feature is that there are four peaks, neither one nor three. This shows the need to consider the vector form of the modes (scalar theory predicts one peak) and to work with the modes of the grating instead of those of the fibre (the fibre's modes produce three peaks).

In all cases, it is assumed that $\delta = 9 \times 10^{-6}$, which corresponds to the elements of the grating having a refractive index 1.3×10^{-5} higher than that of the unperturbed core. Results were generated with smaller values of δ , and the general form of the results was the same, although the spacing between peaks was slightly altered (as expected). However, the size of the resonances was smaller. Typically, for $\delta = 5 \times 10^{-6}$, as much as 50% of power remained in the LP_{01} mode at resonance. For the Y-polarized light, the peaks were not as distinct, i.e. not as useful for highlighting the behaviour of the grating's output.

In each case, four values of anisotropy were used: $\Xi \times 10^4 = 0, 1, 5, 10$. The inclusion of anisotropy produced four clear peaks, arranged more in keeping with experimental observations [8]. Some comments are in order. (i) The anisotropy had a much stronger effect on the X-polarized input, than on the Y-polarized input. This follows as a consequence of the magnitude of α_x being significantly less than that of α_y . (ii) Although the results shown are for positive values of Ξ , the curves obtained for negative values of Ξ are identical. This is because the strongest influence of Ξ is as a square. (iii) It is remarkable how little anisotropy is needed to change the arrangement of the peaks. For a grating with $\delta = 9 \times 10^{-6}$, written in silica, a value of $\Xi = \pm 5 \times 10^{-4}$ gives a difference between the refractive index seen by X- and Y-polarized light of a mere 6.7×10^{-9} .

When the parameters of the fibre were altered so that the grating's resonance corre-

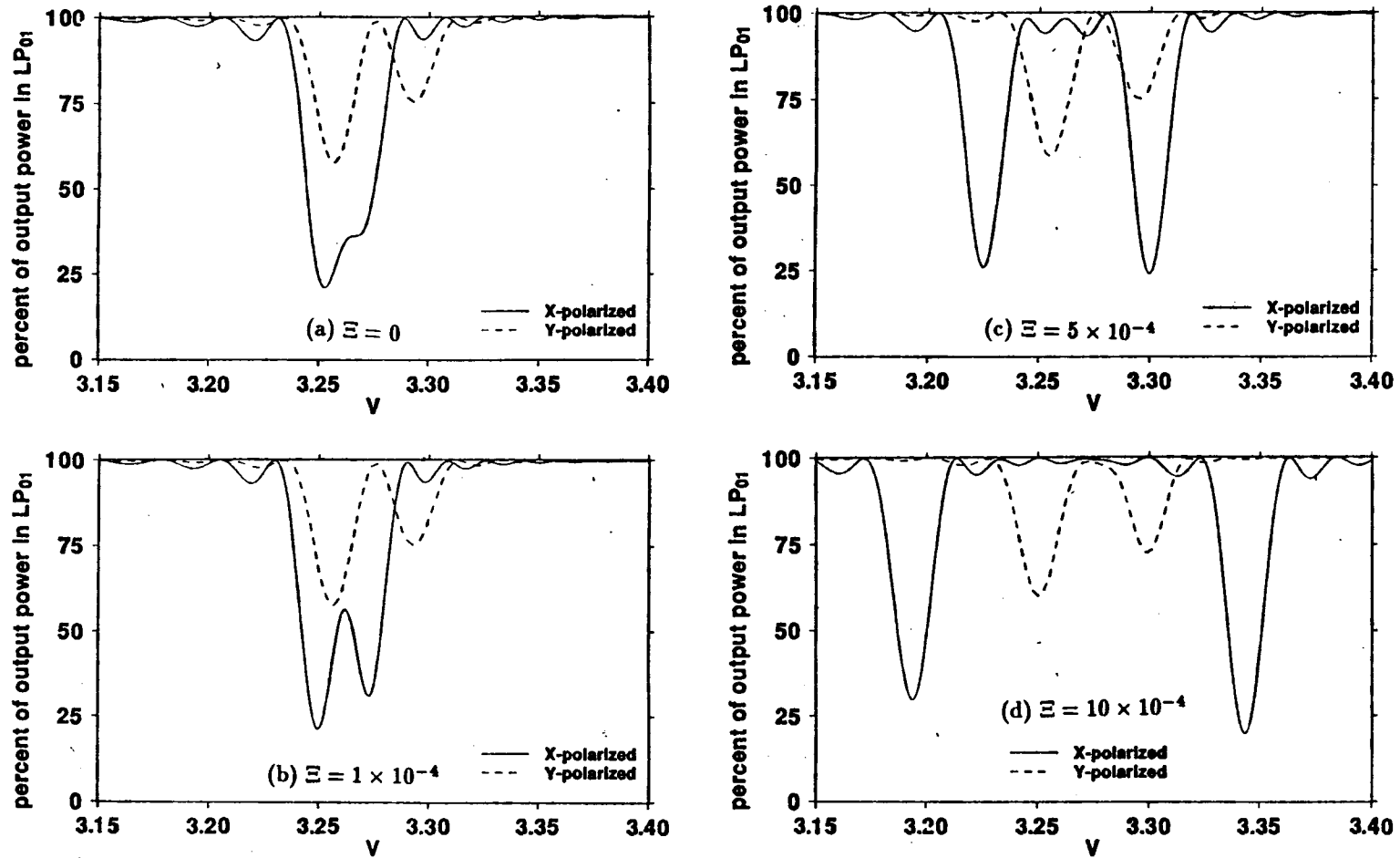


Figure 11: Frequency variation of output in LP₀₁ mode: anisotropy

The amount of power remaining in the LP₀₁ mode after passage through 1000 elements of an LP₀₁ ↔ LP₁₁ grating with $\delta = 9 \times 10^{-6}$, the elements set at angle $\Theta = 2.30^\circ$, $\Lambda = 590 \mu\text{m}$, and $\sigma = 12 \mu\text{m}$. The fibre has $\rho = 4.380 \mu\text{m}$ and a cutoff wavelength of $1.106 \mu\text{m}$. Four values of anisotropy are shown.

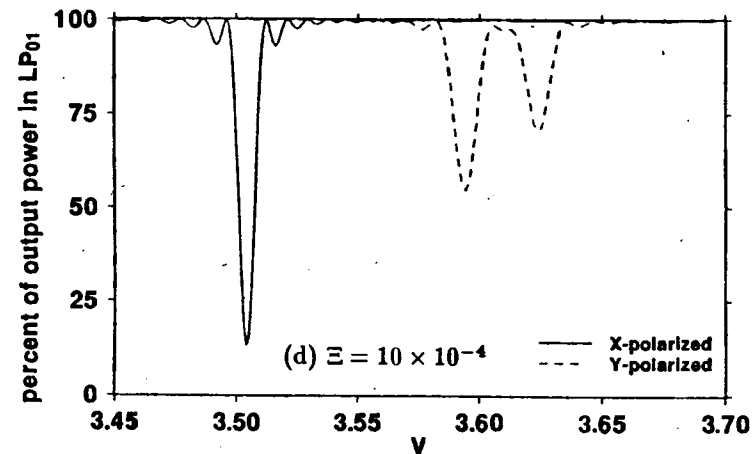
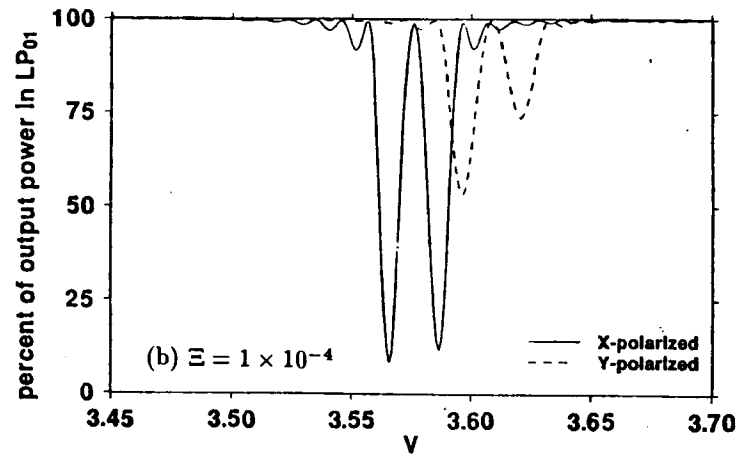
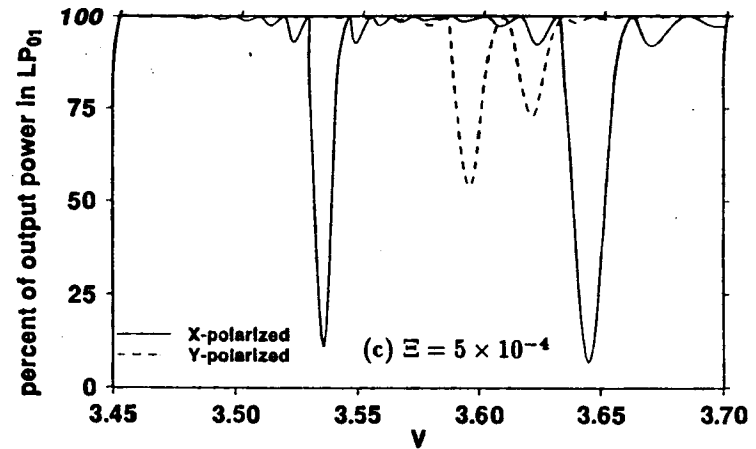
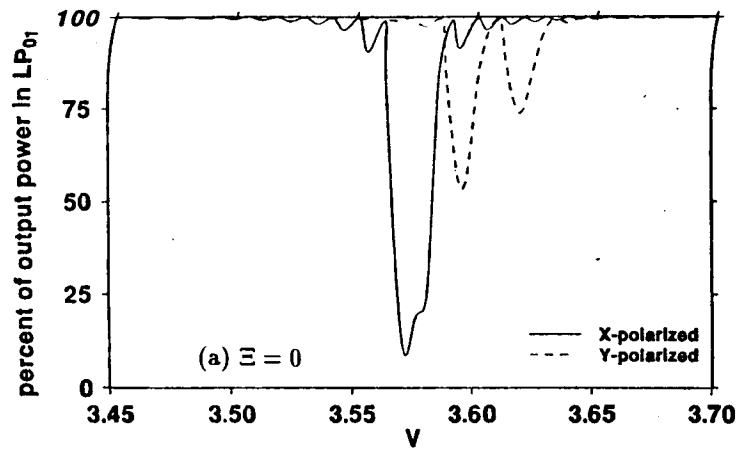


Figure 12: Frequency variation of output in LP_{01} mode: anisotropy

The amount of power remaining in the LP_{01} mode after passage through 1000 elements of an $LP_{01} \leftrightarrow LP_{11}$ grating with $\delta = 9 \times 10^{-6}$, the elements set at angle $\Theta = 2.30^\circ$, $\Lambda = 590 \mu\text{m}$, and $\sigma = 12 \mu\text{m}$. The fibre has $\rho = 4.576 \mu\text{m}$ and a cutoff wavelength of $1.235 \mu\text{m}$. Four values of anisotropy are shown.

sponded to operation near $V = 3.794$, where $\alpha_x = 0$, peculiar results were found. This is expected. As discussed previously, the vector form of the modes is ambiguously defined at that value.

Recall, as shown in Fig. 10, two groups of resonant frequencies may exist, not just one. As $V_{resonant} \rightarrow 3.03$, the resonant peaks on either side in $V = 3.03$ get broader, their tails start to interfere with each other, and eventually the two groups of four peaks become some other pattern. In Fig. 13 this is shown. With the grating's parameters as given above, in Fig. 13(a) the fibre was presumed to have a radius of $\rho = 4.30 \mu\text{m}$ and a profile height of $\Delta = 2.10 \times 10^{-3}$, which corresponds to a higher-mode cut-off wavelength of $1.063 \mu\text{m}$, and in Fig. 13(b) the fibre was presumed to have a radius of $\rho = 4.05 \mu\text{m}$ and a profile height of $\Delta = 1.85 \times 10^{-3}$, which corresponds to a higher-mode cut-off wavelength of $0.940 \mu\text{m}$. Consistently seen results are that the peaks become broader as V gets closer to 3.03, and that the group at the lower frequency has a lower value for the power converted at resonance.

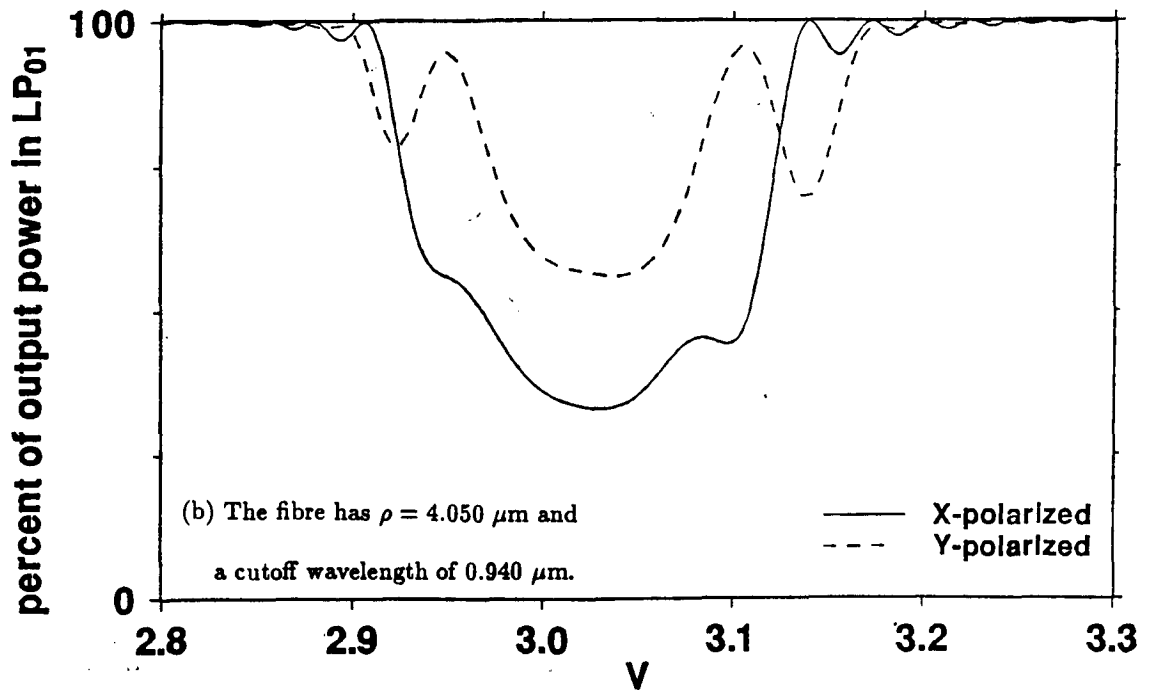
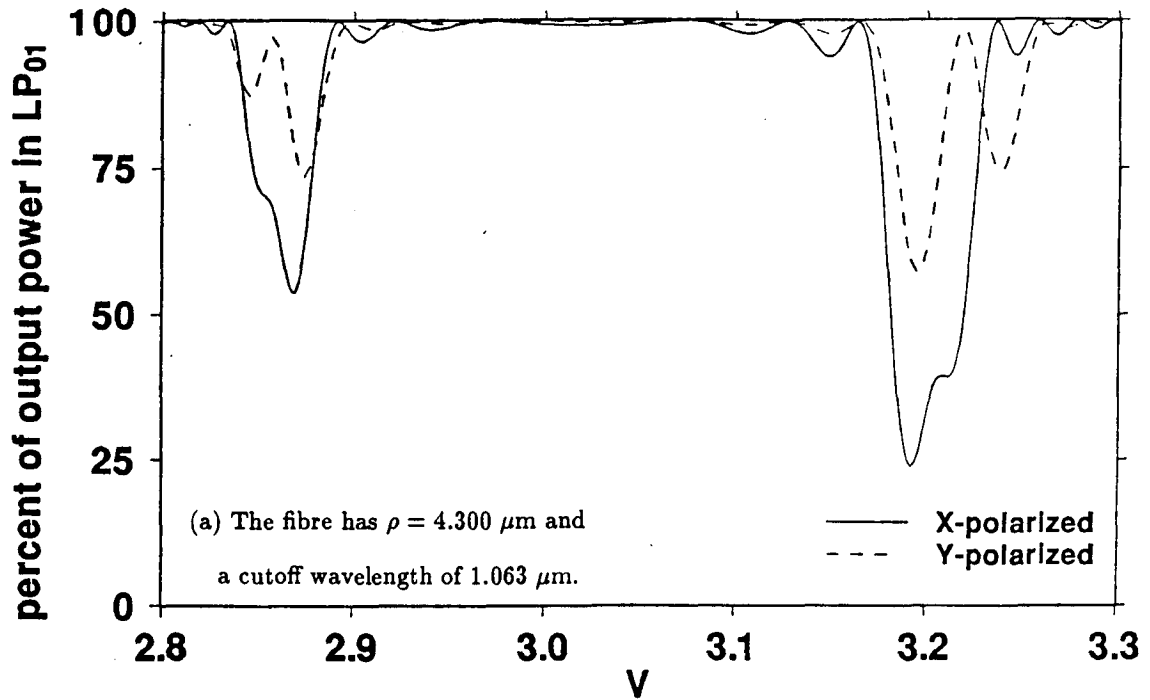


Figure 13: Frequency variation of output in LP_{01} mode

The amount of power remaining in the LP_{01} mode after passage through 1000 elements of an $LP_{01} \leftrightarrow LP_{11}$ grating with $\delta = 9 \times 10^{-6}$, the elements set at angle $\Theta = 2.30^\circ$, $\Lambda = 590 \mu\text{m}$, and $\sigma = 12 \mu\text{m}$.

5.0 NONLINEAR SWITCHING IN $LP_{01} \leftrightarrow LP_{02}$ GRATINGS

The $LP_{01} \leftrightarrow LP_{02}$ mode converting grating in an optical fibre switches power between the LP_{01} and LP_{02} modes which propagate within the fibre [5]. As was shown above, this mode conversion is very frequency dependent, i.e. it has a very narrow spectral response. Any nonlinear effect, caused by intense power being launched in either the LP_{01} or the LP_{02} mode, will destroy the sensitive resonance condition. The question arises, how does the grating perform in switching train of pulses? Such a structure would be the fibre equivalent of the planar device proposed by Trillo et al [9].

Jensen [10] first proposed and studied a nonlinear coherent coupler, made of similar waveguides. Trillo and Wabnitz [11] simplified his equations, and extended the work to dissimilar fibres. These form the mathematical analogue of coupling between dissimilar modes within a waveguide. The equations have been extensively examined [e.g. 12, 13, 14]. Various other improvements on the work of Ref. 10 have followed [e.g. 15, 16, 17], each correcting for some element within the approximations.

Two modes within a nonlinear waveguide will interfere to form a weak, periodic grating that causes coupling between the modes. This grating is independent of any externally written grating designed for mode conversion. Garth and Pask [18] examined the nonlinear coupling between the four forms of LP_{11} modes present in a fibre. Silberberg and Stegeman [19] analysed two modes coupling within a single planar waveguide as the limit of two guides whose separation vanished.

The first step in understanding the switching of pulses in an $LP_{01} \leftrightarrow LP_{02}$ grating is to understand the switching of the normal modes. To do this, make use of two approximate theories: (i) the theory of modal conversion in gratings, and (ii) the theory of nonlinear propagation of modes in fibre.

Concerning the second point, realize that the problem studied has a very weak nonlinearity in a relatively short grating. Hence, it is assumed that the transverse variation of the modal field varies but little from the initial form fixed by the theory of weak guidance (cf.

correction in [15]). This is a common approximation for the analysis of nonlinear fibres.

It is also assumed that the exchange of power between modes along the waveguide is slow, even in this nonlinear régime. This allows the use of the standard analysis of coupled mode theory for a grating. There are also the assumptions of weak-guidance and that the grating is a small perturbation of an otherwise invariant fibre.

5.1 STRUCTURE

The grating is written in a fibre of radius ρ and refractive index given by n_0 , in its cladding, and $n_0(1 + \Delta)$, where $\Delta \ll 1$, in its core. Define, as a normalization of the operating frequency ω (wavelength λ),

$$V^2 = n_0^2 k^2 \rho^2 2\Delta$$

where $k = \frac{2\pi}{\lambda} = \frac{\omega}{c}$. Henceforth, unless otherwise indicated, all lengths are implicitly assumed to be scaled by ρ .

The structure of the $LP_{01} \leftrightarrow LP_{02}$ grating was detailed above (see Fig. 1). It is defined by an increase of magnitude $\delta \ll \Delta$ to the refractive index in the core. The regions of higher index are a fraction $0 < \zeta < 1$ of the whole of the repeated unit defining the grating; the periodicity of this repeated unit is Λ . Thus, the unperturbed refractive index is changed to the perturbed one given by

$$n_0^2(1 + 2\Delta(1 + \frac{\delta}{\Delta}g_z(z))\bar{g}(r)) \quad (5.1)$$

where $g_z(z)$ is a Λ -periodic function whose Fourier series is

$$g_z(z) = g_j e^{ij2\pi z/\Lambda}. \quad (5.2a)$$

In particular, for the grating described herein,

$$g_0 = \zeta \quad ; \quad g_{\pm 1} = -e^{\pm i\pi\zeta} \frac{\sin(\pi\zeta)}{\pi}. \quad (5.2b)$$

Note that both the fibre and this grating are axisymmetric about the axis of modal propagation.

The nonlinearity will be assumed due to the Kerr effect; uniform over the entire infinite cross-section of the fibre; very weak; and isotropic. The local refractive index is given by

$$n^2 \approx n_\ell^2 + 2n_\ell n_I \mathcal{I}$$

where \mathcal{I} is the local intensity and n_ℓ the local refractive index. The problem will be formulated in terms of electric fields \mathcal{E} . Thus, it is more convenient to work with the susceptibility tensor χ_{ijkl} , which can be related to n_I .

Supported by the grating are the LP₀₁ and LP₀₂ modes, denoted as modes 1 and 2, though not necessarily respectively. Initially launched into mode α is power $p_\alpha P_0$, where P_0 is a normalizing, reference power.

5.2 MODES

The two modes present in the grating are either X- or Y-polarized, but both have the same state, namely $\hat{\mathbf{p}}$. Write their electric field vectors as

$$\mathcal{E}_\alpha = \hat{\mathbf{p}} \frac{1}{2} A_\alpha(z) [F_\alpha(r) e^{i(\beta_\alpha z - \omega_0 t)} + \text{c.c.*}]$$

with c.c.* meaning add complex conjugate of terms explicitly listed. Here $A_\alpha(z)$ is some amplitude constant, which varies along the grating, and β_α is the propagation constant, as found by the theory of weak guidance and subsequently corrected for polarization effects [1: ch 14]. Note that modes are linearly polarized.

Normalize the radial variation of the modal fields by defining

$$\hat{F}_\alpha(r) = \frac{1}{\|F_\alpha\|} F_\alpha(r)$$

The total electric field travelling in the fibre is given approximately by the z -varying sum of modes

$$\mathcal{E} = \hat{\mathbf{p}} \frac{1}{2} \left(\frac{\omega_0 P_0}{\pi \rho c^2 \epsilon_0} \right)^{\frac{1}{2}} \left[\frac{1}{\beta_j^{\frac{1}{2}}} \hat{F}_j(r) a_j(z) e^{i(\beta_j z - \omega_0 t)} + \text{c.c.*} \right] \quad (5.3)$$

with the summation convention implied over a Latin index (but not over a Greek index). Constants are chosen for convenient power normalization and give the power in mode α to be

$$P_\alpha = \frac{c^2 \epsilon_0 \beta_\alpha}{2 \rho \omega_0} 2 \pi \rho^2 \int_0^\infty dr r |\mathcal{E}_\alpha|^2 = P_0 |a_\alpha(z)|^2$$

Compared with the previous analysis, here $a_\alpha(z)$ has absorbed an extra phase factor of $e^{i((\beta_\alpha)-\beta_\alpha)z}$.

5.3 NONLINEAR POLARIZATION

The electric field can be written in its spectral form:

$$\mathcal{E} = \hat{p} \frac{1}{2} \int_{-\infty}^{\infty} E_\omega \delta(|\omega| - \omega_0) e^{-i\omega t}; \quad (5.4a)$$

$$E_\omega = \begin{cases} \left(\frac{\omega_0 P_0}{\pi \rho c^2 \epsilon_0} \right)^{\frac{1}{2}} \frac{1}{\beta_j^{\frac{1}{2}}} a_j(z) \hat{F}_j(r) e^{i\beta_j z} & , \text{ if } \omega > 0 \\ E_{-\omega}^* & , \text{ if } \omega < 0 . \end{cases} \quad (5.4b)$$

Clearly, E_ω is needed only at $\omega = \omega_0$. Observe from (5.3) that

$$\begin{aligned} |E_{\omega_0}|^2 &= \frac{\omega_0 P_0}{\pi \rho c^2 \epsilon_0} \frac{1}{(\beta_j \beta_k)^{\frac{1}{2}}} \hat{F}_j(r) \hat{F}_k(r) a_j(z) a_k^*(z) e^{i(\beta_j - \beta_k)z} \\ &= \frac{\omega_0 P_0}{\pi \rho c^2 \epsilon_0} \left(\frac{1}{\beta_1} \hat{F}_1(r) |a_1(z)|^2 + \frac{1}{\beta_2} \hat{F}_2(r) |a_2(z)|^2 + \right. \\ &\quad \left. \frac{1}{(\beta_1 \beta_2)^{\frac{1}{2}}} \hat{F}_1(r) \hat{F}_2(r) (a_1(z) a_2^*(z) e^{i(\beta_1 - \beta_2)z} + a_1^*(z) a_2(z) e^{i(\beta_2 - \beta_1)z}) \right) \end{aligned} \quad (5.5)$$

The nonlinear polarization $\frac{\mathcal{P}}{\epsilon_0}$ follows approximately [27] as

$$\begin{aligned} \mathcal{P} &= \hat{p} \frac{1}{2} \int_{-\infty}^{\infty} P_\omega \delta(|\omega| - \omega_0) e^{-i\omega t} \\ P_\omega &= \begin{cases} \frac{3}{4} \epsilon_0 \chi(-\omega; \omega_0, -\omega_0, \omega) |E_{\omega_0}|^2 E_\omega & , \text{ if } \omega > 0 \\ P_{-\omega}^* & , \text{ if } \omega < 0 , \end{cases} \end{aligned}$$

where $\chi = \chi_{1111}$ because there is Kleinmann symmetry in an isotropic medium, and only one polarization component of the electric field is present in the fibre. Hence, it follows that

$$\begin{aligned} \frac{\rho^2}{c^2} \frac{\partial^2 \mathcal{P}}{\partial t^2 \epsilon_0} &= \hat{p} \frac{1}{2} \frac{-\rho^2 \omega_0^2}{c^2} \left[\frac{3}{4} \chi(-\omega_0; \omega_0, -\omega_0, \omega_0) |E_{\omega_0}|^2 E_{\omega_0} e^{-i\omega_0 t} + \text{c.c.}^* \right] \\ &= \frac{-\rho^2 \omega_0^2}{c^2} \frac{3}{4} \chi(-\omega_0; \omega_0, -\omega_0, \omega_0) |E_{\omega_0}|^2 \mathcal{E}, \end{aligned} \quad (5.6)$$

assuming that χ is real. Define as a shorthand

$$\chi_0 = \chi_{1111}^{(3)}(-\omega_0; \omega_0, -\omega_0, \omega_0) = \frac{4}{3} n_0^2 n_I c \epsilon_0,$$

which relates the susceptibility to n_I .

The final term in (5.5) shows that the nonlinear contribution to the refractive index is equivalent to a $(2\pi/(\beta_1 - \beta_2))$ -periodic grating, caused by the nonlinear interference of the two modes via the Kerr effect. What is this grating's magnitude? It is useful to define

$$\delta_{NL} = \frac{1}{2n_0^2} 2n_0 n_I \frac{P_0}{\pi \rho^2} = \frac{3\chi_0 P_0}{4\pi \rho^2 n_0^3 c \epsilon_0},$$

which is a measure of the change wrought by the nonlinearity on the refractive index. Its interpretation is immediate. If a beam of uniform power P_0 illuminates the fibre's core, a perturbation to the refractive index of size $\delta_{NL} n_0$ is caused. Thus, from (5.5) and (5.6), it follows that

$$\frac{\rho^2}{c^2} \frac{\partial^2 \mathcal{P}}{\partial t^2 \epsilon_0} = -\delta_{NL} \frac{V^3}{2\sqrt{2}\Delta^{\frac{3}{2}}} \frac{1}{(\beta_j \beta_k)^{\frac{1}{2}}} \hat{F}_j(r) \hat{F}_k(r) a_j(z) a_k^*(z) e^{i(\beta_j - \beta_k)z} \mathcal{E}, \quad (5.7)$$

noting $\omega_0^2 = V^2 c^2 / \rho^2 n_0^2 2\Delta$. As $\beta_\alpha \sim \sqrt{\Delta}$, the induced grating has a magnitude of order δ_{NL}/Δ .

5.4 FROM MAXWELL EQUATION TO COUPLING EQUATION

The modes on the unperturbed fibre satisfy

$$[\nabla^2 - \beta_\alpha^2 + k^2 n_0^2 + V^2 \bar{g}(r)] E_\alpha = 0,$$

where ∇^2 is the Laplacean, restricted to operation on the cross-section only. The electric field in the grating satisfies an approximation, derived from the Maxwell equations in a nonlinear medium:

$$[\nabla^2 + \frac{\partial^2}{\partial z^2} + k^2 n_0^2 + V^2 (1 + \frac{\delta}{\Delta} g_z(z)) \bar{g}(r)] \mathcal{E} = \frac{\rho^2}{c^2} \frac{\partial^2 \mathcal{P}}{\partial t^2 \epsilon_0}, \quad (5.8)$$

where $\frac{\mathcal{P}}{\epsilon_0}$ is the nonlinear polarization in the medium. This gives an effective shape function in the perturbed, nonlinear grating of

$$g_{NL}(r, z) = (1 + \frac{\delta}{\Delta} g_z(z)) \bar{g}(r) - \frac{\rho^2}{V^2 c^2} \frac{\partial^2 \mathcal{P}}{\partial t^2 \epsilon_0}.$$

Thus, from (5.3) and (5.8), the customary coupling equations [e.g. 1: ch27] are found to be

$$-2i a'_\alpha(z) = \frac{V^2}{\beta_n^{\frac{1}{2}} \beta_\alpha^{\frac{1}{2}}} \langle \hat{F}_\alpha(r), ((1 + \frac{\delta}{\Delta} g_z(z)) \bar{g}(r) - \frac{\rho^2}{V^2 c^2} \frac{\partial^2 \mathcal{P}}{\partial t^2 \epsilon_0} - \bar{g}(r)) \hat{F}_n(r) \rangle a_n(z) e^{i(\beta_n - \beta_\alpha)z} \quad (5.9)$$

which is the analogous result to that found previously for an axisymmetric grating in a linear medium. The integrals in the right-hand side of (5.9) involve the local change of the refractive index from its unperturbed value. They can be greatly simplified.

Define

$$G_{\alpha\gamma} = \langle \hat{F}_\alpha(r), \bar{g}(r) \hat{F}_\gamma(r) \rangle.$$

Using (5.2a), it follows that

$$\begin{aligned} & \frac{V^2}{\beta_n^{\frac{1}{2}} \beta_\alpha^{\frac{1}{2}}} \langle \hat{F}_\alpha(r), ((1 + \frac{\delta}{\Delta} g_z(z)) \bar{g}(r) - \bar{g}(r)) \hat{F}_n(r) \rangle a_n(z) e^{i(\beta_n - \beta_\alpha)z} \\ &= \frac{\delta \sqrt{2}}{\Delta^{\frac{1}{2}}} V G_{\alpha n} g_j a_n(z) e^{i(\beta_n - \beta_\alpha + j \frac{2\pi}{\Lambda})z} \end{aligned} \quad (5.10)$$

where the approximation $\beta_\alpha \approx V/\sqrt{2}\Delta^{\frac{1}{2}}$ also was made. Further, make this approximation and substitute (5.7) to find

$$\begin{aligned} & - \frac{1}{\beta_n^{\frac{1}{2}} \beta_\alpha^{\frac{1}{2}}} \langle \hat{F}_\alpha(r), \frac{\rho^2}{c^2} \frac{\partial^2}{\partial t^2} \frac{\mathcal{P}}{\epsilon_0} \hat{F}_n(r) \rangle a_n(z) e^{i(\beta_n - \beta_\alpha)z} \\ &= \frac{\sqrt{2}\Delta}{V} \frac{\delta_{NL} V^2}{2\Delta} \langle \hat{F}_\alpha(r), \hat{F}_j(r) \hat{F}_k(r) \hat{F}_n(r) \rangle a_j(z) a_k^*(z) a_n(z) e^{i(\beta_j - \beta_k + \beta_n - \beta_\alpha)z}. \end{aligned} \quad (5.11)$$

5.5 NEAR RESONANCE

As previously established for the linear grating, on the nonlinear grating, resonance occurs when the co-efficient of z in the arguments of the exponentials (5.9), (5.10) and (5.11) is very small. This means that the period of the grating is such that

$$\beta_{>} \approx \beta_{<} + \frac{2\pi}{\Lambda},$$

where $\beta_{<} = \min(\beta_1, \beta_2)$ and $\beta_{>} = \max(\beta_1, \beta_2)$. Hence, it is easy to pick out the strong coupling effects: intermodal- and self-coupling, as in linear régime, and the nonlinear interaction. Near such a resonance β_1 and β_2 are not nearly equal. (If they were, then birefringent-coupling would be present and the nonlinear interaction would be more difficult to analyze.) The argument of the exponential in (5.11) vanishes, if $j = \alpha, k = n$ or $n = \alpha, k = j$. One must be careful in counting these cases: $(\alpha, 1, 1, \alpha), (\alpha, 2, 2, \alpha), (1, 1, \alpha, \alpha), (2, 2, \alpha, \alpha)$. One

of them is a repeat. From (5.9), (5.10) and (5.11), it follows that

$$\begin{aligned}
0 &= 2ia'_1(z) + \frac{\delta\sqrt{2}}{\Delta^{\frac{1}{2}}}V(G_{11}g_0a_1(z) + G_{12}g_{\pm 1}a_2(z)e^{i2\Gamma\Delta^{\frac{3}{2}}z}) \\
&\quad + \frac{\delta_{NL}V}{\sqrt{2}\Delta^{\frac{1}{2}}}(I_1|a_1(z)|^2a_1(z) + 2J|a_2(z)|^2a_1(z)) \\
0 &= 2ia'_2(z) + \frac{\delta\sqrt{2}}{\Delta^{\frac{1}{2}}}V(G_{22}g_0a_2(z) + G_{21}g_{\mp 1}a_1(z)e^{-i2\Gamma\Delta^{\frac{3}{2}}z}) \\
&\quad + \frac{\delta_{NL}V}{\sqrt{2}\Delta^{\frac{1}{2}}}(I_2|a_2(z)|^2a_2(z) + 2J|a_1(z)|^2a_2(z)),
\end{aligned}$$

with the definitions

$$\begin{aligned}
\Gamma &= \frac{1}{2}(\beta_2 - \beta_1 \pm \frac{2\pi}{\Lambda})/\Delta^{\frac{3}{2}} \\
J &= \langle \hat{F}_1(r)^2, \hat{F}_2(r)^2 \rangle \\
I_\alpha &= \langle \hat{F}_\alpha(r), \hat{F}_\alpha(r)^3 \rangle.
\end{aligned}$$

The choice \pm depends upon whether $\beta_1 = \beta_>$ or $\beta_2 = \beta_>$, respectively.

Thus, near resonance, the mode coupling is described by the following equations:

$$\begin{aligned}
0 &= i\frac{d}{dx}a_1(z) + C_1a_1(z) + Ke^{-i\bar{\zeta}}e^{i2\Gamma x}a_2(z) + D_1|a_1(z)|^2a_1(z) + 2B|a_2(z)|^2a_1(z); \\
0 &= i\frac{d}{dx}a_2(z) + C_2a_2(z) + Ke^{i\bar{\zeta}}e^{-i2\Gamma x}a_1(z) + D_2|a_2(z)|^2a_2(z) + 2B|a_1(z)|^2a_2(z),
\end{aligned} \tag{5.12}$$

where the longitudinal length is scaled as $x = z\Delta^{\frac{3}{2}}$. There are the definitions, using (5.2b),

$$C_\alpha = \frac{\delta}{\Delta^2} \frac{V}{\sqrt{2}} G_{\alpha\alpha} \zeta \quad ; \quad Ke^{-i\bar{\zeta}} = \frac{\delta}{\Delta^2} \frac{-e^{\pm i\pi\zeta} \sin \pi\zeta}{\pi\sqrt{2}} V G_{12}$$

with $0 < K$, which is real. These parameters are exactly those found in solving the problem of power switching in a linear grating. Also, there are the definitions

$$D_\alpha = \frac{\delta_{NL}}{\Delta^2} \frac{V}{2\sqrt{2}} I_\alpha \quad ; \quad B = \frac{\delta_{NL}}{\Delta^2} \frac{V}{2\sqrt{2}} J.$$

These show the strength of nonlinear coupling via the parameter δ_{NL} , which depends on the referential power P_0 and n_I .

System (5.12) is precisely that obtained elsewhere [e.g. 9, 11]. Extensive analysis has been applied to the case when $D_1 = D_2$ [e.g. 12, 13], but very little to the case when $D_1 \neq D_2$, despite claims to the contrary. The solution of (5.12) is generally found and discussed in terms of the Stokes parameters.

5.6 CONSTANT AMPLITUDE SOLUTION

One solution to (5.12) is a curiosity: the power in the two modes is constant through the grating, i.e. there is no power coupled between them.

To find this solution, put

$$a_\alpha(z) = p_\alpha^{1/2} e^{i\phi_\alpha(x)},$$

and find, from the real-imaginary decomposition of (5.12), that

$$\begin{aligned}\phi_1'(x) &= C_1 + K\sqrt{\frac{p_2}{p_1}} \cos(-\bar{\zeta} + 2\Gamma x + \phi_2 - \phi_1) + D_1 p_1 + 2B p_2 \\ 0 &= \sin(-\bar{\zeta} + 2\Gamma x - \phi_1(x) + \phi_2(x)) \\ \phi_2'(x) &= C_2 + K\sqrt{\frac{p_1}{p_2}} \cos(\bar{\zeta} - 2\Gamma x - \phi_2 + \phi_1) + D_2 p_2 + 2B p_1.\end{aligned}$$

From the middle equation, the requirement

$$\phi_2(x) = \bar{\zeta} + \phi_1(x) - 2\Gamma x$$

follows. When combined with the first equation, this gives the solution for $\phi_1(x)$, and, thus, for $\phi_2(x)$:

$$\begin{aligned}\phi_1(x) &= \phi_0 + (C_1 + K\sqrt{\frac{p_2}{p_1}} + D_1 p_1 + 2B p_2)x \\ \phi_2(x) &= \bar{\zeta} + \phi_0 + (C_1 + K\sqrt{\frac{p_2}{p_1}} + D_1 p_1 + 2B p_2 - 2\Gamma)x\end{aligned}$$

where ϕ_0 is an arbitrary constant initial phase. The third equation then gives a consistency condition which reduces to

$$\frac{C_1 - C_2 - 2\Gamma}{K} + \sqrt{\frac{p_2}{p_1}} + \frac{D_1 - 2B}{K} p_1 = \sqrt{\frac{p_1}{p_2}} + \frac{D_2 - 2B}{K} p_2.$$

This must be satisfied by the respective powers in the two modes. Given the power in one mode, the necessary power in the other for a constant power solution, is found by solving this. For a specified total power $p = p_1 + p_2$ in two modes, the division of power between the two modes is found by solving for either power.

If a constant power solution exists (Finding a defining equation doesn't guarantee it has a solution), the initial power and phases of the two modes are such that the nonlinear interference exactly counteracts the linear grating. There is no power coupled between modes

1 and 2. If a constant power solution exists, which it will not always do, it has important implications for the possibility of switching.

5.7 GENERAL SOLUTION

To solve the system (5.12), put

$$a_j(z) = A_j^{\frac{1}{2}}(x)e^{i(\phi_j(x)+C_jx)}$$

and define

$$\Phi(x) = \phi_2(x) - \phi_1(x) - \zeta + (2\Gamma + C_2 - C_1)x;$$

$$\gamma = 2\Gamma + C_2 - C_1;$$

$$d_+ = \frac{1}{2}(D_1 + D_2 - 4B) = \frac{\delta_{NL}}{\Delta^2} \frac{1}{4\sqrt{2}} V(I_1 + I_2 - 4J);$$

$$d_- = \frac{1}{2}(D_1 - D_2) = \frac{\delta_{NL}}{\Delta^2} \frac{1}{4\sqrt{2}} V(I_1 - I_2).$$

Note that perfect resonance in the linear coupler corresponds to $\gamma = 0$. Thus, from (5.12), the coupled equations for real variables are

$$-\frac{1}{2}A_1'(x) = K\sqrt{A_1(x)A_2(x)} \sin \Phi(x) \quad (5.13a)$$

$$\frac{1}{2}A_2'(x) = K\sqrt{A_1(x)A_2(x)} \sin \Phi(x) \quad (5.13b)$$

$$\begin{aligned} \Phi'(x) = & d_+(A_2(x) - A_1(x)) - d_-(A_1(x) + A_2(x)) \\ & + K \frac{(A_1(x) - A_2(x))}{\sqrt{A_1(x)A_2(x)}} \cos \Phi(x) + \gamma. \end{aligned} \quad (5.13c)$$

The initial conditions are $A_1(0) = p_1$ and $A_2(0) = p_2$.

The first invariant is immediate:

$$A_1'(x) + A_2'(x) = 0 \Rightarrow A_1(x) + A_2(x) = p$$

which is constant. From the initial conditions, this is $p = p_1 + p_2$. It has an easy physical interpretation: the conservation of energy. The second invariant is harder to find, but follows as

$$4K\sqrt{A_1(x)A_2(x)} \cos \Phi(x) - 2d_+A_1(x)A_2(x) + (pd_- - \gamma)(A_1(x) - A_2(x)) = \mathcal{L}$$

which is constant. From the initial conditions this, too, can be fixed, but it does not have an easy physical interpretation. However, it does provide a means of getting an equation for the power propagating in one mode.

From (5.13a) and (5.13b), it follows that

$$\begin{aligned} -\frac{1}{2}A_1'(x) &= \frac{1}{2}A_2'(x) = K\sqrt{A_1(x)A_2(x)}\sin\Phi(x) \\ \Rightarrow (A_1'(x))^2 &= (A_2'(x))^2 = 4K^2A_1(x)A_2(x) - (2K)^2A_1(x)A_2(x)\cos^2\Phi(x) \end{aligned} \quad (5.14)$$

Recall $A_1(x) = p - A_2(x)$, and use the second invariant to eliminate $\cos\Phi(x)$. This way one obtains a nonlinear ordinary differential equation for either $A_1(x)$ or $A_2(x)$.

For the switching of modes, the interesting initial conditions are all the power in one mode and none in the other. Therefore, with no loss of generality, launch all the power in mode 1, and solve for power in each mode, a distance L along the grating. It is easier to solve for $A_2(x)$, and recover $A_1(x) = p - A_2(x)$. (The accepted wisdom of the literature is to solve for $u(x) = A_1(x) - A_2(x)$.) From these initial conditions, the second invariant is $\mathcal{L} = p(pd_- - \gamma)$, which yields

$$-2K\sqrt{A_1(x)A_2(x)}\cos\Phi(x) = (\gamma - pd_- - pd_+ + d_+A_2(x))A_2(x).$$

Now the right-hand side of (5.14) involves a quartic polynomial in $A_2(x)$:

$$(A_2'(x))^2 = 4K^2(p - A_2(x))A_2(x) - (\gamma - p(d_+ + d_-) + d_+A_2(x))^2A_2^2(x). \quad (5.15)$$

This can be solved either numerically or in terms of the Jacobi elliptic functions [7: ch16,17].

Make the substitutions

$$t = 2Kx \quad ; \quad y(t) = \frac{1}{p}A_2(x),$$

and define the cubic polynomial $Q(\xi)$ to be

$$Q(\xi) = 1 - (1 + (q_0p\tau - \bar{\gamma})^2)\xi + 2(q_0p\tau - \bar{\gamma})\xi^2 - q_0^2p^2\xi^3, \quad (5.16)$$

where

$$0 < q_0 = \frac{|d_+|}{2K} = \frac{\delta_{NL}}{\delta} \frac{\pi}{8\sin\pi\zeta} \frac{|I_1 + I_2 - 4J|}{|G_{12}|} \quad (5.17a)$$

$$\bar{\gamma} = \text{sgn}(d_+) \frac{\gamma}{2K} = \frac{\Delta\pi}{\delta\sqrt{2}\sin\pi\zeta} \text{sgn}(d_+) \frac{2\Gamma + C_2 - C_1}{V|G_{12}|} \quad (5.17b)$$

$$\tau(V) = 1 + \frac{d_-}{d_+} = \frac{2|I_1 - 2J|}{|I_1 + I_2 - 4J|}. \quad (5.17c)$$

These definitions give τ , $\bar{\gamma}$, and q_0 to be independent of the launched power p ; they are functions only of waveguide and grating parameters. Observe that the much studied case corresponds to $d_- = 0$ or, equivalently, $\tau = 1$ and $\bar{\gamma} =$. Conventionally [e.g.10], P_0 has been chosen so that δ_{NL} gives a value such that $q_0 = 2$. However, this would produce a value of P_0 dependent on V ; this would be unsuitable for the purpose of this study.

From (5.15) and (5.16), it follows that

$$y'(t)^2 = -yQ(y) \Rightarrow t = \int_0^{y'(t)} d\xi \frac{1}{\sqrt{\xi Q(\xi)}}. \quad (5.18)$$

The prescribed initial condition $y(0) = 0$ was used. From physical considerations the maximum permissible value of $y(t)$ is 1. Before proceeding, examine the zeroes of $Q(\xi)$, with $0 \leq \xi \leq 1$. These are defined in Appendix D. There exists a value $\xi_0(q_0 p; \tau, \bar{\gamma}) \leq 1$ which is the least positive root of $Q(\xi)$. This value ξ_0 is the maximum value attained by $y(t)$; equivalently, the maximum value attained by $A_2(x)$ is $p\eta_0$.

The form of the solution to (5.18) depends upon the number of roots to $Q(\xi)$. Appendix E lists details of the solution for different numbers of roots, which, for a given parameter pair $(\tau, \bar{\gamma})$ may depend on initial value p . In all cases, at least some power in mode 1 transfers to mode 2. Except for a few singular cases, the solution is oscillatory, i.e. this power is periodically exchanged between modes 1 and 2 during passage through grating. The amplitude of the oscillation is $p\eta_0$ and the period is $4K(\ell)$, which is the complete elliptic integral of the first kind [7: ch16] and ℓ is defined at the appropriate place in Appendix E.

5.8 QUALITATIVE RESULTS OF LINEARLY TUNED GRATING

Initially, to highlight the features of the solution, consider the case of the linearly tuned grating, i.e. a grating whose period and operating wavelength are such that $\gamma = 0 = \bar{\gamma}$. The possible options for the zeroes of $Q(\xi)$ are obtained in Appendix D, and illustrated in Fig. 27. The associated detailed solutions are described in Appendix E.

For $\tau > 1.125$ or $\tau \leq 0$, there is one zero for all values of input power p . The solution is given in form (E.6). The amplitude of the power exchanged between modes 1 and 2 decreases continuously as p increases, and the period of this oscillation increases.

For $\tau = 1.125$, there is one zero and the solution is like (E.6), except when $p = \frac{2\sqrt{6}}{3q_0}$. For $p < \frac{2\sqrt{6}}{3q_0}$, as p increases, the period of the oscillation increases towards infinity and the amplitude of the power exchanged between modes 1 and 2 decreases towards $\frac{3}{4}p$. At $p = \frac{2\sqrt{6}}{3q_0}$, there is a triply degenerate root and the solution is as in (E.2), which gives $A_1(x)$, power in mode 1, decaying with distance, towards value $\frac{3}{4}p$. For $p > \frac{2\sqrt{6}}{3q_0}$, again there is only one zero, and have an exchange of power of declining amplitude and lessening period as p increases.

For the case $1.125 > \tau > 1$, the number of zeroes changes as p changes. There is one root and the solution is given by (E.6) for $p < \frac{w_D}{q_0}$. The amplitude of the power exchanged between modes 1 and 2 decreases as p increases and the coupling length increases towards infinity. At $p = \frac{w_D}{q_0}$, the solution is given by (E.3), as there is doubly degenerate root. The power in mode 1 decays with increasing distance towards value $p(1 - \eta_0)$. For $p > \frac{w_D}{q_0}$, again there is an oscillatory solution, given by (E.5), except at the unique value of p where (E.2) applies. The amplitude of the oscillation decreases. The amplitude of oscillation changes discontinuously by $p\eta_J$ at $p = w_D$.

For the case $0 < \tau \leq 1$, the number of zeroes changes. For $0 < p < \frac{w_D}{q_0}$, the oscillatory solution is given by (E.6). The period of the oscillation increases with p , and, unless $\tau = 1$, the amplitude of the oscillation decreases. At $p = \frac{w_D}{q_0}$, the solution is given by (E.2). The power in mode 1 monotonically approaches $p\eta_0(\tau, 0)$. For $p > \frac{w_D}{q_0}$, the oscillatory solution is given by (E.5), for which the period and amplitude decrease as p increases. The amplitude of the power exchanged alters discontinuously as p passes through the special value $\frac{w_D}{q_0}$.

Physically, there is not a discontinuity in the power switched between modes. A practical grating has a length that is fixed, though the operating frequency varies. The coupling length at which the discontinuity is seen is infinite. Thus, as the power increases towards $\frac{w_D}{q_0}$, the grating's length is a decreasing fraction of the coupling length. Less than complete coupling is observed. As power continues to increase beyond $\frac{w_D}{q_0}$, the coupling length decreases and an increasing fraction of the maximum possible coupling is observed. Consequently, the discontinuity is "smeared out".

5.9 PARAMETERS OF FIBRE

For silica

$$n_0 = 1.46 \quad ; \quad n_I = 2.73 \times 10^{-20} \text{ m}^2/\text{W}$$

the latter being the result for bulk material. Assume the value for a fibre is not very different.

For the fibre of interest

$$\rho = 4.2 \text{ } \mu\text{m} \quad ; \quad \Delta = 3.2 \times 10^{-3}.$$

We wish to operate at $V \in (4, 6.5)$, i.e. wavelength in (550nm, 750nm). For the fabricated gratings

$$\zeta = \frac{1}{2} \quad ; \quad \delta = 4 \times 10^{-6},$$

which produces a resonant coupling length around 210 μm . An error of less than 0.1 μm in the periodicity of the grating yields a detuning parameter $|\bar{\gamma}|$ typically less than 6.

For a step fibre, the modal parameters are obtained from the results of weak-guidance [1: ch14]. The propagation constants are given by

$$\beta_\alpha^2 = \tilde{\beta}_\alpha^2 - \Delta \frac{\chi_\alpha}{\|F_\alpha\|^2}$$

where $\tilde{\beta}_\alpha(V)$ is the value found from numerical solution of problem posed by weak guidance, and

$$\chi_\alpha = U_\alpha J_1(U_\alpha)/J_0(U_\alpha) \quad ; \quad U_\alpha^2 = V^2 - W_\alpha^2 \quad ; \quad W_\alpha^2 = \tilde{\beta}_\alpha^2 - k^2 n_0^2.$$

The modal fields give the following integrals:

$$\begin{aligned} \|F_\alpha\|^2 &= \frac{1}{J_0^2(U_\alpha)} \int_0^1 dr r J_0^2(U_\alpha r) + \frac{1}{K_0^2(W_\alpha)} \int_1^\infty dr r K_0^2(W_\alpha r) = \frac{V^2 \chi_\alpha^2}{2U_\alpha^2 W_\alpha^2} \\ G_{\alpha\alpha} &= \frac{1}{\|F_\alpha\|^2} \frac{1}{J_0^2(U_\alpha)} \int_0^1 dr r J_0^2(U_\alpha r) = \frac{W_\alpha^2}{V^2} \left(1 + \frac{U_\alpha^2}{\chi_\alpha^2}\right) \\ G_{12} &= \frac{1}{\|F_1\| \|F_2\|} \frac{1}{J_0(U_1) J_0(U_2)} \int_0^1 dr r J_0(U_1 r) J_0(U_2 r) = \frac{2U_1 U_2 W_1 W_2}{V^2 (W_2^2 - W_1^2)} \left(\frac{1}{\chi_2} - \frac{1}{\chi_1}\right) \\ I_\alpha &= \frac{1}{\|F_\alpha\|^4} \left(\frac{1}{J_0^4(U_\alpha)} \int_0^1 dr r J_0^4(U_\alpha r) + \frac{1}{K_0^4(W_\alpha)} \int_1^\infty dr r K_0^4(W_\alpha r) \right) \\ J &= \frac{1}{\|F_1\|^2 \|F_2\|^2} \left(\frac{1}{J_0^2(U_1) J_0^2(U_2)} \int_0^1 dr r J_0^2(U_1 r) J_0^2(U_2 r) \right. \\ &\quad \left. + \frac{1}{K_0^2(W_1) K_0^2(W_2)} \int_1^\infty dr r K_0^2(W_1 r) K_0^2(W_2 r) \right) \end{aligned}$$

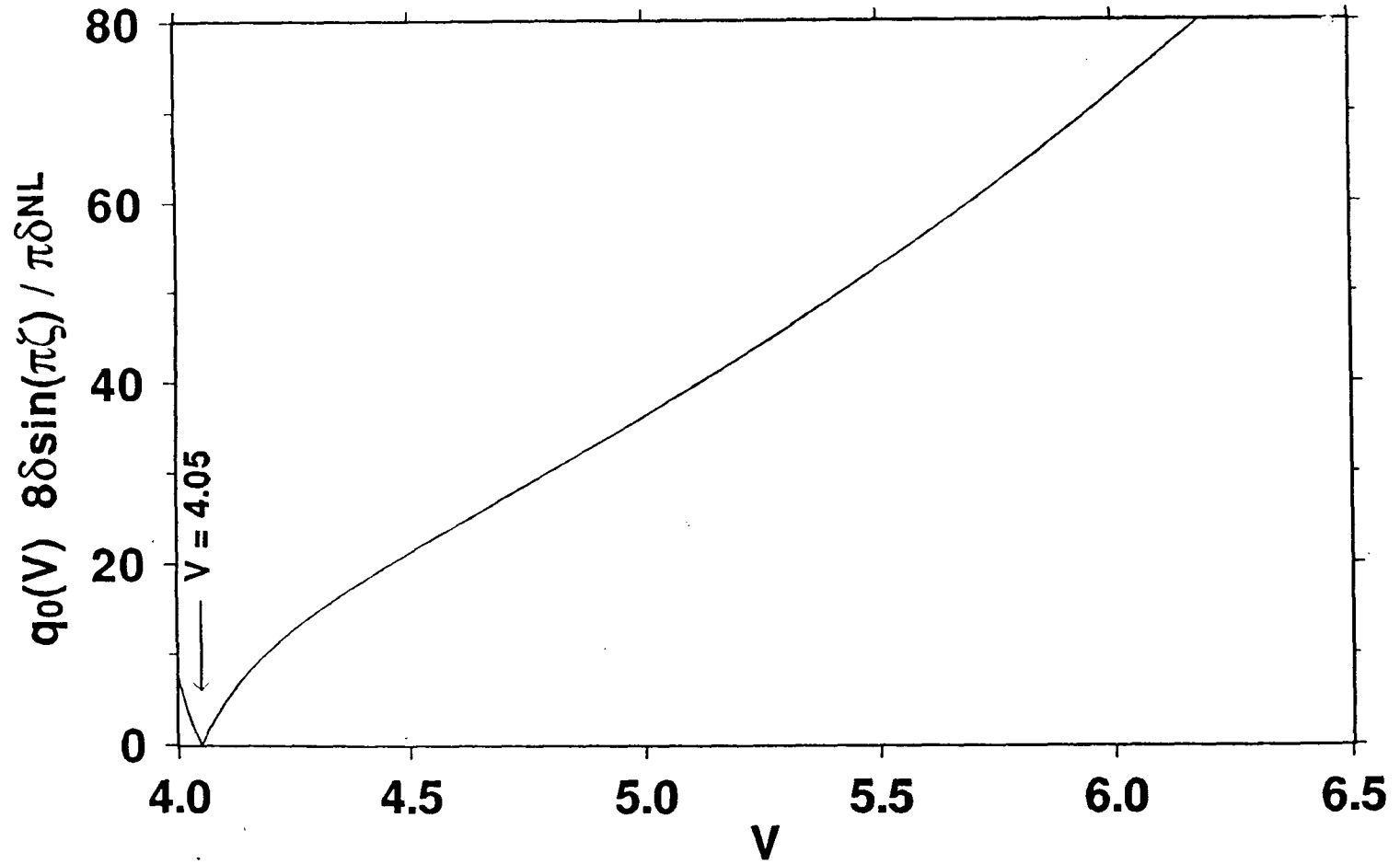


Figure 14: Frequency variation of competition parameter $q_0(V)$

For nonlinear switching in an $LP_{01} \leftrightarrow LP_{02}$ grating, a normalized form of the competition parameter, defined by Eq. (5.17a), is shown as a function of normalized frequency.

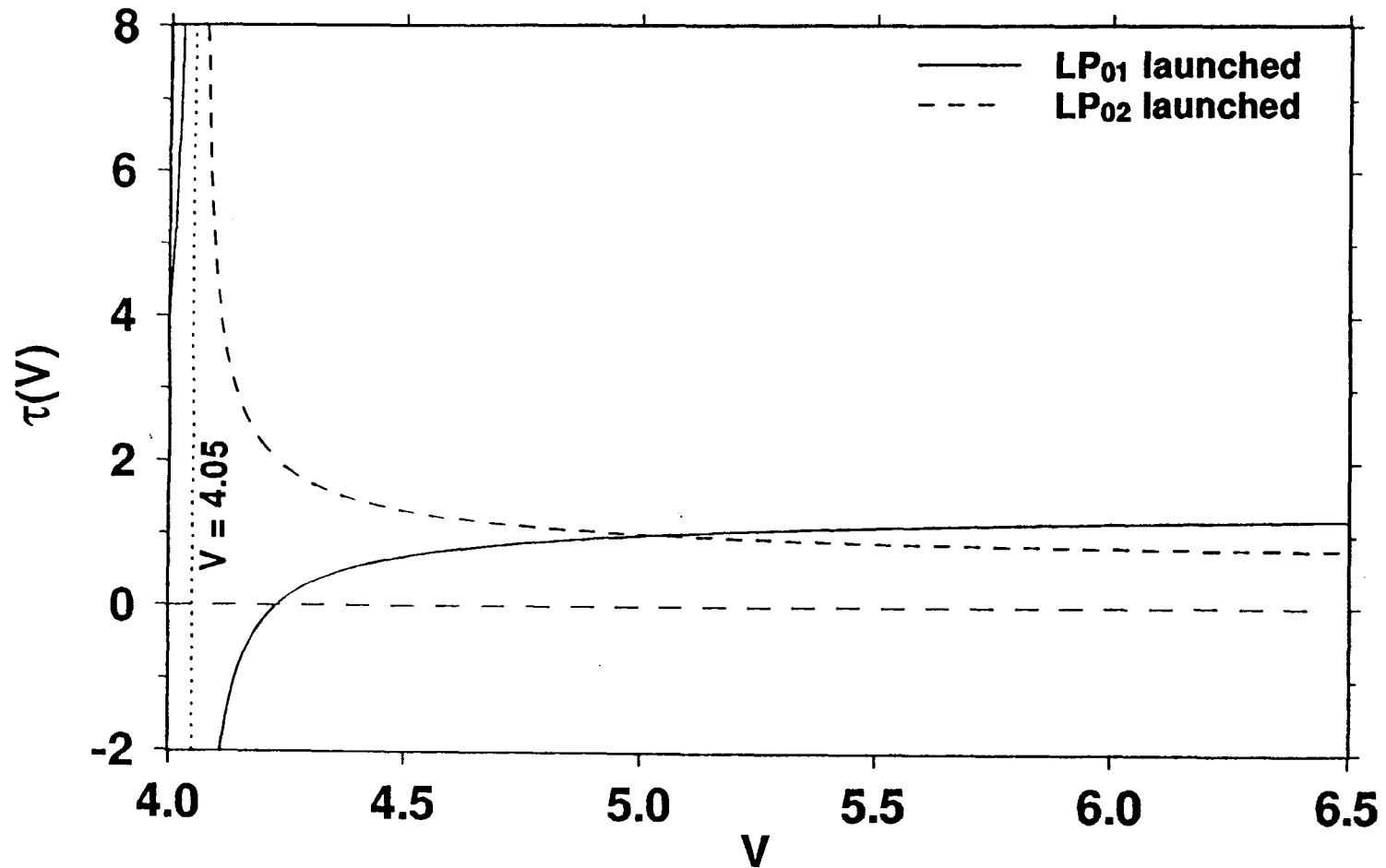


Figure 15: Frequency variation of mismatch parameter $\tau(V)$

For nonlinear switching in an LP₀₁ ↔ LP₀₂ grating, a normalized form of the modal mismatch parameter, defined by Eq. (5.17c), is shown as a function of normalized frequency.

The latter two expressions require numerical evaluation, which is not difficult. Now it is possible to get q_0 and τ . How these vary with V is seen in in Figs. 14 and 15. Of interest is that d_+ changes sign at $V = 4.05$ and $\tau = 1$ at $V = 5.03$.

5.10 NONLINEAR SWITCHING OF LINEARLY TUNED GRATING

For $\bar{\gamma} = 0$, the relevant value of μ is immediate. One finds the power to achieve switching:

$$\begin{aligned} pP_0 &= \frac{P_0 w_D(\frac{8}{9}\tau)}{q_0(V)} = \frac{8\rho^2 \delta n_0 \sin(\pi\zeta)}{n_I} \frac{|G_{12}|}{|I_1 + I_2 - 4J|} w_D(\frac{8}{9}\tau) \\ &= \frac{|G_{12}|}{|I_1 + I_2 - 4J|} w_D(\frac{8}{9}\tau) \quad 3.2 \times 10^4 \text{ Watts,} \end{aligned}$$

using the parameters above. This is shown in Fig. 16. The associated fractional jump in switched power $\xi_J(\frac{8}{9}\tau(V))$ is shown in Fig. 17. For V about 5, the critical power is around 1.6 KW. This is less than the critical power needed for switching in a fibre without a grating. Such a finding is consistent with the finding of Ref. 9.

Observe that the variation with V is very different between switching from the LP_{01} into the LP_{02} mode and switching from the LP_{02} into the LP_{01} mode. For power initially in the LP_{01} mode, switching occurs only if $4.23 < V < 5.62$, and ξ_J is a maximum at $V = 4.69$. For power initially in the LP_{02} mode, switching occurs if $V > 4.74$. The value of ξ_J is approximately constant for $V > 5.5$.

5.11 DETUNING PARAMETER

For linear tuning, the resonant period of the grating Λ_r is related to the operating wavelength by (refer (3.9))

$$\Lambda_r(V) = 2\pi / (\beta_{>} - \beta_{<} + \Delta^{\frac{3}{2}}(C_{>} - C_{<})).$$

For the accuracy worked here, it suffices to use

$$\Lambda_r(V) = 2\sqrt{2}\pi V / \Delta^{\frac{1}{2}}(W_1^2 - W_2^2),$$

which is the scalar approximation for the period of a tuned grating, as obtained previously.

There are two ways to detune the grating.

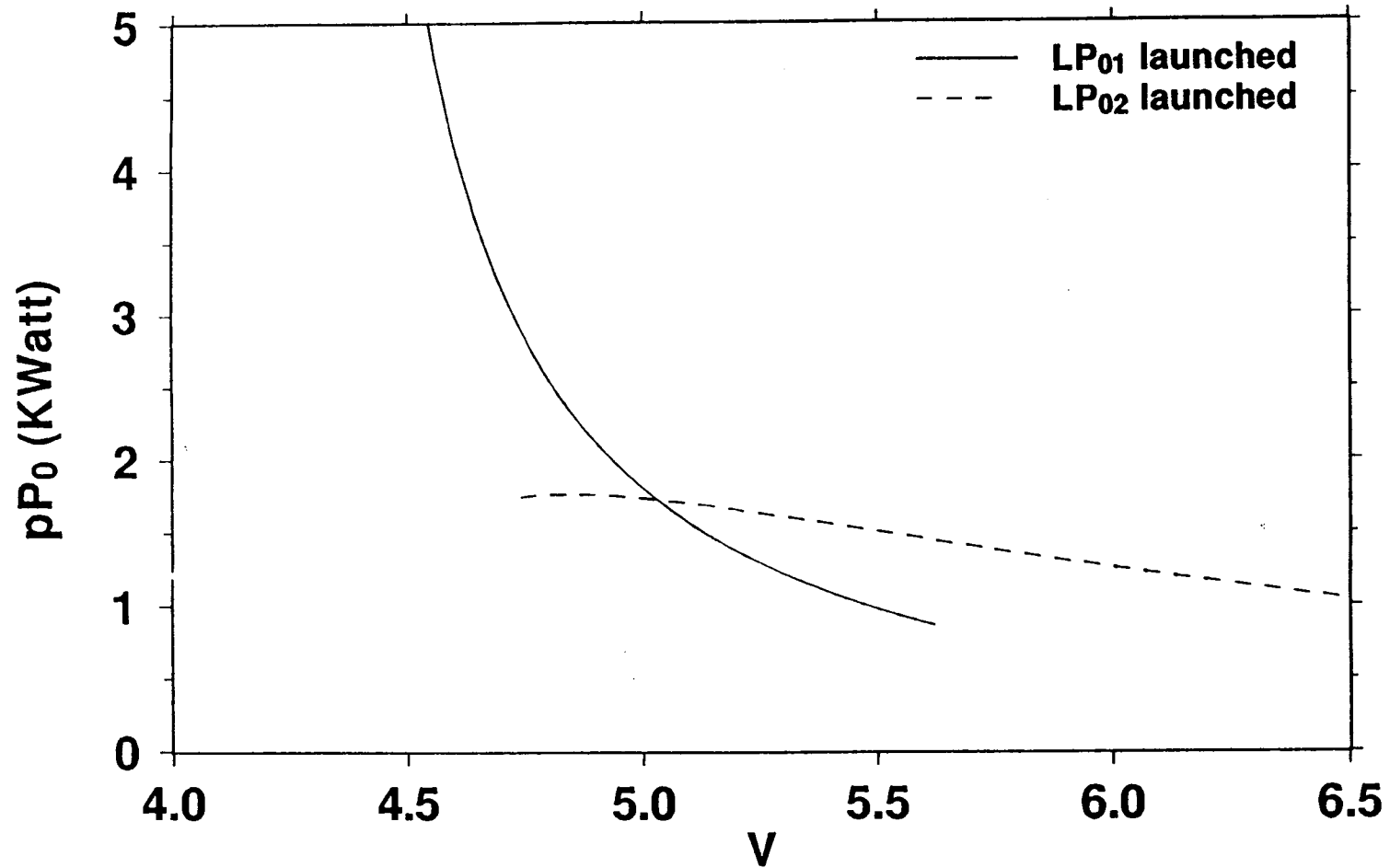


Figure 16: Frequency variation of power required for switching

For the $LP_{01} \leftrightarrow LP_{02}$ grating described in §5.9, the power required to achieve switching, i.e. lowest input power at which the power exchanged between LP_{01} and LP_{02} modes changes discontinuously, is shown as a function of normalized frequency.

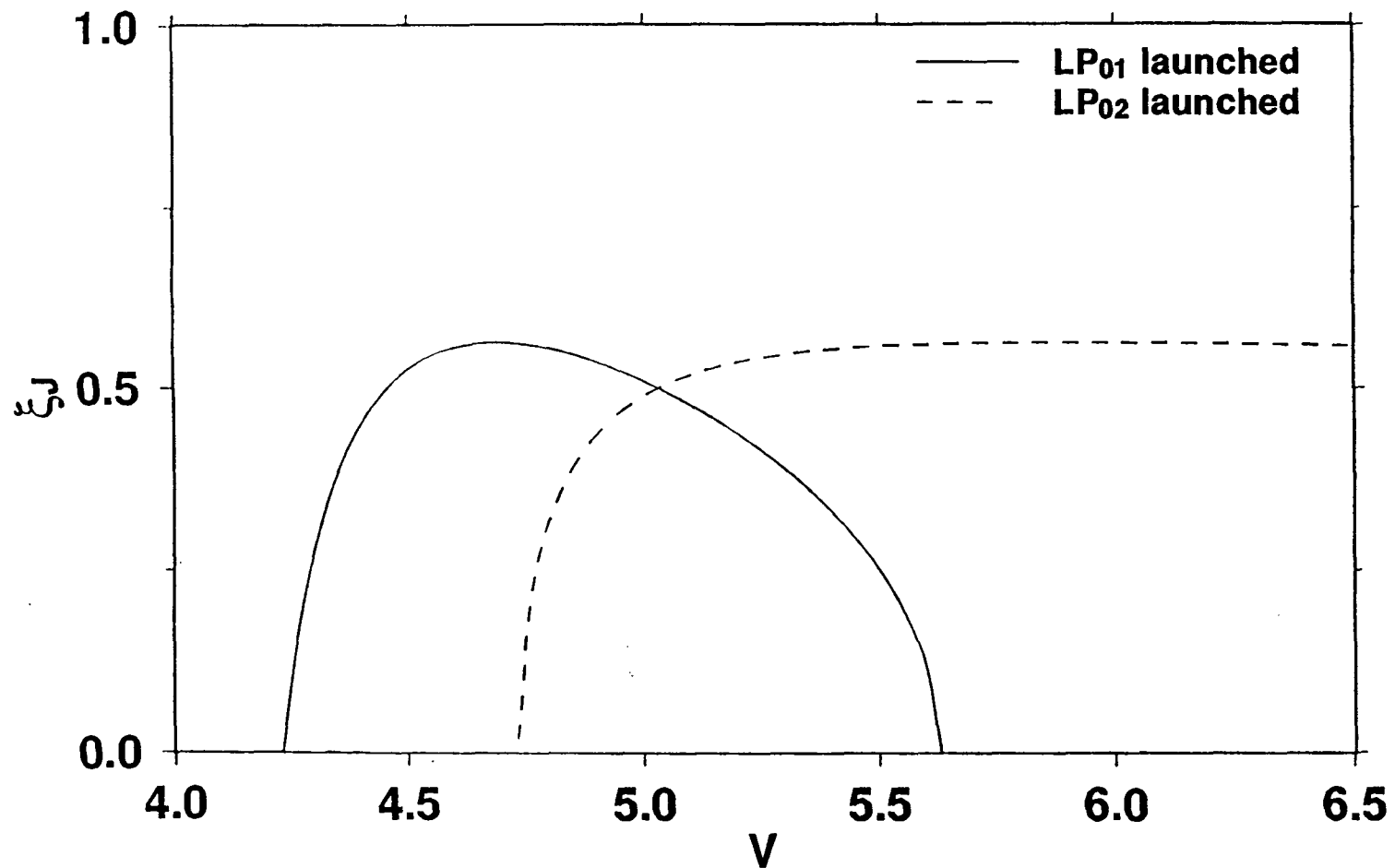


Figure 17: Frequency variation of fractional efficiency of switch

For the $LP_{01} \leftrightarrow LP_{02}$ grating described in §5.9, the size of the discontinuity in the coupled power — as a fraction of input power — is shown as a function of normalized frequency.

Firstly, detune the grating by fixing the operating wavelength and changing the grating's period. With $\Lambda = \Lambda_r \pm \Lambda_\epsilon$, where Λ_ϵ is small, it follows

$$\frac{2\pi}{\Lambda} \approx \frac{2\pi}{\Lambda_r} \mp \Lambda_\epsilon \frac{2\pi}{\Lambda_r^2}$$

$$\Rightarrow \gamma = \Delta^{-\frac{3}{2}} \left(\beta_{<} - \beta_{>} + \frac{2\pi}{\Lambda} \right) + C_{<} - C_{>} \approx \mp \Lambda_\epsilon \Delta^{-\frac{3}{2}} \frac{2\pi}{\Lambda_r^2}.$$

Thus, it follows that

$$\begin{aligned} \bar{\gamma}_\Lambda &= \text{sgn}(d_+) \frac{\Delta^2}{\delta} \frac{\pi}{\sqrt{2} \sin \pi \zeta} \frac{1}{V |G_{12}|} \frac{\mp \Lambda_\epsilon 2\pi}{\Delta^{\frac{3}{2}} \Lambda_r^2} \\ &= \mp \Lambda_\epsilon \text{sgn}(d_+) \frac{1}{\sqrt{\Delta}} \frac{\Delta^2}{\delta} \frac{1}{4\sqrt{2} \sin \pi \zeta} \frac{(W_1^2 - W_2^2)^2}{V^3 |G_{12}(V)|} \\ &= \mp \Lambda_\epsilon \text{sgn}(d_+) 8 \frac{(W_1^2 - W_2^2)^2}{V^3 |G_{12}(V)|}, \end{aligned} \quad (5.19)$$

using the scalar approximation for $\Lambda_r(V)$ and the values for the fibre's parameters given above.

Secondly, detune the grating by fixing its period, and changing the operating frequency from the resonant value V_r to $V_r \pm V_\epsilon$ with $V_\epsilon \ll V_r$. This is the more useful procedure. Previously, it was shown that

$$\gamma(V_r \pm V_\epsilon) \approx \pm V_\epsilon \gamma'(V_r) = \pm V_\epsilon \frac{1}{2\sqrt{2}\Delta V^2} (W_2^2(1 + 2\frac{U_2^2}{\chi_2^2}) - W_1^2(1 + 2\frac{U_1^2}{\chi_1^2})).$$

The value of $V G_{12}(V)$ changes very slowly; it is assumed constant for the small change in V . Hence,

$$\begin{aligned} \bar{\gamma}_\nu &= \text{sgn}(d_+) \frac{\Delta^2}{\delta} \frac{\pi}{\sqrt{2} \sin \pi \zeta} \frac{1}{V |G_{12}|} \frac{\pm V_\epsilon}{2\sqrt{2}\Delta V^2} (W_2^2(1 + 2\frac{U_2^2}{\chi_2^2}) - W_1^2(1 + 2\frac{U_1^2}{\chi_1^2})) \\ &= \pm V_\epsilon \text{sgn}(d_+) \frac{\Delta}{\delta} \frac{\pi}{4 \sin \pi \zeta} \frac{W_2^2(1 + 2\frac{U_2^2}{\chi_2^2}) - W_1^2(1 + 2\frac{U_1^2}{\chi_1^2})}{V_r^3 |G_{12}(V_r)|} \\ &= \pm V_\epsilon \text{sgn}(d_+) 628.3 \frac{W_2^2(1 + 2\frac{U_2^2}{\chi_2^2}) - W_1^2(1 + 2\frac{U_1^2}{\chi_1^2})}{V_r^3 |G_{12}(V_r)|}, \end{aligned} \quad (5.20)$$

where the values of W_α and U_α are those pertinent to V_r . For slight frequency detuning, observe that $(V - V_r)/V_r = (\omega - \omega_r)/\omega_r = (l_r - l)/l_r$.

The variation of $\bar{\gamma}$ with V , via the two forms $\bar{\gamma}_\nu$ and $\bar{\gamma}_\Lambda$, is seen in Fig. 18.

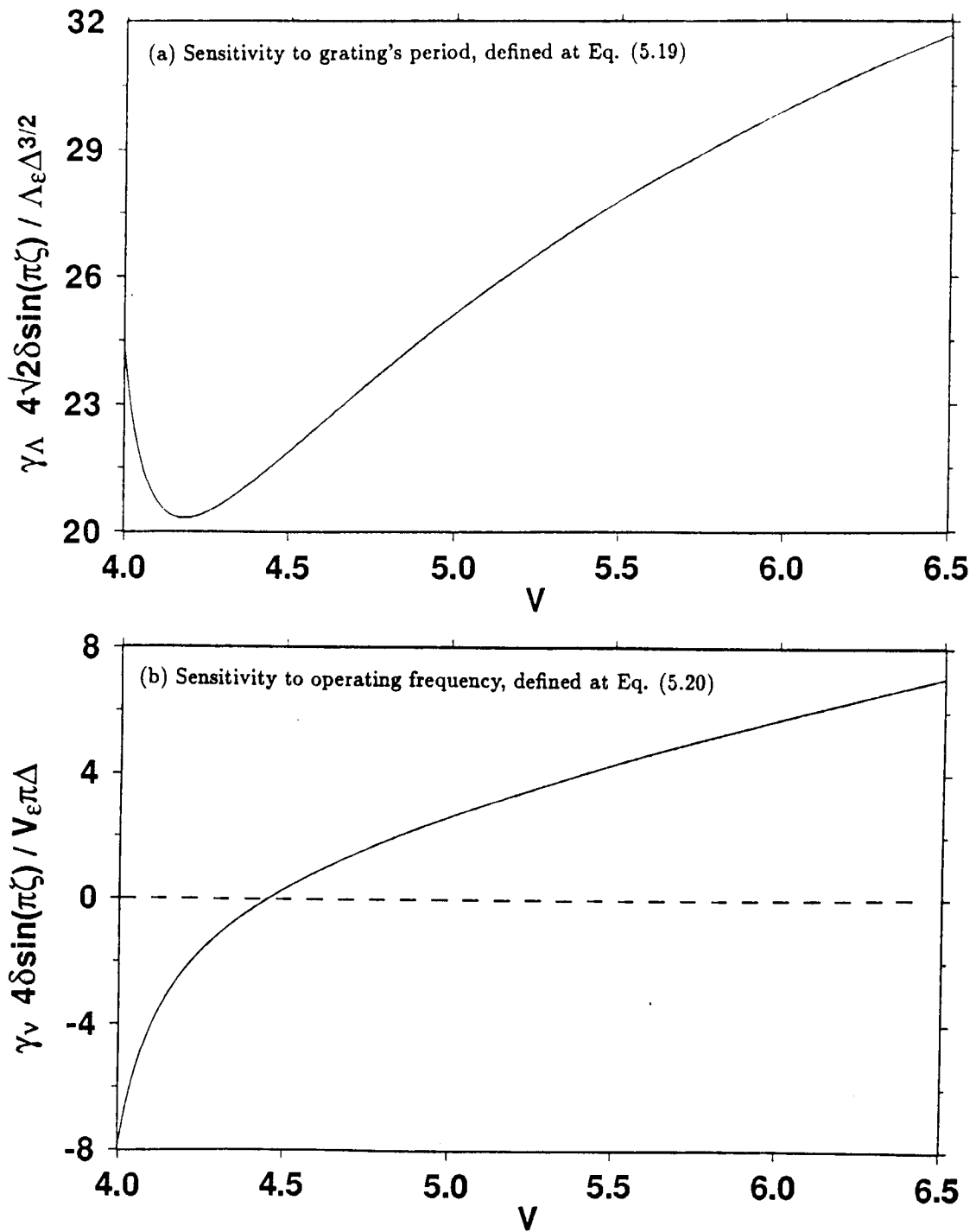


Figure 18: Frequency variation of detuning parameters

For nonlinear switching in an $LP_{01} \leftrightarrow LP_{02}$ grating, normalized forms of the detuning parameter's sensitivity is shown as a function of normalized frequency.

5.12 NONLINEAR SWITCHING OF DETUNED GRATING

The same qualitative findings apply to the detuned grating as to the tuned grating. The amount of power exchanged between the guides may change discontinuously as the launched power increases. To see if this happens, study Fig. 28. By finding the value of μ relevant to the pair $(\tau, \bar{\gamma})$, as fixed by (D.2), one finds the power to achieve switching:

$$\begin{aligned} pP_0 &= \frac{P_0 w_D(\mu)}{q_0(V)} = \frac{8\rho^2 \delta n_0 \sin(\pi\zeta)}{n_I} \frac{|G_{12}|}{|I_1 + I_2 - 4J|} w_D(\mu) \\ &= \frac{|G_{12}|}{|I_1 + I_2 - 4J|} w_D(\mu) \quad 3.2 \times 10^4 \text{ Watts,} \end{aligned}$$

using the parameters above.

Compared with the case of $\bar{\gamma} = 0$, the detuned grating offers the possibility of a lower value of the switching power. Selecting the value of $\mu(V)$ to maximize ξ_J fixes $w_D(\mu)$. The value of $\bar{\gamma}$ can be varied to keep μ fixed, while the value of $\tau(V)$ is varied to increase the value of $q_0(V)$ and thus decrease pP_0 . Within the range of operation shown, this can reduce the required power by about a half. Suppose the optimal value of μ , notably $\frac{3}{4}$, is selected, and power is launched in the LP_{01} mode. For $\bar{\gamma} = 0$, this value of μ corresponds to $V = 4.69$ and $q_0(4.69) = 26.9$. Since $q_0(5.53) = 53.8$, then the value of pP_0 , when operating at $V = 5.53$ and $\mu = \frac{3}{4}$, is half that needed when operating at $\bar{\gamma} = 0$ and $V = 4.69$. As $\tau(5.53) = 1.11$, to retain $\mu = \frac{3}{4}$ it follows that $\bar{\gamma} = 0.736$. To obtain this value of $\bar{\gamma}$ by detuning, choose either $\Lambda_\epsilon = 3.29 \times 10^{-3}$ or $V_\epsilon = 2.65 \times 10^{-4}$.

6.0 CONCLUSION

A comprehensive mathematical description of the phenomena of mode conversion by a grating written in an optical fibre was presented. It improved upon previous theories by taking cognition of the possibility that the grating may not be axisymmetric. This couples modes in more complicated combinations than previously considered, and means that true modes, and not LP modes, have to be used.

The theory took two parts: the exchange of power between modes; the exact form of the higher-order modes, a form which changes during passage through a non-axisymmetric grating. The latter produced a curious result: while a mode seen on an axisymmetric fibre approaches the limiting form of one of the well-known LP₁₁ modes, which particular form changes during transit through the grating and may, indeed, be frequency dependent.

The former allowed quite good modelling of the measurable output of actual gratings — both LP₀₁ ↔ LP₀₂ and LP₀₁ ↔ LP₁₁. The theory predicted that, in forming the grating, the slight changes made to the refractive index are very weakly anisotropic. The relative difference between the variations to the two transverse indices (i.e those sensed by X- or Y-polarized light) is of the order of 0.1%. Also, an analysis was able to bound the theoretic linewidth as seen in the spectral response curve. This bound was less than that observed experimentally, and, under typical design, sets a limit of a FWHM of approximately $\frac{1}{2}\Delta$ on the response peak in the V -spectrum.

The feasibility of using the LP₀₁ ↔ LP₀₂ grating as an all-optical switch was demonstrated. Although its properties were found to be quite frequency dependent, quite general mathematical results allowed their determination. For example, with power initially in the LP₀₁ mode at the resonant wavelength, switching occurs only if $4.23 < V < 5.62$. The maximum fractional jump in switched power that can be achieved, under any operating conditions, is 9/16. The power needed to operate such a switch was shown to be reduced by operating the switch away from the wavelength corresponding to resonance in the linear régime. in either the LP₀₁ or LP₀₂ mode. The theory showed that the behaviour of the

switch depends on the choice of initial mode.

Of course, work remains to be done. In particular, to better illustrate the operation of nonlinear switching in an $LP_{01} \leftrightarrow LP_{02}$ grating, spectral response curves akin to Fig. 5 could be generated for various levels of input power.

7.0 ACKNOWLEDGEMENTS & REFERENCES

ACKNOWLEDGEMENTS

I must begin by acknowledging that this work owes its existence to the direction of Dr Ken Hill. I wish to thank my other colleagues at DOCT for useful discussions on the matters described herein and, especially, Mr Bernard Malo who carefully performed so many experiments at my prompting.

Dr Richard Black of the Ecole Polytechnique, Montréal, provided the scalar propagation constants $U_\alpha(V)$ and $W_\alpha(V)$ of the LP_{01} , LP_{11} and LP_{02} modes on a step fibre. I also thank him for a pre-publication copy of Ref. 24, and helpful discussions on the theory expounded in Appendix B.

REFERENCES

- 1 A.W.Snyder & J.D.Love, *Optical Waveguide Theory*, Chapman & Hall, London (1983).
- 2 A.Yariv & P.Yeh, *Optical Waves in Crystals*, Wiley, New York (1984).
- 3 E.A.Coddington & N.Levinson, *Theory of Ordinary Differential Equations*, McGraw-Hill, New York (1955)
- 4 G.Meltz, W.W.Morey & W.H.Glenn, "Formation of Bragg gratings in optical fibers by a transverse holographic method", *Opt Lett* 14 (1989) 823-825
- 5 F.Bilodeau, K.O.Hill, B.Malo, D.C.Johnson & I.M.Skinner, "Efficient, narrowband $LP_{01} \leftrightarrow LP_{02}$ mode converters fabricated in photosensitive fibre: spectral response", *Electron Lett.* 27 (1991) 682-684
- 6 D.K.W.Lam & B.K.Garside, "Characterization of single-mode optical fiber filters", *Appl Optics* 20 (1981) 440-445
- 7 M.Abramowitz & I.A.Stegun (eds), *Handbook of Mathematical Functions*, National Bureau of Standards, Washington (1964)

- 8 K.O.Hill, B.Malo, K.A.Vineberg, F.Bilodeau, D.C.Johnson & I.M.Skinner, "Efficient mode conversion in telecommunication fibre using externally written gratings", *Electron. Lett.* **26** (1990) 1270-1271.
- 9 S.Trillo, S.Wabnitz & G.I.Stegeman, "Nonlinear codirectional guided wave mode conversion in grating structures", *J Lightwave Technol* **6** (1988) 971-976
- 10 S.M.Jensen, "The nonlinear coherent coupler", *J Quantum Electron* **18** (1982) 1580-1583
- 11 S.Trillo & S.Wabnitz, "Nonlinear nonreciprocity in a coherent mismatched directional coupler", *Appl Phys Lett* **49** (1986) 752-754
- 12 B.Daino, G.Gregori & S.Wabnitz, "Stability analysis of nonlinear coherent coupling" *J Appl Phys* **58** (1985) 4512-4514
- 13 K.L.Sala, "Nonlinear refractive-index phenomena in isotropic media subjected to a dc electric field: Exact solutions", *Phys Rev A* **29** (1984) 1944-1956
- 14 F.Matera & S.Wabnitz, "Nonlinear polarization evolution and instability in a twisted birefringent fiber", *Opt Lett* **11** (1986) 467-469
- 15 A.Ankiewicz, "Novel effects in nonlinear coupling", *Opt Quantum Electron* **20** (1988) 329-337
- 16 Y.Chen, "Solution to full coupled wave equations of nonlinear coupled systems", *J Quantum Electron* **25** (1989) 2149-2153
- 17 F.J.Fraile-Pelaez & G.Assanto, "Coupled-mode equations for nonlinear directional couplers", *Appl Opt* **29** (1990) 2216-2217
- 18 S.J.Garth & C.Pask, "Polarization rotation in nonlinear bimodal optical fibers", *J Lightwave Technol* **8** (1990) 129-137
- 19 Y.Silberberg & G.I.Stegeman, "Nonlinear coupling of waveguide modes", *Appl Phys Lett* **50** (1987) 801-803

- 20 I.M.Skinner & C.Pask, "Raman frequency shift and second-order solitons in optical fibres", to be submitted to *Opt Lett*
- 21 R.Courant & D.Hilbert, *Methods of Mathematical Physics*, vol 1, Interscience, New York (1953).
- 22 A.W.Snyder, J.D.Love & R.A.Sammut, "Green's function methods for analyzing optical fiber perturbations", *J Opt Soc Am* **72**(1982) 1131-1135
- 23 A.W.Snyder & W.R.Young, "Modes of Optical Waveguides", *J Opt Soc Am* **68** (1978) 297-309
- 24 R.J.Black, L.Gagnon & G.E.Stedman, "Symmetry principles for lightguides. I. Single-core and few-mode fibers and basic formalism", to be submitted to *J Opt Soc Am A*
- 25 J.Mathews & R.L.Walker, *Mathematical Methods of Physics*, 2nd ed., Benjamin/Cummings, Menlo Park (1970)
- 26 R.J.Black & C.Pask, "Equivalent optical waveguides", *J Lightwave Technol* **2** (1984) 268-276
- 27 A.Erdélyi, W.Magnus, F.Oberhettinger, & F.G.Tricomi, *Higher Transcendental Functions*, vol 2, McGraw-Hill, New York (1953)
- 28 I.S.Gradstein & I.M.Ryshik, *Tables of Series, Products and Integrals*, Verlag Harri Deutsch, Frankfurt (1981)

APPENDIX A

Two Coupled Linear Differential Equations

A.1 PERIODIC SOLUTION

Consider the system defining functions of a real variable x

$$\begin{pmatrix} a_1'(x) \\ a_2'(x) \end{pmatrix} = i \begin{pmatrix} 0 & M e^{i2\Gamma x} \\ M^* e^{-i2\Gamma x} & 0 \end{pmatrix} \begin{pmatrix} a_1(x) \\ a_2(x) \end{pmatrix},$$

with Γ real.

With the definition

$$\mu^2 = |M|^2 + \Gamma^2,$$

the solution can be written as

$$\begin{aligned} a_1(x) &= e^{i\Gamma x} (B \cos(\mu x) + C \sin(\mu x)) \\ &= e^{i\Gamma x} \left(\frac{B - iC}{2} e^{i\mu x} + \frac{B + iC}{2} e^{-i\mu x} \right) \\ a_2(x) &= e^{-i\Gamma x} \left(\frac{B\Gamma - iC\mu}{M} \cos(\mu x) + \frac{C\Gamma + iB\mu}{M} \sin(\mu x) \right) \\ &= e^{-i\Gamma x} \left(\frac{(B - iC)(\Gamma + \mu)}{2M} e^{i\mu x} + \frac{(B + iC)(\Gamma - \mu)}{2M} e^{-i\mu x} \right), \end{aligned}$$

where B and C are constants, determined by the boundary conditions imposed. For all $|M|$ and Γ , these solutions are strictly periodic.

Of particular interest are the boundary conditions $a_1(0) = 1$ and $a_2(0) = 0$, which gives

$$\begin{aligned} B = 1 & \quad ; \quad C = \frac{-i\Gamma}{\mu}; \\ B\Gamma - iC\mu = 0 & \quad ; \quad \frac{C\Gamma + iB\mu}{M} = \frac{iM^*}{\mu}. \end{aligned}$$

This gives the familiar result

$$|a_1(x)|^2 = 1 - \frac{1}{1 + \frac{\Gamma^2}{|M|^2}} \sin^2(\mu x).$$

A.2 EXPONENTIAL SOLUTION

Consider the system defining functions of a real variable x

$$\begin{pmatrix} a_1'(x) \\ a_2'(x) \end{pmatrix} = i \begin{pmatrix} 0 & M e^{i2\Gamma x} \\ -M^* e^{-i2\Gamma x} & 0 \end{pmatrix} \begin{pmatrix} a_1(x) \\ a_2(x) \end{pmatrix},$$

with Γ real.

With the definition

$$\mu^2 = |M|^2 - \Gamma^2,$$

the solution can be written as

$$\begin{aligned} a_1(x) &= e^{i\Gamma x} (B \cosh(\mu x) + C \sinh(\mu x)) \\ &= e^{i\Gamma x} \left(\frac{B+C}{2} e^{\mu x} + \frac{B-C}{2} e^{-\mu x} \right) \\ a_2(x) &= -e^{-i\Gamma x} \left(\frac{iB\Gamma + C\mu}{M} \cosh(\mu x) + \frac{iC\Gamma + B\mu}{M} \sinh(\mu x) \right) \\ &= -e^{-i\Gamma x} \left(\frac{(i\Gamma + \mu)(B+C)}{2M} e^{\mu x} + \frac{(i\Gamma - \mu)(B-C)}{2M} e^{-\mu x} \right), \end{aligned}$$

where B and C are constants, determined by the boundary conditions imposed. For $|\Gamma| < |M|$, these solutions are exponential in form. When $|\Gamma| > |M|$, then μ becomes imaginary, and these solutions are strictly periodic.

Consider the case when $|\Gamma| < |M|$. Of particular interest are the boundary conditions $a_1(0) = 1$ and $a_2(L) = 0$, which give

$$B = 1 \quad ; \quad C = - \left(\frac{\mu \tanh(\mu L) + i\Gamma}{\mu + i\Gamma \tanh(\mu L)} \right).$$

This gives the result that

$$|a_2(0)|^2 = \sinh^2(\mu L) / (\cosh^2(\mu L) - \frac{\Gamma^2}{|M|^2}).$$

APPENDIX B

Modes in Periodically, Axi-Asymmetrically Perturbed Fibre

For completeness, we first enumerate the relevant properties of the straight circular fibre, and then develop the z -dependent properties of the modes by perturbation methods [e.g. 1]. Attention is restricted to the first six modes of the waveguide, but other modes can be examined by analogous methods. These six are the two polarization states of the fundamental mode which correspond to the LP_{01} mode; and the odd and even HE_{21} mode, the TE_{01} mode, and the TM_{01} mode, which all correspond to the LP_{11} mode.

Position within the cross-section of the fibre is given by polar coordinates (r, θ) . The refractive index profile of the axisymmetric fibre is given by

$$n^2(r) = n_0^2(1 + 2\Delta\bar{g}(r)),$$

where n_0 is the constant refractive index of the cladding and Δ is the customary profile height parameter. Working with weakly guiding fibres means $\Delta \ll 1$. The periodic axisymmetric feature of the refractive index is described by the Λ -periodic function $g_1(r, \theta, z)$ so that the shape function becomes

$$g(r, \theta, z) = \bar{g}(r) + \frac{\delta}{\Delta}g_1(r, \theta, z)$$

where the perturbation is weak, i.e. $\delta \ll \Delta$.

As a notational device, a tilde over a modal property will indicate it applies to the local scalar modes of the waveguide. A bar over a quantity indicates it applies to the axially invariant waveguide. The normalized frequency is defined as

$$V^2 = k^2\rho^2n_0^22\Delta,$$

where k is the free-space wavenumber and ρ is the core radius. Henceforth, all length quantities will be scaled by ρ , unless otherwise explicitly stated.

B.1 INDEXING MODES

The VC modes on the unperturbed fibre will be enumerated by the system

$$\begin{aligned}\bar{\mathbf{E}}_1 &= F_0(r) \hat{\mathbf{x}} \quad ; \quad \bar{\mathbf{E}}_2 = F_0(r) \hat{\mathbf{y}} \\ \bar{\mathbf{E}}_3 &= F_1(r)(\cos \theta \hat{\mathbf{x}} - \sin \theta \hat{\mathbf{y}}) \quad ; \quad \bar{\mathbf{E}}_4 = F_1(r)(\cos \theta \hat{\mathbf{x}} + \sin \theta \hat{\mathbf{y}}) \\ \bar{\mathbf{E}}_5 &= F_1(r)(\sin \theta \hat{\mathbf{x}} + \cos \theta \hat{\mathbf{y}}) \quad ; \quad \bar{\mathbf{E}}_6 = F_1(r)(-\sin \theta \hat{\mathbf{x}} + \cos \theta \hat{\mathbf{y}})\end{aligned}\tag{B.1}$$

so that $\bar{\mathbf{E}}_1$ is the X-polarized fundamental mode; $\bar{\mathbf{E}}_2$ is the Y-polarized fundamental mode; $\bar{\mathbf{E}}_3$ is the even HE_{21} mode; $\bar{\mathbf{E}}_4$ the TM_{01} mode; $\bar{\mathbf{E}}_5$ the odd HE_{21} mode; and $\bar{\mathbf{E}}_6$ the TE_{01} mode. Notice there is a change in the customary convention [e.g. 1: p304], by reversing the sign of the TE_{01} mode. When the local modes in the grating are examined, they, too, will be enumerated by this system so that the index j will be on the mode which corresponds to $\bar{\mathbf{E}}_j$ on the straight circular fibre. The corresponding index will be meaningful on the propagation constants β_j , which include the polarization corrections.

Working with scalar modes on this same waveguide, there are the fundamental or LP_{01} mode, indexed by f , and two forms — an odd and an even — of the LP_{11} mode, which will be indexed separately by subscripts o, e or together by h . The odd-even symmetry is determined from the symmetry axes defined by the perturbation, and is usually obvious from inspection. It will be assumed that it is. (If it is not, then the separation of the two families described below will not happen, but the analysis can proceed [e.g. 1: pp289,633f].) Certainly the perturbation motivating this study — the $\text{LP}_{01} \leftrightarrow \text{LP}_{11}$ grating — has obvious symmetry. So do the much examined elliptical perturbations of circular cores.

B.2 MODES OF STRAIGHT CIRCULAR FIBRE

For the straight, circular fibre, the vector form of the six modes was given at (B.1) above.

The polarization corrections to the propagation constants follow [e.g. 1: p304] as

$$\begin{aligned}\bar{\beta}_1^2 &= \bar{\beta}_2^2 = \beta_f^2 - \Delta I_0 \\ \bar{\beta}_3^2 &= \bar{\beta}_5^2 = \beta_h^2 - \Delta(I_1 - I_2) \\ \bar{\beta}_4^2 &= \beta_h^2 - \Delta 2(I_1 + I_2) \\ \bar{\beta}_6^2 &= \beta_h^2\end{aligned}\tag{B.2}$$

where β_f and β_h are the scalar propagation constants of the LP₀₁ and LP₁₁ modes, respectively, as determined by the weak guidance theory, $F_1(r)$ and $F_0(r)$ are the radial dependence of the LP₁₁ and LP₀₁ scalar modes, respectively, with $\|F_j\|^2 = \int_0^\infty dr r F_j^2(r)$, and

$$\begin{aligned} I_0 &= \frac{1}{\|F_0\|^2} \int_0^\infty dr r F_0(r) F_0'(r) g'(r); \\ I_1 &= \frac{1}{\|F_1\|^2} \int_0^\infty dr r F_1(r) F_1'(r) g'(r); \\ I_2 &= \frac{1}{\|F_1\|^2} \int_0^\infty dr F_1^2(r) g'(r). \end{aligned}$$

These are known, at least numerically.

B.3 PERTURBED SOLUTIONS FOR LOCAL MODES

Using perturbation analysis [e.g. 1: p376], the properties of the local modes can be found very easily from those of the modes on the unperturbed fibre. The sub-domain $\mathcal{D}(z)$ of the infinite cross-section of the fibre is that portion in which $g_1(r, \theta, z) \neq 0$ at position z . The scalar propagation constants $\tilde{\beta}_j$, with $j = f, e, o$, follow as

$$\begin{aligned} \tilde{\beta}_j^2 &= \bar{\beta}_j^2 + \frac{\delta}{\Delta} \frac{V^2}{\|\bar{\psi}_j\|^2} \int_{\mathcal{D}(z)} dS g_1(r, \theta, z) \bar{\psi}_j^2 \\ &= \bar{\beta}_j^2 + \frac{\delta}{\Delta} V^2 \xi_j + \frac{\delta}{\Delta} V^2 q_j(z), \end{aligned} \quad (\text{B.3})$$

with the definitions

$$q_j(z) = -\xi_j + \frac{1}{\|\bar{\psi}_j\|^2} \int_{\mathcal{D}(z)} dS g_1(r, \theta, z) \bar{\psi}_j^2, \quad (\text{B.4})$$

$$\begin{aligned} \xi_j &= \frac{1}{\|\bar{\psi}_j\|^2 \Lambda} \int_0^\Lambda dz \int_{\mathcal{D}(z)} dS g_1(r, \theta, z) \bar{\psi}_j^2 \\ &= \frac{1}{\|\bar{\psi}_j\|^2} \int_{\mathcal{C}_\infty} dS \bar{\psi}_j^2 \frac{1}{\Lambda} \int_0^\Lambda dz g_1(r, \theta, z), \end{aligned} \quad (\text{B.5})$$

The value of these definitions is that the average of $q_j(z)$, over the period Λ , vanishes.

Similarly, there exist perturbation methods to generate corrections to the scalar modal fields. In particular, use of Green functions [e.g. 21, 22] gives a workable solution. However, these corrections will not be relevant in the ensuing analysis and so the details of such corrections will not be pursued here.

B.4 DETAILS: FUNDAMENTAL MODES

Explicitly, from (B.3), (B.4) and (B.5), for the scalar fundamental mode it follows that

$$\tilde{\beta}_f^2(s(z)) = \bar{\beta}_f^2 + \frac{\delta}{\Delta} V^2(\xi_f + q_f(z)), \quad (\text{B.6})$$

with

$$q_f(z) = -\xi_f + \frac{1}{\|F_0\|^2} \int_0^\infty dr r F_0^2(r) \frac{1}{2\pi} \int_0^{2\pi} d\theta g_1(r, \theta, z)$$

$$\xi_f = \frac{1}{\|F_0\|^2} \int_0^\infty dr r F_0^2(r) \frac{1}{2\pi\Lambda} \int_0^\Lambda dz \int_0^{2\pi} d\theta g_1(r, \theta, z).$$

The two vector forms of the scalar fundamental mode continue to be the X- and Y-polarized HE₂₁ modes throughout the z -variation.

As mentioned above, the scalar field will include a perturbation correction term that does not contribute to any further details, and will be ignored. Why? The usual formalism [1: p288] gives the vector correction to β from the scalar modal field $\bar{\psi}$ by

$$\beta^2(z) \approx \tilde{\beta}^2(z) - \frac{2\Delta}{\|\bar{\psi}_f\|^2} \left\langle \frac{\partial \bar{\psi}_f}{\partial P}, \bar{\psi}_f \frac{\partial g}{\partial P} \right\rangle$$

for the P -polarized fundamental mode. Since the perturbation corrections to ψ are of order $\frac{\delta}{\Delta}, \Delta$, their contribution to the vector correction of β is at least an order of magnitude smaller than the correction found without them. This is why corrections to ψ are ignored.

Thus, the vector correction to the fundamental scalar propagation constant, anywhere in the z -varying fibre, is exactly the vector correction to the fundamental scalar propagation constant on the unperturbed fibre. At position z along the grating, the local values of $\beta_1(z)$ and $\beta_2(z)$ follow:

$$\beta_1^2(z) = \beta_2^2(z) = \bar{\beta}_f^2 + \frac{\delta}{\Delta} V^2 \xi_f + \frac{\delta}{\Delta} V^2 q_f(z) - \Delta I_0 + O(\delta) + O(\Delta^2). \quad (\text{B.7})$$

The first term in this expression is the scalar approximation of the unperturbed axisymmetric fibre; the second is the average correction to this scalar value over a period Λ ; the third is the effect of the local axi-asymmetry; the fourth term is the polarization correction to the propagation constant.

B.5 DETAILS: HIGHER-ORDER MODES

For the even and odd modes, substitution of $\bar{\psi} = F_1(r) \cos \theta$ and $\bar{\psi} = F_1(r) \sin \theta$, respectively, into (B.3), (B.4) and (B.5) produces

$$\tilde{\beta}_e^2(z) = \bar{\beta}_h^2 + \frac{\delta}{\Delta} V^2 (\xi_e + q_e(z)) \quad (\text{B.8})$$

$$q_e(z) = -\xi_e + \frac{1}{\pi \|F_1\|^2} \int_{\mathcal{D}(z)} dS g_1(r, \theta, z) F_1^2(r) \cos^2 \theta$$

$$\xi_e = \frac{1}{\pi \|F_1\|^2 \Lambda} \int_{\mathcal{C}_\infty} dS F_1^2(r) \cos^2 \theta \int_0^\Lambda dz g_1(r, \theta, z),$$

$$\tilde{\beta}_o^2(z) = \bar{\beta}_h^2 + \frac{\delta}{\Delta} V^2 (\xi_o + q_o(z)) \quad (\text{B.9})$$

$$q_o(z) = -\xi_o + \frac{1}{\pi \|F_1\|^2} \int_{\mathcal{D}(z)} dS g_1(r, \theta, z) F_1^2(r) \sin^2 \theta$$

$$\xi_o = \frac{1}{\pi \|F_1\|^2 \Lambda} \int_{\mathcal{C}_\infty} dS \int_0^\Lambda dz F_1^2(r) \sin^2 \theta g_1(r, \theta, z).$$

Also define the average, local, higher-order scalar propagation constant as

$$\begin{aligned} \tilde{\beta}_h^2(z) &= \frac{1}{2} (\tilde{\beta}_o^2(z) + \tilde{\beta}_e^2(z)) = \bar{\beta}_h^2 + \frac{\delta}{\Delta} V^2 \frac{1}{2} (\xi_o + \xi_e + q_e(z) + q_o(z)) \\ &= \tilde{\beta}_a^2 + \frac{\delta}{\Delta} V^2 \frac{1}{2} (q_e(z) + q_o(z)), \end{aligned} \quad (\text{B.10})$$

thus defining $\tilde{\beta}_a$, which is the average of $\tilde{\beta}_h(z)$ over one period.

It is necessary to find the vector form of the local higher-order modes, as well as the vector corrections to the propagation constants.

As with the modes on an axially symmetric fibre, we find that the scalar local modes of the grating form the vector local modes by combining in pairs $\{\bar{\psi}_e(r, \theta) \hat{x}, \bar{\psi}_o(r, \theta) \hat{y}\}$ and $\{\bar{\psi}_o(r, \theta) \hat{x}, \bar{\psi}_e(r, \theta) \hat{y}\}$. These are called the X- and Y-set, respectively, thus indicating the axis of symmetry. A subscript x, y indicates to which set something is relevant. With $a_x(z), a_y(z)$ the coefficients, respectively, of the x- and y-components in these sets, the standard formalism [e.g. 1: ch13] gives the pair of equations

$$(\beta^2 - \tilde{\beta}_{\{e\}}^2) a_x(z) \|\bar{\psi}_h\|^2 = -2\Delta (a_x \langle \frac{\partial \bar{\psi}_{\{e\}}}{\partial x}, \bar{\psi}_{\{e\}} \frac{\partial g}{\partial x} \rangle + a_y \langle \frac{\partial \bar{\psi}_{\{e\}}}{\partial x}, \bar{\psi}_{\{e\}} \frac{\partial g}{\partial y} \rangle) \quad (\text{B.11a})$$

$$(\beta^2 - \tilde{\beta}_{\{e\}}^2) a_y(z) \|\bar{\psi}_h\|^2 = -2\Delta (a_x \langle \frac{\partial \bar{\psi}_{\{e\}}}{\partial y}, \bar{\psi}_{\{e\}} \frac{\partial g}{\partial x} \rangle + a_y \langle \frac{\partial \bar{\psi}_{\{e\}}}{\partial y}, \bar{\psi}_{\{e\}} \frac{\partial g}{\partial y} \rangle) \quad (\text{B.11b})$$

with the upper and lower choices being for the X- and Y-set, respectively. Advantage was taken of the fact that $\|\bar{\psi}_h\| = \|\bar{\psi}_e\| = \|\bar{\psi}_o\|$. A little thought shows that other corrections to β , due to corrections to ψ of order Δ and $\frac{\delta}{\Delta}$, would be second order small. Hence, they are neglected. Hence, the reason for not evaluating corrections to the scalar modal field for higher-order modes.

From (B.11), it follows that the vector corrections to $\beta(z)$ and the vector directions of the modal fields, as specified by $a_x(z), a_y(z)$, are found as a solution to a matrix eigenvalue problem. Namely,

$$\|\bar{\psi}_h\|^2 \frac{(\beta^2 - \tilde{\beta}_e^2)}{2\Delta} \begin{pmatrix} a_x(z) \\ a_y(z) \end{pmatrix} = \begin{pmatrix} -\langle \frac{\partial \bar{\psi}_{\{e\}}}{\partial x}, \bar{\psi}_{\{e\}} \frac{\partial q}{\partial x} \rangle + \{-Q(z)\|F_1\|^2 V^2 \delta / \Delta^2\} & -\langle \frac{\partial \bar{\psi}_{\{e\}}}{\partial x}, \bar{\psi}_{\{e\}} \frac{\partial q}{\partial y} \rangle \\ -\langle \frac{\partial \bar{\psi}_{\{e\}}}{\partial y}, \bar{\psi}_{\{e\}} \frac{\partial q}{\partial x} \rangle & -\langle \frac{\partial \bar{\psi}_{\{e\}}}{\partial y}, \bar{\psi}_{\{e\}} \frac{\partial q}{\partial y} \rangle + \{-Q(z)\|F_1\|^2 V^2 \delta / \Delta^2\} \end{pmatrix} \times \begin{pmatrix} a_x(z) \\ a_y(z) \end{pmatrix}, \quad (\text{B.12})$$

where we define, from (B.9) and (B.8),

$$Q(z) = \frac{\pi \Delta^2 (\tilde{\beta}_e^2 - \tilde{\beta}_o^2)}{2V^2 \delta \Delta} = \frac{\pi}{2} (\xi_e - \xi_o + q_e(z) - q_o(z)) \quad (\text{B.13a})$$

$$= \frac{1}{2\|F_1\|^2} \int_{\mathcal{D}(z)} dS g_1(r, \theta, z) F_1^2(r) \cos 2\theta \quad (\text{B.13b})$$

Thus, can be obtained the vector corrections to the propagation constants.

The matrices on the right-hand side of (B.12) for the X and Y-sets, are, respectively,

$$\frac{1}{4} \begin{pmatrix} -I_2 - 3I_1 & -3I_2 - I_1 \\ -3I_2 - I_1 & -I_2 - 3I_1 - 2\frac{2\delta}{\pi\Delta^2} V^2 Q(z) \end{pmatrix}$$

and

$$\frac{1}{4} \begin{pmatrix} I_2 - I_1 - 2\frac{2\delta}{\pi\Delta^2} V^2 Q(z) & I_2 - I_1 \\ I_2 - I_1 & I_2 - I_1 \end{pmatrix}.$$

For ease of subsequent analysis, define the obvious constants

$$\alpha_x = \frac{\pi \Delta^2 (-3I_2 - I_1)}{2\delta V^2} = \frac{\pi \Delta^2 \sqrt{2} (\delta\beta_4 - \delta\beta_3)}{2\delta \Delta^{\frac{3}{2}} V} \quad (\text{B.14a})$$

$$\alpha_y = \frac{\pi \Delta^2 (I_1 - I_2)}{2\delta V^2} = \frac{\pi \Delta^2 \sqrt{2} (-\delta\beta_5)}{2\delta \Delta^{\frac{3}{2}} V}. \quad (\text{B.14b})$$

where $\delta\beta_j$ is the polarization correction to the propagation constant. The third expressions in (B.14) show a physical interpretation for α_j , as the difference in the propagation constants, corrected for first order polarization effects, of the two modes of the J-set.

The local polarization corrections to the propagation constants follow by solving (B.12) for the eigenvalues.

$$\begin{aligned}\frac{2(\beta_{\{4\}}^2 - \tilde{\beta}_e^2)}{\Delta} &= \frac{2(\beta_{\{\mp\}}^2 - \tilde{\beta}_e^2)}{\Delta} \\ &= -I_2 - 3I_1 - \frac{2\delta}{\pi\Delta^2}V^2Q(z) \mp \frac{2\delta}{\pi\Delta^2}V^2\text{sgn}(\alpha_x)|\alpha_x^2 + Q^2(z)|^{\frac{1}{2}}. \\ \frac{2(\beta_{\{6\}}^2 - \tilde{\beta}_e^2)}{\Delta} &= \frac{2(\beta_{\{\pm\}}^2 - \tilde{\beta}_e^2)}{\Delta} \\ &= I_2 - I_1 - \frac{2\delta}{\pi\Delta^2}V^2Q(z) \mp \frac{2\delta}{\pi\Delta^2}V^2\text{sgn}(\alpha_y)|\alpha_y^2 + Q^2(z)|^{\frac{1}{2}}.\end{aligned}$$

The sign on the radicals is fixed by ensuring continuity of the vector direction of the modes if $Q(z)$ changes sign, which, in general, it may do. The implications of this choice is discussed below.

Notice from (B.8) and (B.13a) that

$$\begin{aligned}\tilde{\beta}_e^2(z) - \Delta\frac{2\delta}{\pi\Delta^2}V^2\frac{1}{2}Q(z) &= \tilde{\beta}_h^2 + \frac{\delta}{\Delta}V^2\frac{1}{2}(\xi_e + \xi_o) + \frac{\delta}{\Delta}V^2\frac{1}{2}(q_e(z) + q_o(z)) \\ &= \tilde{\beta}_a^2 + \frac{\delta}{\Delta}V^2\frac{1}{2}(q_e(z) + q_o(z)).\end{aligned}\tag{B.15}$$

The vector corrections to the modal propagation constants are now fully determined:

$$\begin{aligned}\beta_3^2(z) &= \tilde{\beta}_a^2 + \frac{\delta}{\Delta}V^2\frac{1}{2}(q_e(z) + q_o(z)) - \Delta(I_1 - I_2) \\ &\quad - \Delta\frac{2\delta}{\pi\Delta^2}V^2\frac{1}{2}\text{sgn}(\alpha_x)(|\alpha_x^2 + Q^2(z)|^{\frac{1}{2}} - |\alpha_x|); \end{aligned}\tag{B.16a}$$

$$\begin{aligned}\beta_4^2(z) &= \tilde{\beta}_a^2 + \frac{\delta}{\Delta}V^2\frac{1}{2}(q_e(z) + q_o(z)) - \Delta 2(I_1 + I_2) \\ &\quad + \Delta\frac{2\delta}{\pi\Delta^2}V^2\frac{1}{2}\text{sgn}(\alpha_x)(|\alpha_x^2 + Q^2(z)|^{\frac{1}{2}} - |\alpha_x|); \end{aligned}\tag{B.16b}$$

$$\begin{aligned}\beta_5^2(z) &= \tilde{\beta}_a^2 + \frac{\delta}{\Delta}V^2\frac{1}{2}(q_e(z) + q_o(z)) - \Delta(I_1 - I_2) \\ &\quad - \Delta\frac{2\delta}{\pi\Delta^2}V^2\frac{1}{2}\text{sgn}(\alpha_y)(|\alpha_y^2 + Q^2(z)|^{\frac{1}{2}} - |\alpha_y|); \end{aligned}\tag{B.16c}$$

$$\begin{aligned}\beta_6^2(z) &= \tilde{\beta}_a^2 + \frac{\delta}{\Delta}V^2\frac{1}{2}(q_e(z) + q_o(z)) + 0 \\ &\quad + \Delta\frac{2\delta}{\pi\Delta^2}V^2\frac{1}{2}\text{sgn}(\alpha_y)(|\alpha_y^2 + Q^2(z)|^{\frac{1}{2}} - |\alpha_y|). \end{aligned}\tag{B.16d}$$

Written in this form, they show that the first correction term, common to all four, is the local variation of the scalar propagation constant; the second term is exactly the same as the correction to the scalar propagation constant of the corresponding mode on the unperturbed waveguide; the third term is the local correction due to the asymmetric perturbation.

The local vector modes from solving (B.12) for the eigenvectors.

$$\mathbf{E}_{\pm}(z) = \begin{cases} \text{constant}_{\pm} (\alpha_x \bar{\psi}_e \hat{\mathbf{x}} + (\pm \text{sgn}(\alpha_x) |\alpha_x^2 + Q^2|^{\frac{1}{2}} - Q) \bar{\psi}_o \hat{\mathbf{y}}) & , \text{ for X-set} \\ \text{constant}_{\pm} (\alpha_y \bar{\psi}_o \hat{\mathbf{x}} + (\pm \text{sgn}(\alpha_y) |\alpha_y^2 + Q^2|^{\frac{1}{2}} - Q) \bar{\psi}_e \hat{\mathbf{y}}) & , \text{ for Y-set} \end{cases}$$

where the constants come from arbitrarily prescribed normalization conditions. Define the two angles $\phi_x(z)$ and $\phi_y(z)$ by

$$\phi_{\gamma}(z) = \arctan\left(\frac{-Q(z)}{\text{sgn}(\alpha_{\gamma}) |\alpha_{\gamma}^2 + Q^2(z)|^{\frac{1}{2}} + \alpha_{\gamma}}\right) = -\frac{1}{2} \arctan\left(\frac{Q(z)}{\alpha_{\gamma}}\right). \quad (\text{B.17})$$

Both of these are in $[-\frac{\pi}{4}, \frac{\pi}{4}]$. By suitably choosing the normalization conditions, the local vector modes can be rewritten:

$$\begin{aligned} \mathbf{E}_3(z) &= \sqrt{2} \cos(\phi_x(z) - \frac{\pi}{4}) \bar{\psi}_e(r, \theta) \hat{\mathbf{x}} + \sqrt{2} \sin(\phi_x(z) - \frac{\pi}{4}) \bar{\psi}_o(r, \theta) \hat{\mathbf{y}} \\ &= \cos \phi_x \bar{\mathbf{E}}_3 + \sin \phi_x \bar{\mathbf{E}}_4; \\ \mathbf{E}_4(z) &= -\sqrt{2} \sin(\phi_x(z) - \frac{\pi}{4}) \bar{\psi}_e(r, \theta) \hat{\mathbf{x}} + \sqrt{2} \cos(\phi_x(z) - \frac{\pi}{4}) \bar{\psi}_o(r, \theta) \hat{\mathbf{y}} \\ &= -\sin \phi_x \bar{\mathbf{E}}_3 + \cos \phi_x \bar{\mathbf{E}}_4; \\ \mathbf{E}_5(z) &= \sqrt{2} \cos(\phi_y(z) + \frac{\pi}{4}) \bar{\psi}_o(r, \theta) \hat{\mathbf{x}} + \sqrt{2} \sin(\phi_y(z) + \frac{\pi}{4}) \bar{\psi}_e(r, \theta) \hat{\mathbf{y}} \\ &= \cos \phi_y \bar{\mathbf{E}}_5 + \sin \phi_y \bar{\mathbf{E}}_6; \\ \mathbf{E}_6(z) &= -\sqrt{2} \sin(\phi_y(z) + \frac{\pi}{4}) \bar{\psi}_o(r, \theta) \hat{\mathbf{x}} + \sqrt{2} \cos(\phi_y(z) + \frac{\pi}{4}) \bar{\psi}_e(r, \theta) \hat{\mathbf{y}} \\ &= -\sin \phi_y \bar{\mathbf{E}}_5 + \cos \phi_y \bar{\mathbf{E}}_6. \end{aligned}$$

Thus, the evolution of the vector form of the modes on the z -varying perturbed waveguide can be written concisely in terms of a rotation matrix $D_{\ell}(z)$.

$$\begin{pmatrix} \mathbf{E}_j(z) \\ \mathbf{E}_k(z) \end{pmatrix} = \begin{pmatrix} \cos \phi_{\ell}(z) & \sin \phi_{\ell}(z) \\ -\sin \phi_{\ell}(z) & \cos \phi_{\ell}(z) \end{pmatrix} \begin{pmatrix} \bar{\mathbf{E}}_j \\ \bar{\mathbf{E}}_k \end{pmatrix} = D_{\ell}(z) \begin{pmatrix} \bar{\mathbf{E}}_j \\ \bar{\mathbf{E}}_k \end{pmatrix} \quad (\text{B.18a})$$

$$= \sqrt{2} \begin{pmatrix} \cos(\phi_{\ell}(z) \mp \frac{\pi}{4}) & \sin(\phi_{\ell}(z) \mp \frac{\pi}{4}) \\ -\sin(\phi_{\ell}(z) \mp \frac{\pi}{4}) & \cos(\phi_{\ell}(z) \mp \frac{\pi}{4}) \end{pmatrix} \begin{pmatrix} \bar{\psi}_{\{o\}} \hat{\mathbf{x}} \\ \bar{\psi}_{\{e\}} \hat{\mathbf{y}} \end{pmatrix} \quad (\text{B.18b})$$

with the upper or lower choice being for the X- or Y-set, respectively, and where j, k, ℓ are 3, 4, x or 5, 6, y , respectively. The angle very concisely shows which particular form of LP₁₁

mode is more like the nominated mode of the grating at position z , as can be seen from Fig. 19.

B.6 SIGN OF α_j AND LP₁₁ MODES

What is new in the analysis? It follows the standard procedure [23]. The results worthy of comment are the consequences of the choice of sign, as mentioned, and the description of the vector direction of the local modes in terms of rotation matrices.

The higher-order modes of a significantly axi-asymmetric waveguide are the four familiar forms of the LP₁₁ mode: $\bar{\psi}_e(r, \theta) \hat{x}$, $\bar{\psi}_e(r, \theta) \hat{y}$, $\bar{\psi}_o(r, \theta) \hat{x}$, and $\bar{\psi}_o(r, \theta) \hat{y}$. The modes of an axisymmetric waveguide are equally familiar, and are obtained from these by simple rotations and a dilation through $\frac{\pi}{4}$:

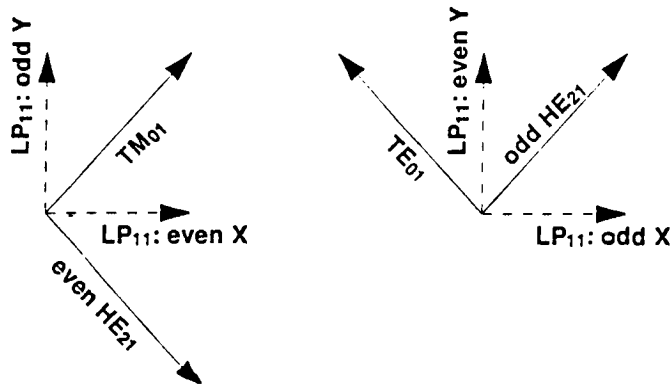
$$\begin{pmatrix} \bar{E}_3 \\ \bar{E}_4 \end{pmatrix} = \sqrt{2} \begin{pmatrix} \frac{1}{\sqrt{2}} & \frac{-1}{\sqrt{2}} \\ \frac{1}{\sqrt{2}} & \frac{1}{\sqrt{2}} \end{pmatrix} \begin{pmatrix} \bar{\psi}_e(r, \theta) \hat{x} \\ \bar{\psi}_o(r, \theta) \hat{y} \end{pmatrix}$$

$$\begin{pmatrix} \bar{E}_5 \\ \bar{E}_6 \end{pmatrix} = \sqrt{2} \begin{pmatrix} \frac{1}{\sqrt{2}} & \frac{1}{\sqrt{2}} \\ \frac{-1}{\sqrt{2}} & \frac{1}{\sqrt{2}} \end{pmatrix} \begin{pmatrix} \bar{\psi}_o(r, \theta) \hat{x} \\ \bar{\psi}_e(r, \theta) \hat{y} \end{pmatrix}.$$

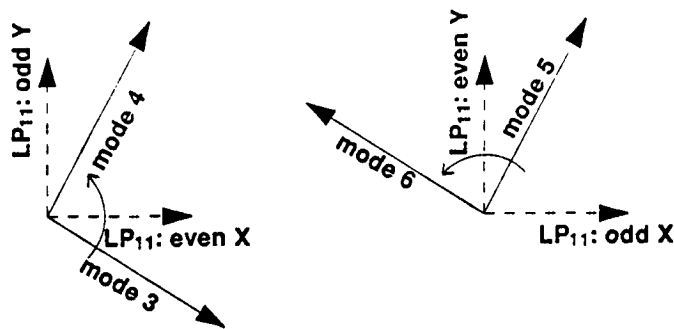
At (B.18), it is apparent that the local modes on the perturbed waveguide are somewhere between these two extremes.

For very little asymmetry, i.e. $Q(z)$ very small, it follows from (B.17) that $\phi_y, \phi_x \rightarrow 0$, and the modes are, indeed the same as those of the unperturbed axisymmetric waveguide. As the amount of axi-asymmetry increases or the parameter α_j becomes small, the way the two sets approach the LP₁₁ modes differs. This can be seen best by taking the limiting forms of (B.17) as $Q(z)$ becomes large or α_j becomes small. This gives $\phi_j \rightarrow -\text{sgn}(Q)\text{sgn}(\alpha_j)\frac{\pi}{4}$. The sign of $Q(z)$ indicates whether the imposition of the asymmetry has made the even or the odd scalar mode the "faster" mode, i.e. when $Q(z) > 0$, the even mode has the higher propagation constant. Thus, within each set of modes, the mode, which has the higher propagation constant on the unperturbed waveguide, becomes more like the even LP₁₁ mode.

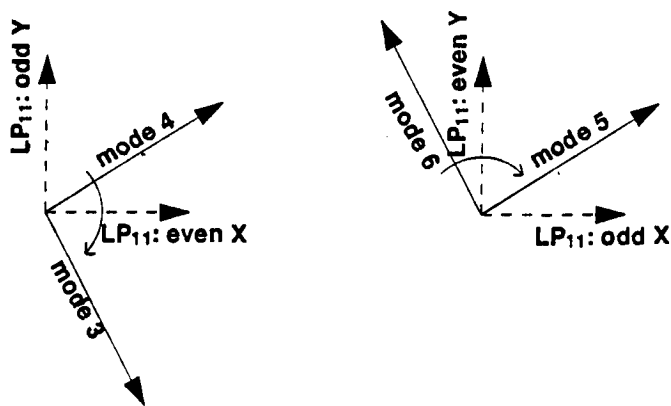
The behaviour, during passage through a period of the perturbation, is described in detail for the X-set. There are four possibilities. Consider firstly $Q(z) > 0$. If $\alpha_x > 0$,



(a) Graphical representation of the relationship between the first group of true (VC) higher-order modes and the LP₁₁ modes — identified by direction of polarization and symmetry property about the X-axis — of an axisymmetric fibre.



(b) Direction of “rotation”, i.e. form of transformation, of the true modes to LP₁₁ modes, when $0 < \phi_j$, as defined by Eq. (B.17).



(c) Direction of “rotation”, i.e. form of transformation, of the true modes to LP₁₁ modes, when $0 > \phi_j$, as defined by Eq. (B.17).

Figure 19: Modal rotation and limiting forms

mode 3, which corresponds to the even HE_{21} mode, becomes like the Y-polarized odd LP_{11} mode, and mode 4, which corresponds to the TM_{01} mode, becomes like the X-polarized even mode. However, if $\alpha_x < 0$, mode 3 becomes like the X-polarized even LP_{11} mode, and mode 4 becomes like the Y-polarized odd mode. Now consider $Q(z) < 0$. With $\alpha_x > 0$, mode 3 becomes like the X-polarized even LP_{11} mode, and mode 4 the Y-polarized odd mode; whereas, if $\alpha_x < 0$, mode 3 becomes like the Y-polarized odd LP_{11} mode, and mode 4 the X-polarized even mode. This is illustrated in Fig. 19. This apparently strange swapping of modal behaviour has an explanation. When $\alpha_x > 0$, the even HE_{21} mode on the axisymmetric waveguide has a higher propagation constant than the TM_{01} mode, and thus mode 3 becomes more like the LP_{11} mode with the higher propagation constant, which, for $Q(z) > 0$, is the even mode, and mode 4 becomes like that with the lower propagation constant, namely the odd mode. For $\alpha_x < 0$, the behaviour switches because the TM_{01} mode has the higher value of β .

The same number of cases occurs for the Y-family, but they are not described in detail. They also are illustrated in Fig. 19.

If we recall from (B.13) that $Q(z)$ measures the local difference $\tilde{\beta}_e(z) - \tilde{\beta}_o(z)$, then it follows that $\frac{Q(z)}{\alpha_x} \sim \frac{\tilde{\beta}_e - \tilde{\beta}_o}{\delta\beta_4 - \delta\beta_3}$ (with a similar expression involving α_y). This is the Λ -parameter defined elsewhere [1: p288], wherein the limit of an LP_{11} mode was shown to apply as this gets large, which is equivalent to α_j getting small or $Q(z)$ getting big. However, that the choice of LP_{11} mode approached is dependent on the sign of $Q(z)/\alpha_j$ was not remarked in Ref. 1. It is discussed in Ref. 24.

What happens at $\alpha_j = 0$? Recall from (B.14) that this means that two propagation constants, as evaluated by first-order corrections to the weak guidance approximation, are equal for the two modes of the J-set. In the neighbourhood of $\alpha_j = 0$, taking more terms in the polarization corrections to β_j and evaluating the electric fields beyond the weak guidance approximation, may show continuous, though very rapid, change of behaviour as the value of V (and hence $\alpha_j(V)$) changes. However, there would still remain a value of V (namely such that $\alpha_j(V) = 0$) where the vector direction of the modes was ambiguous [25: p293]. At this special value of V , the LP_{11} modes are equally valid as a description of the modes of

the axisymmetric fibre as the VC modes.

B.7 AVERAGE PROPAGATION CONSTANTS

Since the perturbation is assumed to evolve slowly along the waveguide, i.e. $\Lambda \gg 1$, and $\rho \gg \lambda$, the adiabatic approximation can be used. This means that the modes vary slowly and that the total phase of the mode accumulates approximately in some average fashion [1: p407f]. Define the average propagation constant over the period of the grating by

$$\langle \beta_j \rangle = \frac{1}{\Lambda} \int_0^\Lambda dz \beta_j(z).$$

Since it is trivial that, correct to the order of the accuracy worked above, $\langle \beta_j \rangle^2 = \langle \beta_j^2 \rangle$, we can work with the average value of the square of the propagation constants.

Recall how the functions $q_j(z)$ were defined so that their averages vanish over a period. From (B.7) it is almost immediate that

$$\langle \beta_1 \rangle^2 = \langle \beta_2 \rangle^2 = \bar{\beta}_f^2 + \frac{\delta}{\Delta} V^2 \xi_f - \Delta I_0. \quad (\text{B.19})$$

The second correction term is, of course, the polarization correction to the propagation constant of an unperturbed fibre. The interpretation of the first correction term is equally transparent. It shows the net result of the perturbation, either lowering or raising the average scalar propagation, as the average effective guidance parameter rises or falls.

In evaluating the vector average $\langle \beta_j \rangle$, for $j = 3, \dots, 6$, from (B.16), recall that the average value of $q_e(z) + q_o(z)$ vanishes. It is apparent that the average value of the polarization correction to the scalar propagation constants contains a term that is exactly the vector correction of the corresponding mode on the unperturbed waveguide. The other term exists only on the non axisymmetric fibre, i.e. when $Q(z) \neq 0$. Thus, with the definition

$$L(x) = \frac{1}{\Lambda} \int_0^\Lambda dz (|x^2 + Q^2(z)|^{\frac{1}{2}} - |x|), \quad (\text{B.20})$$

the complete set of average propagation constants for the higher-order modes follows:

$$\langle \beta_3 \rangle^2 = \bar{\beta}_a^2 - \Delta(I_1 - I_2) - \Delta \frac{\delta}{\pi \Delta^2} \text{sgn}(\alpha_x) L(|\alpha_x|); \quad (\text{B.21a})$$

$$\langle \beta_4 \rangle^2 = \bar{\beta}_a^2 - \Delta 2(I_1 + I_2) + \Delta \frac{\delta}{\pi \Delta^2} \text{sgn}(\alpha_x) L(|\alpha_x|); \quad (\text{B.21b})$$

$$\langle \beta_5 \rangle^2 = \tilde{\beta}_a^2 - \Delta(I_1 - I_2) - \Delta \frac{\delta}{\pi \Delta^2} \text{sgn}(\alpha_y) L(|\alpha_y|); \quad (\text{B.21c})$$

$$\langle \beta_6 \rangle^2 = \tilde{\beta}_a^2 + 0 + \Delta \frac{\delta}{\pi \Delta^2} \text{sgn}(\alpha_y) L(|\alpha_y|). \quad (\text{B.21d})$$

with $\tilde{\beta}_a$ given at (B.10) and which includes a correction cognisant of the average guidance parameter of the grating. The average value of the polarization correction to the scalar propagation constants contains a term that is exactly the polarization correction of the corresponding propagation constant on the unperturbed waveguide. The final term in these expressions is due only to the presence of the non-axisymmetric z -variation, i.e. that $Q(z) \neq 0$. For $\delta \sim \Delta^2$, it is the same order of magnitude as other corrections to $\bar{\beta}_h$.

An important finding is that there are four distinct values of $\langle \beta_j \rangle$, instead of three. The degeneracy between the odd and even HE_{21} modes has been broken. As functions of frequency, it follows that the $\langle \beta_j \rangle$ are discontinuous at any point where the relevant α_j vanishes. This is a consequence of the discontinuity in the way the two modes oscillate between the two different LP_{11} modes. Next, an example of this peculiar behaviour is presented: the $\text{LP}_{01} \leftrightarrow \text{LP}_{11}$ grating.

B.8 EXAMPLE: LOCAL MODES OF $\text{LP}_{01} \leftrightarrow \text{LP}_{11}$ GRATING

The form of the perturbation can best be appreciated from Fig. 9, and is described in detail at §4.1.

Recall the definition for $s(z)$ given by (4.2). This allows us to write

$$g_1(r, \theta, z) = H(1 - r)H(r \cos \theta - 1 + 2\frac{z}{\ell_c})H(r \cos \theta + 1 - 2\frac{z - \ell_1}{\ell_c}), \quad (\text{B.22})$$

where $H(x)$ is the Heaviside step function, and so make some progress in evaluating the integrals in (B.4) and (B.3).

To determine the solution for a grating written in an arbitrary fibre, the integrals below (B.2) are needed, and can be found numerically, if not analytically. These give immediately α_x and α_y , from (B.14).

Proceeding, define the familiar scalar modal efficiencies η_f, η_h for the LP₀₁ and LP₁₁ families of modes, respectively, as the integrals

$$\eta_j = \frac{\int_C dS \bar{\psi}_j^2(r, \theta)}{\|\bar{\psi}_j\|^2}$$

where $j = f, h$ and C indicates the domain of integration is the core of the fibre. With a little ingenuity, from (B.5) it is possible to show

$$\xi_f = \frac{\ell_1}{\Lambda} \eta_f \quad \text{and} \quad \xi_e = \xi_o = \frac{\ell_1}{\Lambda} \eta_h \equiv \xi_h. \quad (\text{B.23})$$

The equality $\xi_e = \xi_o$ has a profound consequence. Recalling that the average of $q_j(z)$ over one period vanishes, from (B.4) and (B.5) it follows that the average scalar propagation constants of the odd and even scalar modes are identical. This means that for part of the grating $\tilde{\beta}_e > \tilde{\beta}_o$ and for part $\tilde{\beta}_o > \tilde{\beta}_e$. It is this that ensures the ‘‘average’’ higher-order modes in the grating are not LP₁₁ modes, and that, as detailed above, the higher-order modes approach, in turn, the forms of two different LP₁₁ modes during transit through the grating.

With the perturbation defining the grating, in general the functions $q_j(z)$ follow as

$$q_j(z) = \begin{cases} -\xi_f + \frac{2}{\|\bar{\psi}_j\|^2} \int_s^1 dr r \int_0^{\arccos(\frac{s}{r})} d\theta \bar{\psi}_j^2(r, \theta) & , \text{ if } 1 \geq s(z) \geq 0 \\ -\xi_f + \eta_f - \frac{2}{\|psb_j\|^2} \int_{-s}^1 dr r \int_{\arccos(\frac{s}{r})}^{\pi} \bar{\psi}_j^2(r, \theta) & , \text{ if } 0 > s(z) \geq -1 \end{cases}$$

so that changing the angular variable of integration in the second case and noting the symmetry about the Y-axis of $\bar{\psi}^2$ gives

$$\begin{aligned} q_f(z) &= \begin{cases} -\xi_f + \frac{1}{\pi \|F_0\|^2} \int_s^1 dr r F_0^2(r) \arccos(\frac{s}{r}) & , \text{ if } 1 \geq s(z) \geq 0 \\ -\xi_f + \eta_f - \frac{1}{\pi \|F_0\|^2} \int_{-s}^1 dr r F_0^2(r) \arccos(\frac{-s}{r}) & , \text{ if } 0 > s(z) \geq -1 \end{cases} \\ q_e(z) &= \begin{cases} -\xi_h + \frac{1}{\pi \|F_1\|^2} \int_s^1 dr r F_1^2(r) (\arccos(\frac{s}{r}) + s \sqrt{1 - \frac{s^2}{r^2}}) & , \text{ if } 1 \geq s(z) \geq 0 \\ -\xi_h + \eta_h - \frac{1}{\pi \|F_1\|^2} \int_{-s}^1 dr r F_1^2(r) (\arccos(\frac{-s}{r}) - s \sqrt{1 - \frac{s^2}{r^2}}) & , \text{ if } 0 > s(z) \geq -1 \end{cases} \\ q_o(z) &= \begin{cases} -\xi_h + \frac{1}{\pi \|F_1\|^2} \int_s^1 dr r F_1^2(r) (\arccos(\frac{s}{r}) - s \sqrt{1 - \frac{s^2}{r^2}}) & , \text{ if } 1 \geq s(z) \geq 0 \\ -\xi_h + \eta_h - \frac{1}{\pi \|F_1\|^2} \int_{-s}^1 dr r F_1^2(r) (\arccos(\frac{-s}{r}) + s \sqrt{1 - \frac{s^2}{r^2}}) & , \text{ if } 0 > s(z) \geq -1 \end{cases} \end{aligned}$$

This fixes $Q(z)$ as

$$Q(z) = s(z) \frac{1}{\|F_1\|^2} \int_{|s|}^1 dr r F_1^2(r) \sqrt{1 - \frac{s^2}{r^2}}.$$

As expected, this gives $Q = 0$ if $z \in (\ell_c, \ell_1) \cup (\ell_1 + \ell_c, \Lambda)$, which is where the cross-section of the grating is axisymmetric. Also, it is antisymmetric in the parameter s , so will change sign during transit of the grating. It is easy to get α_x and α_y , given at (B.14), ϕ_x and ϕ_y , given at (B.17), and, from (B.20),

$$L(x) = 2\xi \int_0^1 ds (|x^2 + Q^2(\frac{\ell_c s}{2})|^{\frac{1}{2}} - |x|).$$

All the information is assembled to fully describe the modes of the grating, written in the fibre. They are illustrated for the case of a grating written in a step fibre.

For a circular step fibre, the expressions for all the necessary quantities can be extracted from standard references [e.g. 1: p313,319]. With the definitions

$$\chi_0 = U_f \frac{J_1(U_f)}{J_0(U_f)} \quad \text{and} \quad \chi_1 = 1 - U_h \frac{J_0(U_h)}{J_1(U_h)},$$

they follow as

$$F_0(r) = \begin{cases} \frac{J_0(U_f r)}{J_0(U_f)} & , \text{ if } r < 1 \\ \frac{K_0(W_f r)}{K_0(W_f)} & , \text{ if } 1 < r \end{cases} ; \quad F_1(r) = \begin{cases} \frac{J_1(U_h r)}{J_1(U_h)} & , \text{ if } r < 1 \\ \frac{K_1(W_h r)}{K_1(W_h)} & , \text{ if } 1 < r \end{cases}$$

$$\eta_f = \frac{W_f^2(U_f^2 + \chi_0^2)}{V^2 \chi_0^2} ; \quad \eta_h = \frac{W_h^2(U_h^2 + \chi_1^2 - 1)}{V^2(\chi_1^2 - 1)}$$

$$\|F_0\|^2 = \frac{V^2 \chi_0^2}{2U_f^2 W_f^2} ; \quad \|F_1\|^2 = \frac{V^2(\chi_1^2 - 1)}{2U_h^2 W_h^2}$$

$$I_0 = \chi_0 / \|F_0\|^2 ; \quad I_1 = \chi_1 / \|F_1\|^2 ; \quad I_2 = -1 / \|F_1\|^2$$

These give

$$\alpha_x = \frac{\pi \Delta^2 (3 - \chi_1)}{2\delta V^2 \|F_1\|^2} ; \quad \alpha_y = \frac{\pi \Delta^2 (1 + \chi_1)}{2\delta V^2 \|F_1\|^2}.$$

Normalized forms of these, namely $\frac{2\delta}{\pi \Delta^2} \alpha_j$, are shown, as functions of V , in Fig. 20. They are important parameters in determining the way the vector form of the modes changes during passage through the grating. It is apparent that α_x changes sign at $V = 3.794$, but α_y does not anywhere; it is worth noting that $\alpha_y > \alpha_x$ everywhere. Indeed, for much of the domain shown, α_x is quite small.

Shown in Fig. 21 is the variation of the angles ϕ_x and ϕ_y during passage through a grating with parameters $\frac{\pi \Delta^2}{\delta} = 3$. It is clear how little axi-asymmetry is needed for

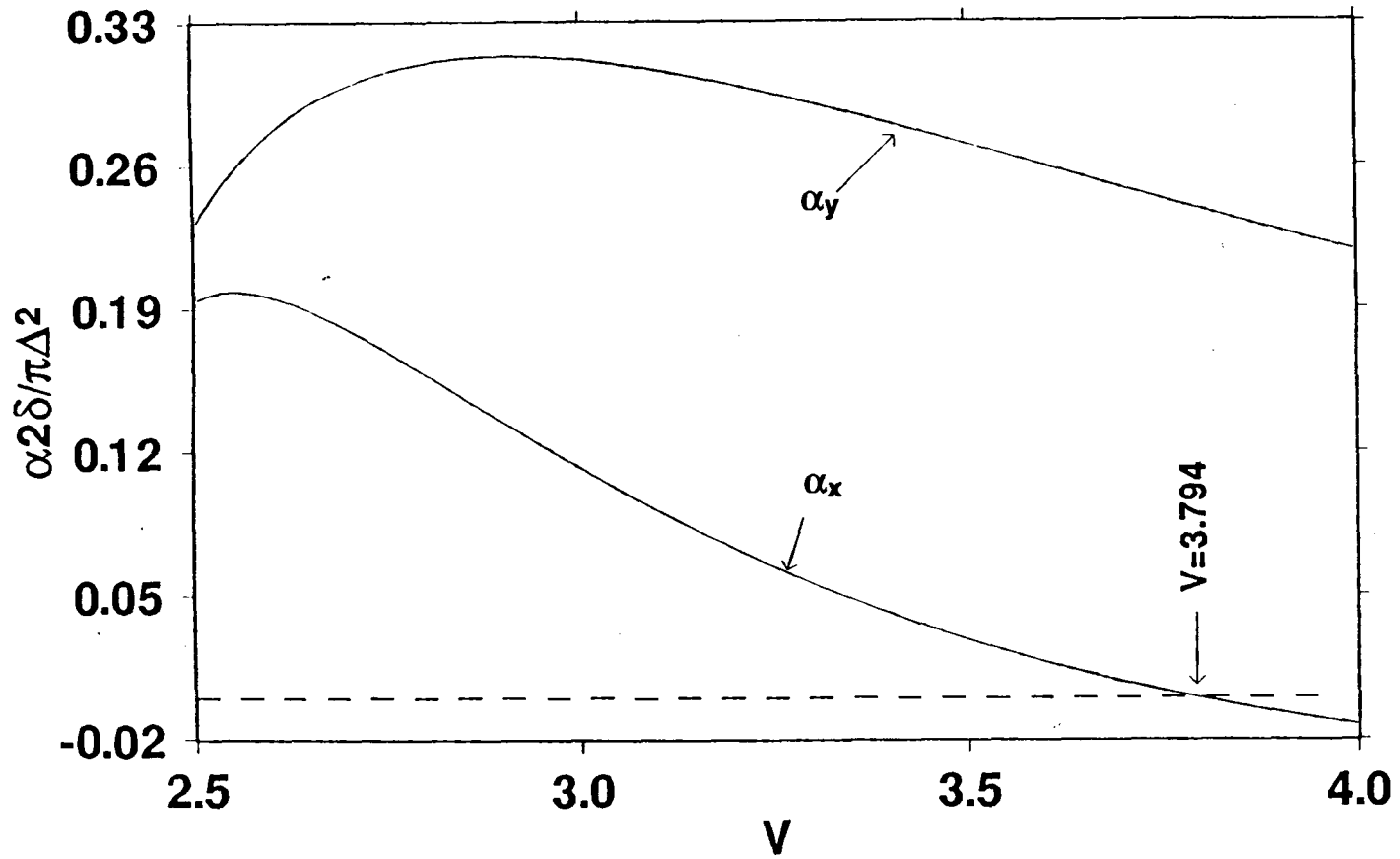


Figure 20: Frequency variation of interference parameters: step-profile

For a step-profile fibre, the normalized form of the interference parameters α_j , defined by Eq. (B.14), as a function of normalized frequency.

the effective modes to be the LP_{11} modes, which are present when $\phi_j \rightarrow \pm \frac{\pi}{4}$. This is particularly true as $|\alpha_x| \rightarrow 0$. A similar quantification that very little asymmetry is needed to establish LP_{11} modes was made previously [1], for the case of an elliptical core in a fibre [p361, 385f, 635f]. Using the angles together with Fig. 19, it is seen how each particular mode approaches two different LP_{11} modes during its passage through the grating. This means that on “average” the modes are VC modes! It is doubtful that such an average has any meaning. Finally, it is apparent how the evolution of modes 3 and 4 in the grating is frequency dependent, i.e. the way they approach the two different LP_{11} modes depends on the value of V . As V goes through 3.794, the sign of ϕ_x switches. As V passes through 3.794, the sign of ϕ_x flips over.

Fig. 22 shows the normalized variation from $\bar{\beta}_h$ of the four higher order propagation constants during passage of the respective modes through one period of the grating. To illustrate the way that the behaviours of modes 3 and 4 interchange, one value of V less than 3.794 and one greater are used. The dominant behaviour seen in Fig. 22 is how all the propagation constants follow the local variation in the scalar constant, i.e. the local perturbation of the effective guidance parameter [26]. The actual forms of the LP_{11} modes or VC modes approached by each mode in each section of the grating are better appreciated by taking a local birefringence as a measure of z -variation of β . One possible form of this, i.e. $\langle \beta_\gamma \rangle - \tilde{\beta}_e(z)$ which is the local variation from the local value of β for the even LP_{11} mode, and an explicit listing of the limiting forms approached by the modes are shown in Fig. 23.

It requires some ingenuity, but it is possible to show that $L(|\alpha_x|) > L(\alpha_y)$ everywhere. Together with (B.21), this inequality shows that the degeneracy between the even and odd HE_{21} modes is broken, i.e. that $\langle \beta_5 \rangle \neq \langle \beta_3 \rangle$, for all frequencies. The evaluation of $Q(z)$ is done numerically, involving as it does Bessel functions, but presents no serious difficulties. For the combination of parameters $\frac{\pi \Delta^2}{\delta} = 3$, the results for $\langle \beta_j \rangle$ are seen in Fig. 24. The discontinuity at $V = 3.794$ in the effective or average values of the propagation constants for modes 3 and 4 is apparent. This discontinuity is not surprising, considering the way that the modes evolve changes at this value of V . Indeed, as can be seen from Fig. 23, their behaviours swap.

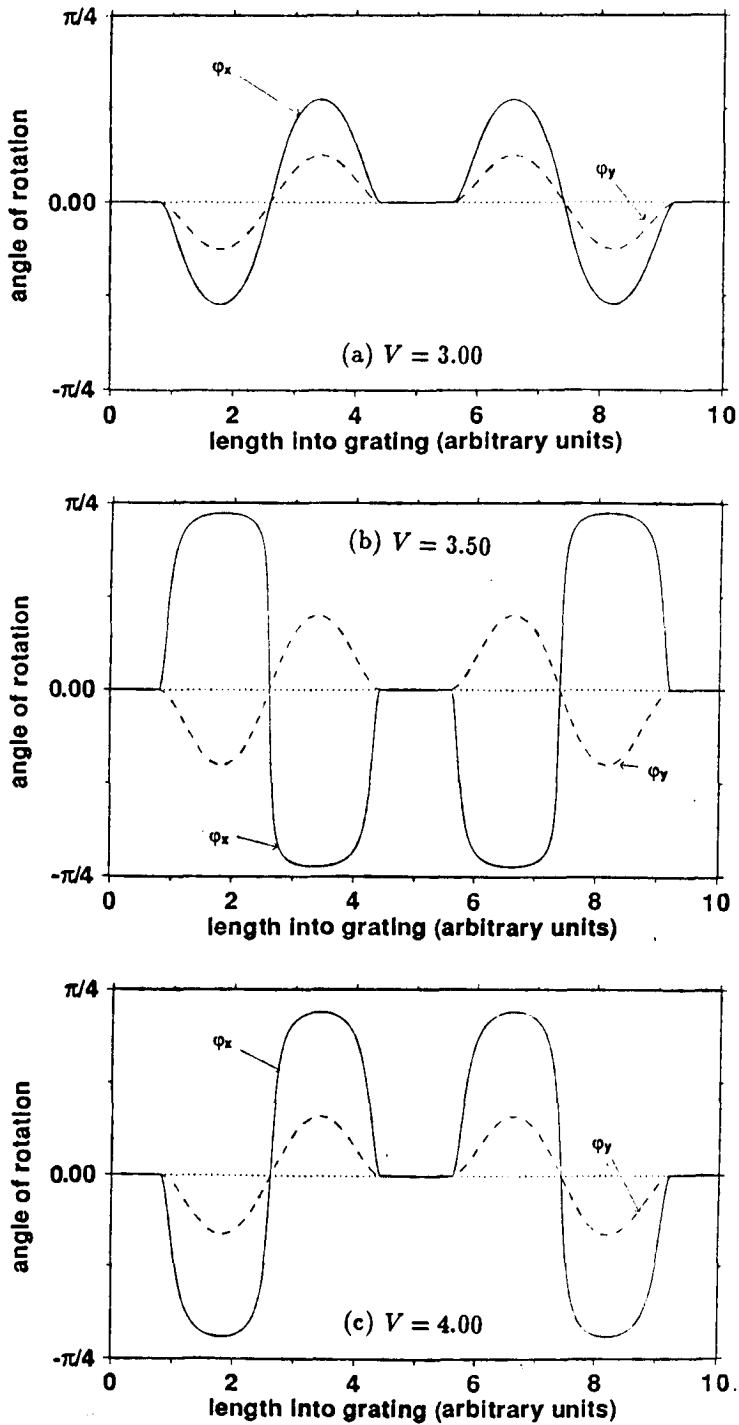


Figure 21: Modal rotation during passage through grating

For a step-profile fibre, angles of rotation ϕ_j of the modal sets during transit through one period of the $LP_{01} \leftrightarrow LP_{11}$ grating. Here $\pi\Delta^2/\delta = 3.0$. Three different values of V are shown.

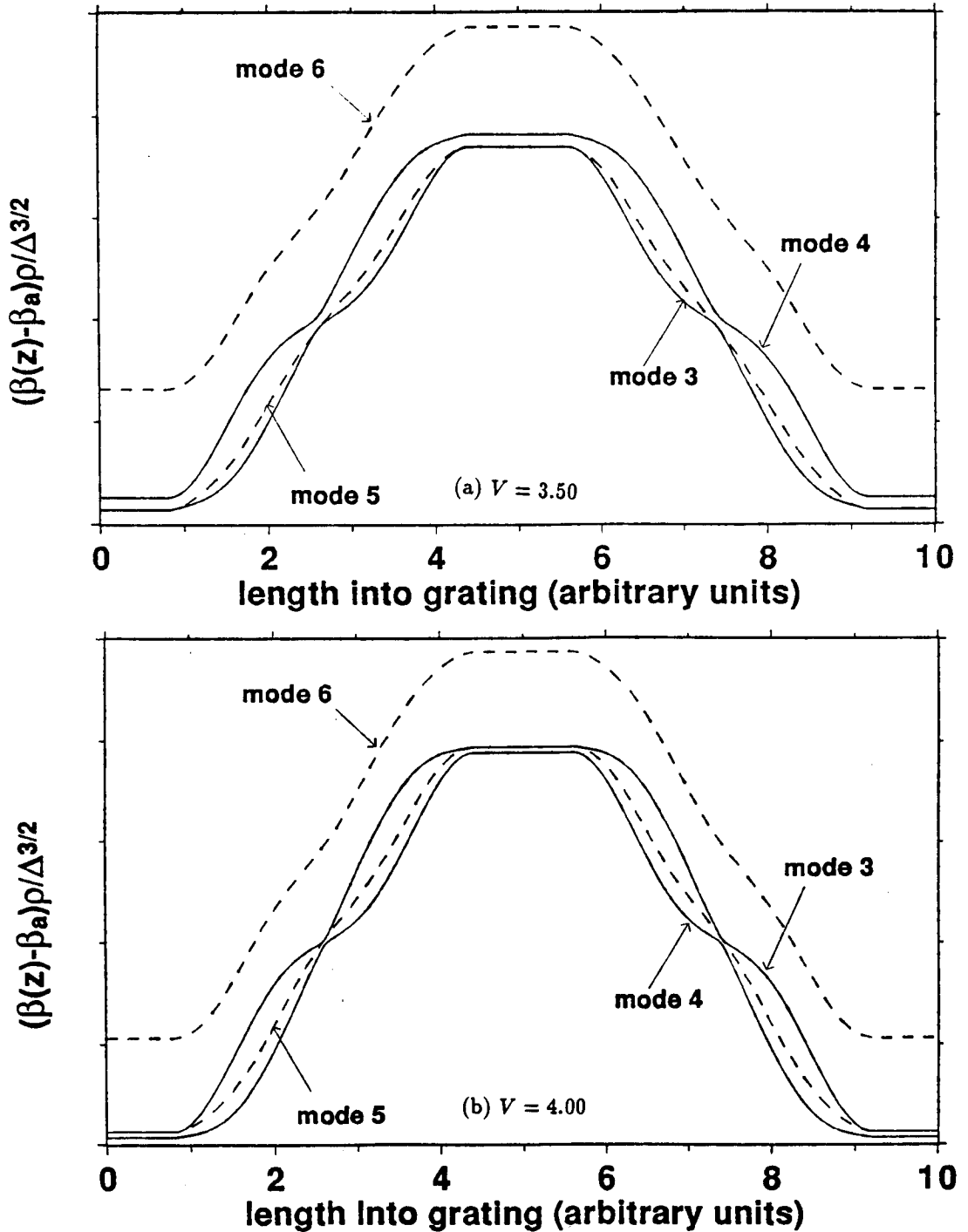


Figure 22: Change in β during passage through grating

For an $LP_{01} \leftrightarrow LP_{11}$ grating in a step-fibre, variation of the local propagation constant $\beta_j(z)$, given by Eq. (B.16), during transit through one period of the $LP_{01} \leftrightarrow LP_{11}$ grating. Here $\pi\Delta/\delta = 3.0$ and the modes are indexed as in §B.1. Two different values of V are shown.

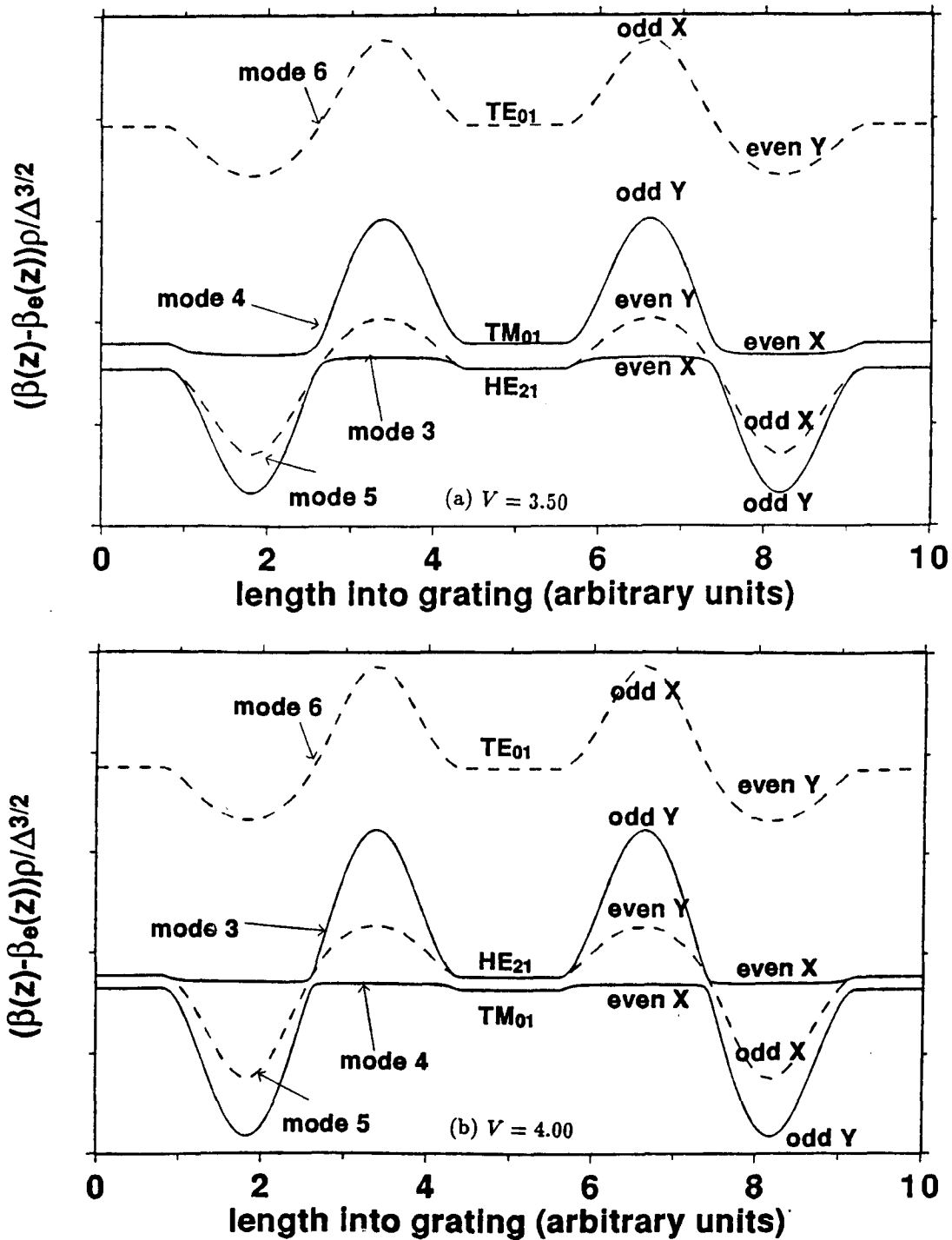


Figure 23: "Local birefringence" during passage through grating

For an $LP_{01} \leftrightarrow LP_{11}$ grating in a step-fibre, variation of the local birefringence $\beta_j(z) - \tilde{\beta}_h(z)$ during transit through one period of the $LP_{01} \leftrightarrow LP_{11}$ grating. On the left, modes are indexed as in §B.1; in the middle, modes are identified by their axisymmetric form; on the right, are listed the two different LP_{11} modes, which are limiting forms. Here $\pi\Delta/\delta = 3.0$. Two different values of V are shown.

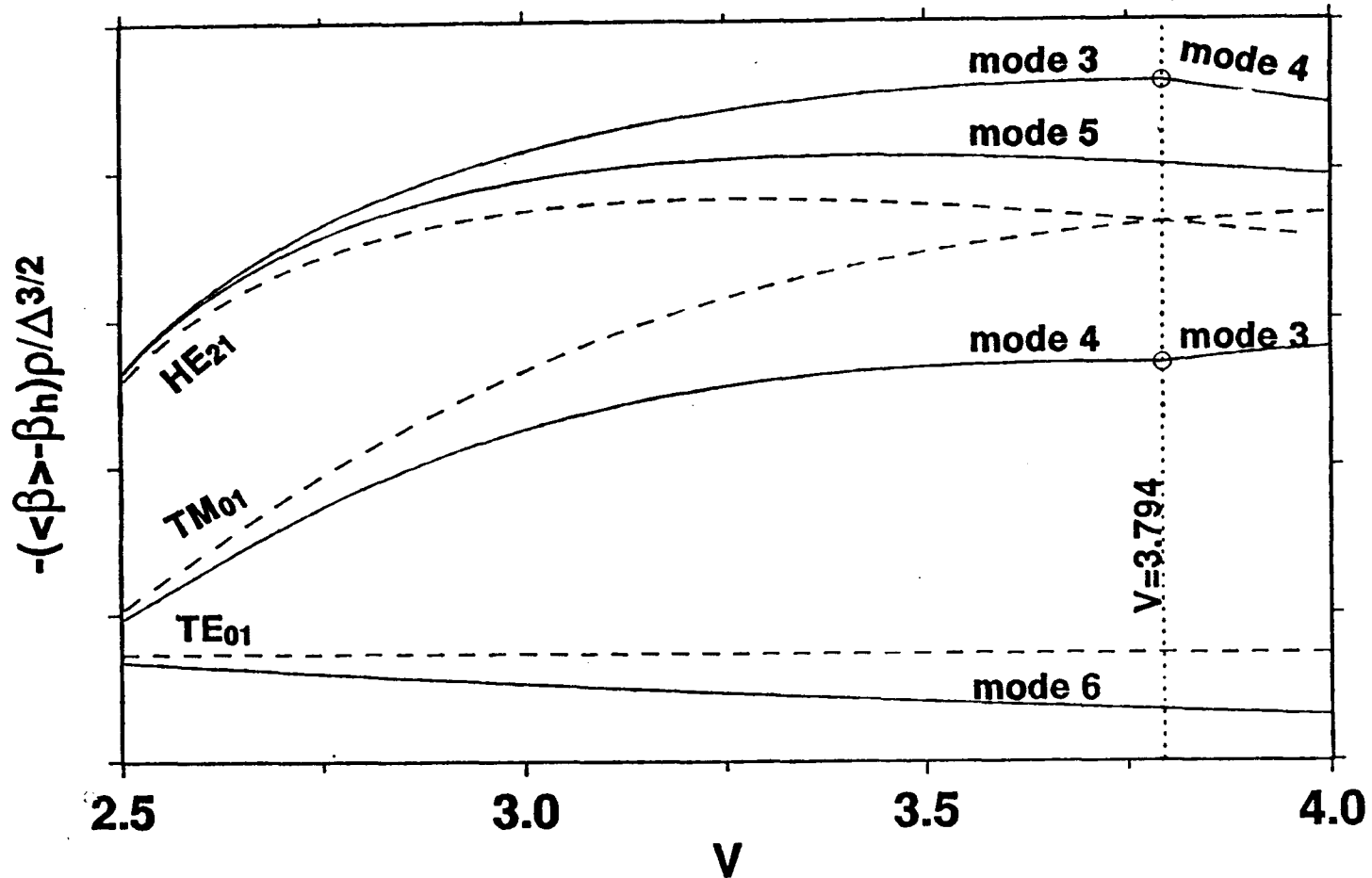


Figure 24: Frequency variation of β averaged over one period

For an $LP_{01} \leftrightarrow LP_{11}$ grating in a step-fibre, the frequency dependence of corrections to the propagation constants, averaged over one period of the grating, as given by Eq. (B.21), are shown as solid curves. Broken curves are the corresponding results on an axisymmetric step-fibre. Here $\pi\Delta/\delta = 3.0$ and the modes are indexed as in §B.1.

B.9 INCLUSION OF ANISOTROPY

It may be that the weak perturbations forming the periodic structure have an anisotropic nature, i.e. $\delta_x \neq \delta_y$, where δ_j is the perturbation seen by the j -polarized light. For simplicity, it is assumed that the optical axes, defined by the anisotropic refractive index tensor, are the Cartesian axes used in the problem, defined by the symmetry of the form of the perturbation. This is not an unreasonable assumption. The anisotropy is frequently induced by the same symmetry structure as produces the perturbation. As a notational device, put

$$\delta_x = \delta \quad ; \quad \delta_y = (1 + \Xi)\delta.$$

As the anisotropic axes are aligned with the Cartesian axes, the two states of polarization are the X- and Y-polarized modes, mentioned above. The respective polarization constants are found by replacing δ with δ_x and δ_y in (B.7).

For the higher-order modes, we again proceed as above. The problem is only more cumbersome.

As in (B.8) and (B.9), derive four values for $\tilde{\beta}$, by replacing δ with either δ_x or δ_y . Next, in (B.11a) and (B.11b), respectively, it is important to realize that $\tilde{\beta}_{\{e\}}$ and $\tilde{\beta}_{\{o\}}$ are replaced by $\tilde{\beta}_{\{e\}}^{(X)}$ and $\tilde{\beta}_{\{o\}}^{(Y)}$. Further, in the left-hand side of (B.12), $\tilde{\beta}_e$ becomes $\tilde{\beta}_e^{\{\{X\}\}}$, and in the right-hand side of (B.12) it follows

$$\begin{aligned} Q(z) &= \frac{\pi \Delta^2}{2V^2 \delta} \frac{\tilde{\beta}_e^{\{\{X\}\}2} - \tilde{\beta}_o^{\{\{Y\}\}2}}{\Delta} \\ &= (1 + \frac{\Xi}{2})Q_-(z) + \{\mp\} \frac{\Xi}{2} Q_+(z), \end{aligned}$$

using the definitions (B.8), (B.9) and

$$Q_+(z) = q_e(z) + q_o(z) + \xi_e + \xi_o = \frac{1}{2\|F_1\|^2} \int_{\mathcal{D}(z)} dS g_1(r, \theta, z) F_1^2(r) \quad (\text{B.24a})$$

$$Q_-(z) = q_e(z) - q_o(z) + \xi_e - \xi_o = \frac{1}{2\|F_1\|^2} \int_{\mathcal{D}(z)} dS g_1(r, \theta, z) F_1^2(r) \cos 2\theta. \quad (\text{B.24b})$$

The latter is the same as $Q(z)$ defined at (B.13b). However, in this anisotropic case, $Q(z)$ depends on the family of modes examined. Define

$$Q_{\{z\}}(z) = (1 + \frac{\Xi}{2})Q_-(z) + \{\mp\} \frac{\Xi}{2} Q_+(z). \quad (\text{B.25})$$

Given the appropriate choice of $Q_j(z)$, the above results about the modes' vector forms — defined by the angles given in (B.17) — all carry over. It is important to note that, while $Q_-(z)$ vanishes in the region in which the perturbation is axisymmetric and is an antisymmetric function over a period, $Q_+(z)$ does not have these properties. Thus, in this region, the modes are not the same as on an axisymmetric fibre, as can be seen because $\phi_x \neq 0 \neq \phi_y$. This is expected. In this region, the original axisymmetric fibre is perturbed to an anisotropic one. An example of the form of the actual modes, as described by the angles ϕ_x and ϕ_y , during passage through the grating is shown in Fig. 25, which is interpreted together with Fig. 19. In this case $\frac{\pi\Delta^2}{\delta} = 3$.

For the propagation constants, observe that the analogous result to (B.15) is

$$\tilde{\beta}_e^{(X)} - \Delta \frac{2\delta}{\pi\delta^2} V^2 \frac{1}{2} Q_j(z) = \tilde{\beta}_h^2 + \frac{\delta}{\pi\Delta} V^2 \left(\left(1 + \frac{\Xi}{2}\right) Q_+(z) \mp \frac{\Xi}{2} Q_-(z) \right).$$

Hence, using (B.24) and defining the average scalar constant in the obvious way as

$$\tilde{\beta}_a^2 = \tilde{\beta}_h^2 + \frac{\delta V^2}{2\Delta} \left(1 + \frac{\Xi}{2}\right) (\xi_e + \xi_o),$$

it follows that

$$\begin{aligned} \beta_{\{3\}}^2(z) &= \tilde{\beta}_a^2 - \frac{\delta\Xi V^2}{4\Delta} (\xi_e - \xi_o) + \frac{\delta V^2}{2\Delta} \left(\left(1 + \frac{\Xi}{2}\right) (q_e(z) + q_o(z)) - \frac{\Xi}{2} (q_e(z) - q_o(z)) \right) \\ &\quad - \Delta \left\{ \frac{1}{2} \right\} (I_1 + \{\mp\} I_2) + \{\mp\} \Delta \frac{\delta V^2}{\pi\Delta^2} \text{sgn}(\alpha_x) (|\alpha_x^2 + Q_x^2(z)|^{\frac{1}{2}} - |\alpha_x|) \\ \beta_{\{5\}}^2(z) &= \tilde{\beta}_a^2 + \frac{\delta\Xi V^2}{4\Delta} (\xi_e - \xi_o) + \frac{\delta V^2}{2\Delta} \left(\left(1 + \frac{\Xi}{2}\right) (q_e(z) + q_o(z)) + \frac{\Xi}{2} (q_e(z) - q_o(z)) \right) \\ &\quad - \Delta \left\{ \begin{matrix} I_1 - I_2 \\ 0 \end{matrix} \right\} + \{\mp\} \Delta \frac{\delta V^2}{\pi\Delta^2} \text{sgn}(\alpha_y) (|\alpha_y^2 + Q_y^2(z)|^{\frac{1}{2}} - |\alpha_y|). \end{aligned}$$

The average values for the propagation constants of the X- and Y-families are different; there are the terms $\mp \frac{\Xi}{2} (\xi_e - \xi_o)$. For $j = x, y$, define $L_j(x)$ as in (B.20) with the appropriate choice of $Q_j(z)$ replacing $Q(z)$. The average values of β_ϵ follow:

$$\langle \beta_\epsilon \rangle = \tilde{\beta}_a^2 + \{\mp\} \Delta \frac{\delta\Xi V^2}{4\Delta^2} (\xi_e - \xi_o) - \Delta B_\epsilon + \{\pm\} \Delta \frac{\delta V^2}{\pi\Delta^2} \text{sgn}(\alpha_\gamma) L_\gamma(|\alpha_\gamma|),$$

where γ indicates the family to which $\langle \beta_\epsilon \rangle$ belongs, the choice of sign on the second term is dependent on $\gamma = \left\{ \begin{matrix} x \\ y \end{matrix} \right\}$, and the third term and the choice of sign on the fourth term are those relevant to ϵ , as found in (B.21).

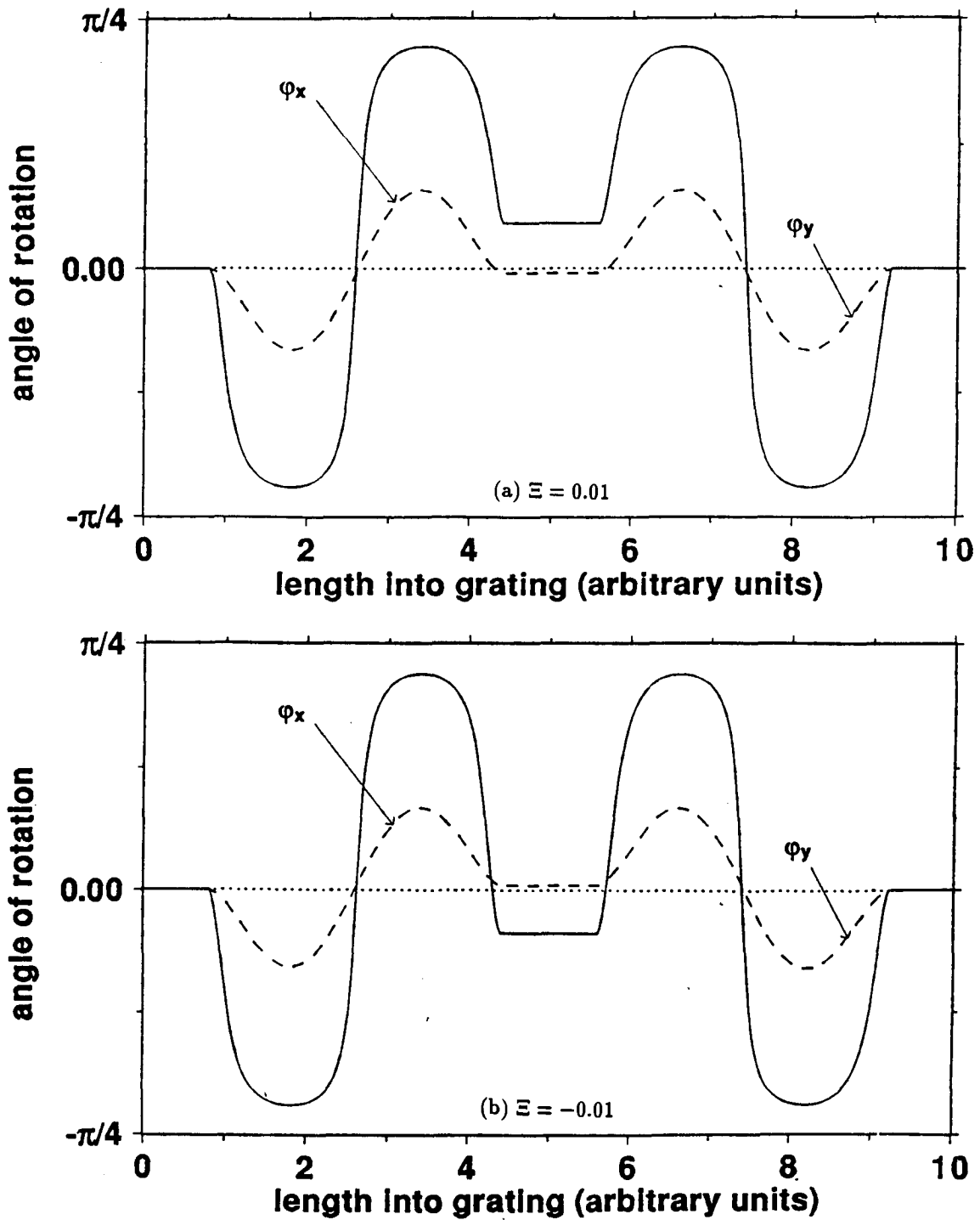


Figure 25: Modal rotation during passage through anisotropic grating

For a step-profile fibre, angles of rotation ϕ_j of the modal sets during transit through one period of an anisotropic $LP_{01} \leftrightarrow LP_{11}$ grating. Here $\pi\Delta^2/\delta = 3.0$ and $V = 3.50$. Compare with Fig. 21(b).

APPENDIX C

Three Coupled, Linear Differential Equations

We are interested in finding the solution of the system

$$\begin{pmatrix} a_1'(x) \\ a_2'(x) \\ a_3'(x) \end{pmatrix} = i \begin{pmatrix} 0 & K_2 e^{i\psi} e^{i\theta_2 x} & K_3 e^{i\psi} e^{i\theta_3 x} \\ K_2 e^{-i\psi} e^{-i\theta_2 x} & C_2 & iM e^{i(\theta_3 - \theta_2)x} \\ K_3 e^{-i\psi} e^{-i\theta_3 x} & -iM e^{-i(\theta_3 - \theta_2)x} & C_3 \end{pmatrix} \begin{pmatrix} a_1(x) \\ a_2(x) \\ a_3(x) \end{pmatrix} \quad (\text{C.1})$$

together with the initial conditions

$$a_1(0) = 1 \quad ; \quad a_2(0) = 0 = a_3(0). \quad (\text{C.2})$$

All of $K_2, K_3, M, \psi, \theta_2,$ and θ_3 are real.

It is straightforward to verify that the solution of the system can be described by

$$a_\alpha(x) = A_{\alpha j} e^{i(\mu_j - \theta_\alpha)x},$$

with $\theta_1 = 0$ and the summation convention implied for a Latin index, but not for a Greek one. The coefficients satisfy

$$\begin{pmatrix} -\mu_\alpha & K_2 e^{i\psi} & K_3 e^{i\psi} \\ K_2 e^{-i\psi} & \bar{\theta}_2 - \mu_\alpha & iM \\ K_3 e^{-i\psi} & -iM & \bar{\theta}_3 - \mu_\alpha \end{pmatrix} \begin{pmatrix} A_{1\alpha} \\ A_{2\alpha} \\ A_{3\alpha} \end{pmatrix} = \begin{pmatrix} 0 \\ 0 \\ 0 \end{pmatrix},$$

where it is defined that for, $\beta = 2, 3,$

$$\bar{\theta}_\beta = \theta_\beta + C_\beta.$$

This gives $A_{1\alpha}$ arbitrary; it follows that

$$A_{2\alpha} = A_{1\alpha} (K_2(\mu_\alpha - \bar{\theta}_3) + iM K_3) e^{-i\psi} / (\mu_\alpha - \bar{\theta}_3)(\mu_\alpha - \bar{\theta}_2) - M^2;$$

$$A_{3\alpha} = A_{1\alpha} (K_3(\mu_\alpha - \bar{\theta}_2) - iM K_2) e^{-i\psi} / (\mu_\alpha - \bar{\theta}_3)(\mu_\alpha - \bar{\theta}_2) - M^2.$$

The μ_α are three solutions of the cubic equation

$$\mu_\alpha^3 - (\bar{\theta}_2 + \bar{\theta}_3)\mu_\alpha^2 - (K_2^2 + K_3^2 + M^2 - \bar{\theta}_2\bar{\theta}_3)\mu_\alpha + K_2^2\bar{\theta}_3 + K_3^2\bar{\theta}_2 = 0.$$

Further notational changes

$$X = (\bar{\theta}_2 + \bar{\theta}_3)/6 \quad ; \quad Y = (\bar{\theta}_2 - \bar{\theta}_3)/2 \quad ;$$

$$\mu_\alpha = \gamma_\alpha + \frac{1}{3}(\bar{\theta}_2 + \bar{\theta}_3) = \gamma_\alpha + 2X$$

give the cubic equation

$$0 = \gamma_\alpha^3 - (K_2^2 + K_3^2 + M^2 + 3X^2 + Y^2)\gamma_\alpha + K_2^2(X - Y) + K_3^2(X + Y) + 2X(X^2 - Y^2 - M^2). \quad (\text{C.3})$$

The important feature of this equation is that the coefficient of γ_α is real and negative, so that three real solutions for γ_α are assured.

With the definitions

$$\begin{aligned} \sigma &= K_2^2 + K_3^2 + M^2 + 3X^2 + Y^2 \\ \cos(\phi) &= -\frac{3(K_2^2(X - Y) + K_3^2(X + Y) + 2X(X^2 - Y^2 - M^2))}{\sigma 2\sqrt{\sigma/3}}, \end{aligned}$$

where ϕ is fixed between 0 and π , it follows that these three solutions of (C.3) are [7: #3.8.2]

$$\begin{aligned} \gamma_1 &= 2\sqrt{\sigma/3} \cos(\phi/3) \\ \gamma_2 &= -2\sqrt{\sigma/3} \cos((\phi - \pi)/3) \\ \gamma_3 &= -2\sqrt{\sigma/3} \cos((\phi + \pi)/3). \end{aligned}$$

With the initial conditions prescribed at (C.2), it is straightforward to obtain the equation for the $A_{1\alpha}$, which was left arbitrary above. Noting that $(\mu_\alpha - \bar{\theta}_3)(\mu_\alpha - \bar{\theta}_2) = (\gamma_\alpha - X)^2 - Y^2$, this is

$$\begin{pmatrix} e^{-i\psi} \frac{K_2(\mu_1 - \bar{\theta}_3) + iMK_3}{(\gamma_1 - X)^2 - Y^2 - M^2} & e^{-i\psi} \frac{K_2(\mu_2 - \bar{\theta}_3) + iMK_3}{(\gamma_2 - X)^2 - Y^2 - M^2} & e^{-i\psi} \frac{K_2(\mu_3 - \bar{\theta}_3) + iMK_3}{(\gamma_3 - X)^2 - Y^2 - M^2} \\ e^{-i\psi} \frac{K_3(\mu_1 - \bar{\theta}_2) - iMK_2}{(\gamma_1 - X)^2 - Y^2 - M^2} & e^{-i\psi} \frac{K_3(\mu_2 - \bar{\theta}_2) - iMK_2}{(\gamma_2 - X)^2 - Y^2 - M^2} & e^{-i\psi} \frac{K_3(\mu_3 - \bar{\theta}_2) - iMK_2}{(\gamma_3 - X)^2 - Y^2 - M^2} \end{pmatrix} \begin{pmatrix} A_{11} \\ A_{12} \\ A_{13} \end{pmatrix} = \begin{pmatrix} 1 \\ 0 \\ 0 \end{pmatrix},$$

which yields the solution

$$\begin{aligned} A_{11} &= ((\gamma_1 - X)^2 - Y^2 - M^2)/(\gamma_1 - \gamma_2)(\gamma_1 - \gamma_3) \\ A_{12} &= ((\gamma_2 - X)^2 - Y^2 - M^2)/(\gamma_2 - \gamma_3)(\gamma_2 - \gamma_1) \\ A_{13} &= ((\gamma_3 - X)^2 - Y^2 - M^2)/(\gamma_3 - \gamma_1)(\gamma_3 - \gamma_2). \end{aligned}$$

As the γ_α are all real, it follows that the $A_{1\alpha}$ are, too.

Thus, the solutions for the $a_\alpha(z)$ can be recovered, though they won't be reproduced here. It is possible to rearrange the expression for $|a_1|^2(x)$ — which is power — to a more useful form:

$$|a_1|^2(x) = 1 - \eta_1 \sin^2(\nu_1 x) - \eta_2 \sin^2(\nu_2 x) - \eta_3 \sin^2(\nu_3 x), \quad (\text{C.4})$$

where the frequencies are defined by

$$\begin{aligned}
\nu_1 &= \frac{1}{2}(\gamma_1 - \gamma_2) = \sqrt{\sigma} \sin((\phi + \pi)/3) \\
\nu_2 &= \frac{1}{2}(\gamma_2 - \gamma_3) = -\sqrt{\sigma} \sin(\phi/3) \\
\nu_3 &= \frac{1}{2}(\gamma_3 - \gamma_1) = \sqrt{\sigma} \sin((\phi - \pi)/3)
\end{aligned} \tag{C.5}$$

and the coefficients (or “efficiencies”) by

$$\begin{aligned}
\eta_1 &= ((X - \gamma_1)^2 - Y^2 - M^2)((X - \gamma_2)^2 - Y^2 - M^2)/4\nu_1^2\nu_2\nu_3 \\
\eta_2 &= ((X - \gamma_2)^2 - Y^2 - M^2)((X - \gamma_3)^2 - Y^2 - M^2)/4\nu_1\nu_2^2\nu_3 \\
\eta_3 &= ((X - \gamma_3)^2 - Y^2 - M^2)((X - \gamma_1)^2 - Y^2 - M^2)/4\nu_1\nu_2\nu_3^2.
\end{aligned} \tag{C.6}$$

For a resonance to occur in this solution, the requirement is simply that $\cos(\phi) \rightarrow \pm 1$, i.e. $\phi \rightarrow 0$ or $\phi \rightarrow \pi$. Under these circumstances, from (C.5) and (C.6), it follows that $\nu_2 \rightarrow 0$ and $\eta_2 \rightarrow 1$ or $\nu_3 \rightarrow 0$ and $\eta_3 \rightarrow 1$, respectively. In other words, with ϕ close to 0, the conversion is very strong and the frequency very small on the second term in (C.5), and, with ϕ close to π , the same happens on the third term. We can use this requirement to recover the conditions for resonance.

For a small angle, replace the trigonometric functions above with their limiting forms, and replace these in the expressions for η_j at (C.6). The “resonant” efficiency has a square of the small angle in the denominator, so the condition to keep it bounded at 1 is that the numerator vanish. This gives the condition $(X \pm \sqrt{\frac{\sigma}{3}})^2 \rightarrow Y^2 + M^2$, and the \pm indicates two possibilities, which correspond to the two options $\phi \rightarrow 0, \pi$, though not necessarily respectively. Thus, the resonance condition is

$$0 < K_2^2 + K_3^2 = 2\sqrt{M^2 + Y^2}(\sqrt{M^2 + Y^2} \pm 3X)$$

which has two solutions, corresponding to \pm .

APPENDIX D

Zeroes of Polynomial

D.1 FUNCTION FOR ZEROES

Consider the cubic polynomial given by

$$Q(\xi) = 1 - (1 + (w\tau - \bar{\gamma})^2)\xi + 2w(w\tau - \bar{\gamma})\xi^2 - w^2\xi^3 \quad (\text{D.1})$$

and defined on $\xi \in [0, 1]$. How do the zeroes of $Q(\xi)$ vary as the parameter w changes, with $w \geq 0$? Since all functional dependence is continuous, there is continuous variation with parameters $\bar{\gamma}, \tau$. Trivially, for all $R > 0$, it follows that $q(1+R) < 0$ and $q(-R) > 0$. Hence, all the roots of $Q(\xi)$ are in $[0, 1]$. Of particular interest is the smallest root of $Q(\xi)$. Define it to be $\xi = \xi_0(w; \tau, \bar{\gamma})$, which is a function of w , with parameters $\tau, \bar{\gamma}$.

Rather than finding the zeroes of $Q(\xi)$ as functions of w , consider w to be a function of the zeroes and get $w(\xi)$ by solving $Q(\xi) = 0$ for w . Trivially, this gives two branches of a function defined for $\xi \in [0, 1]$:

$$w_{\pm}(\xi) = \frac{-\bar{\gamma}}{\xi - \tau} \pm \frac{\sqrt{1 - \xi}}{(\xi - \tau)\sqrt{\xi}}$$

To define $w(\xi)$, retain only the portions of these with $w_{\pm} \geq 0$. If such a choice doesn't exist, then no w is defined for the value of ξ , i.e. no value of the parameter w will make such a value ξ into a root of $Q(\xi)$. Also, $w(\xi)$ may be multiple valued, i.e. both $w_{\pm}(\xi) \geq 0$. Examine functional form of $w(\xi)$. As a simplification, note

$$w_{\pm}(\xi; \tau, -\bar{\gamma}) = -w_{\mp}(\xi; \tau, \bar{\gamma})$$

so that one can assume $\bar{\gamma} \geq 0$ and then take the solutions $w < 0$ for the case $\bar{\gamma} < 0$.

It follows that $w(\frac{1}{1+\bar{\gamma}^2}) = 0$, since $w_+(\frac{1}{1+\bar{\gamma}^2})$. This combines with a knowledge of the limiting behaviour of $w_{\pm}(\xi)$ near any asymptotes to give an indication of which branches $w_{\pm}(\xi)$ exist in which portions of the domain $[0, 1]$, for the specific choice of parameters $\tau, \bar{\gamma}$.

There is a vertical asymptote at $\xi = 0$. As $\epsilon \rightarrow 0^+$, it follows that

$$w_{\pm}(\epsilon) \rightarrow \begin{cases} \mp 1/\tau\epsilon^{\frac{1}{2}} & , \text{ if } \tau \neq 0 \\ \pm 1/\epsilon^{\frac{3}{2}} & , \text{ if } \tau = 0 \end{cases}$$

where the need is to distinguish the special case $\tau = 0$. For this special case, $w_+ > 0$ and $w_- < 0$. In general, w_+ has the opposite sign to that of τ , and w_- has the same one. There is another vertical asymptote at $\xi = \tau$. With $\tau \neq 0$ and $\epsilon \rightarrow 0^+$, it follows that

$$\begin{aligned} w_+(\tau \pm \epsilon) &\rightarrow \begin{cases} (\pm\sqrt{\frac{1-\tau}{\tau}} \mp \bar{\gamma})/\epsilon & , \text{ if } \tau \neq \frac{1}{1+\bar{\gamma}^2} \\ -(1+\bar{\gamma}^2)/2\bar{\gamma} & , \text{ if } \tau = \frac{1}{1+\bar{\gamma}^2} \end{cases} \\ w_-(\tau \pm \epsilon) &\rightarrow \begin{cases} (\mp\sqrt{\frac{1-\tau}{\tau}} \mp \bar{\gamma})/\epsilon & , \text{ if } \tau \neq \frac{1}{1+\bar{\gamma}^2} \\ \mp 2\bar{\gamma}/\epsilon & , \text{ if } \tau = \frac{1}{1+\bar{\gamma}^2} \end{cases} \end{aligned}$$

where the need is to distinguish the exceptional case $\tau = \frac{1}{1+\bar{\gamma}^2}$. If $\tau = \frac{1}{1+\bar{\gamma}^2}$, then there is a finite limit for $w_+(\tau)$. Otherwise, it is necessary to know if $\tau > \frac{1}{1+\bar{\gamma}^2}$, since then $\bar{\gamma} > \sqrt{\frac{1-\tau}{\tau}}$. If $\tau > \frac{1}{1+\bar{\gamma}^2}$, then the limit is positive for $w_{\pm}(\tau - \epsilon)$ and negative for $w_{\pm}(\tau + \epsilon)$. If $\tau < \frac{1}{1+\bar{\gamma}^2}$, then the limit is positive for $w_+(\tau + \epsilon)$ and $w_-(\tau - \epsilon)$ and negative for other pair.

Trivially, $w(1) = w_{\pm}(1) = \frac{\bar{\gamma}}{\tau-1}$, which is valid only if $\tau \neq 1$. It is positive or negative if $\tau > 1$ or $\tau < 1$, respectively. Below it is shown that the derivative is infinite at $\xi = 1$.

It is useful to have the derivatives of $w_{\pm}(\xi)$. Their vanishing tells whether any stationary points exist on the branches $w_{\pm}(\xi)$. Thus,

$$w'_{\pm}(\xi) = \frac{\bar{\gamma}}{(\xi - \tau)^2} \pm \frac{\tau - 3\xi + 2\xi^2}{2(\xi - \tau)^2 \xi^{\frac{3}{2}} \sqrt{1 - \xi}}$$

which is undefined for $\xi = 1, 0, \tau$. The latter two values are expected as they are vertical asymptotes. $\xi = 1$ is the only point $w_{\pm}(\xi)$ have in common. Stationary values are not immediate — finding them involves solving a quartic polynomial in ξ :

$$2\xi^2 - 3\xi + \tau = \mp 2\bar{\gamma}\xi\sqrt{\xi(1 - \xi)}$$

for w_{\pm} (Recall it is assumed $\bar{\gamma} > 0$). The number and some details of the solutions can be found graphically. Refer to Fig. 26 and Table 1, where $w_+(\xi)$ corresponds to the lower and $w_-(\xi)$ to the upper solid branch. Thought shows that critical values of $w(\xi)$ represent values for which $Q(\xi)$ has a degenerate root.

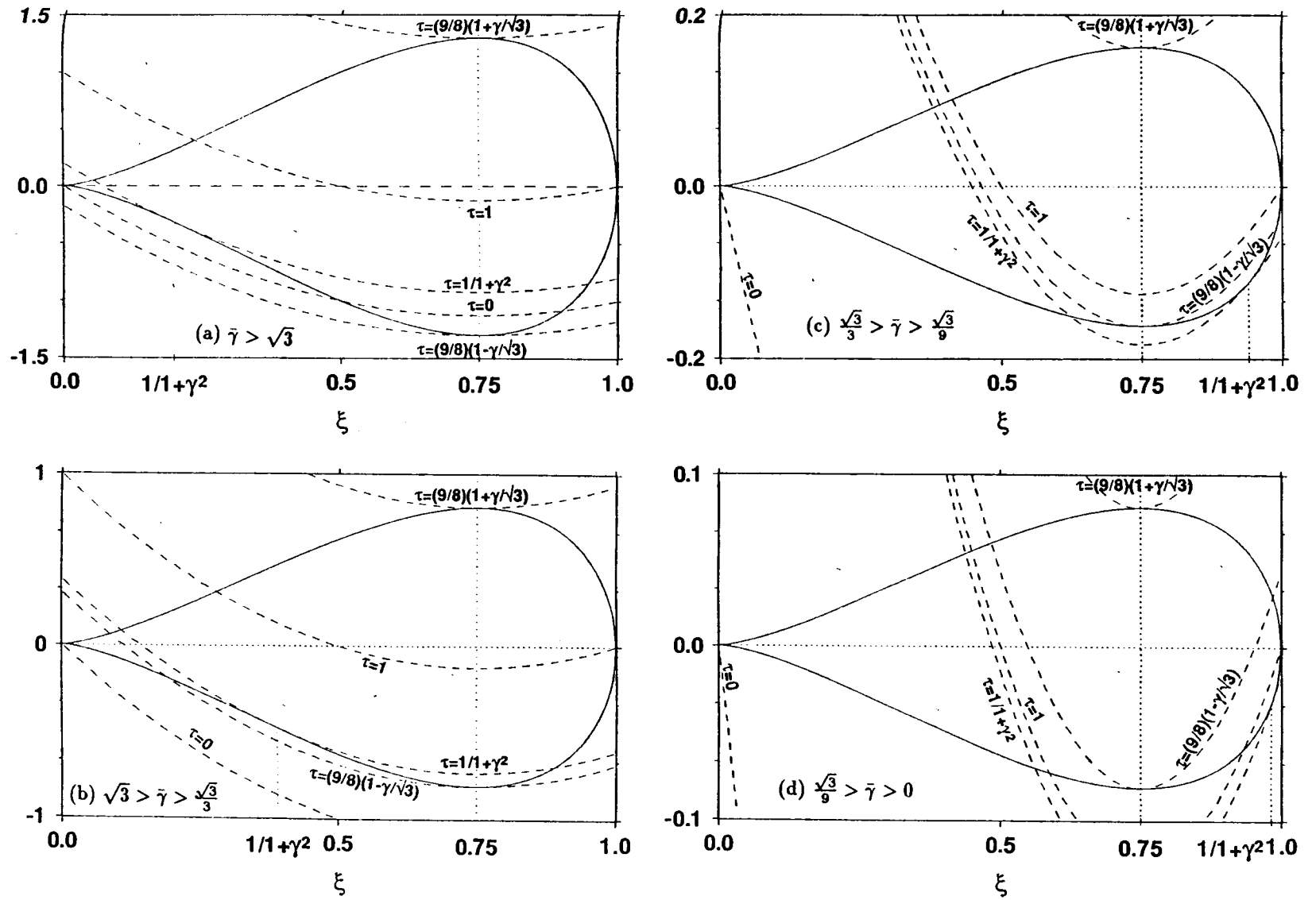


Figure 26: Graphical solution for critical points

Graphical solution of the equation for the critical points of $w(\eta)$, for various combinations $(\tau, \bar{\gamma})$.

Table 1: Solutions for critical points

List of the number of solutions for the critical points, illustrated by Fig. 26.

(a) Solutions for $w_-(\xi)$, i.e. upper curve

$\tau > R_+$	0
$\tau = R_+$	1
$R_+ > \tau \geq 1$	2
$1 > \tau \geq 0$	1
$0 > \tau$	0

(b) Solutions for $w_+(\xi)$, i.e. lower curve

$\gamma > \sqrt{3}$ $\frac{1}{4} > \frac{1}{1+\gamma^2}$		$\sqrt{3} > \gamma > \frac{\sqrt{3}}{3}$ $\frac{3}{4} > \frac{1}{1+\gamma^2} > \frac{1}{4}$		$\frac{\sqrt{3}}{3} > \gamma > \frac{\sqrt{3}}{9}$ $\frac{27}{28} > \frac{1}{1+\gamma^2} > \frac{3}{4}$		$\frac{\sqrt{3}}{9} > \gamma$ $\frac{1}{1+\gamma^2} > \frac{27}{28}$	
$\tau > 1$	0	$\tau > 1$	0	$\tau > 1$	0	$\tau > R_-$	0
						$\tau = R_-$	1
						$R_- > \tau > 1$	2
$\tau = 1$	1	$\tau = 1$	1	$\tau = 1$	1	$\tau = 1$	3
				$1 > \tau > R_-$	1		
$1 > \tau > \frac{1}{1+\gamma^2}$	1	$1 > \tau > \frac{1}{1+\gamma^2}$	1	$\tau = R_-$	2	$1 > \tau > \frac{1}{1+\gamma^2}$	3
				$R_- > \tau > \frac{1}{1+\gamma^2}$	3		
$\tau = \frac{1}{1+\gamma^2}$	2	$\tau = \frac{1}{1+\gamma^2}$	2	$\tau = \frac{1}{1+\gamma^2}$	2	$\tau = \frac{1}{1+\gamma^2}$	2
		$\frac{1}{1+\gamma^2} > \tau > R_-$	3				
$\frac{1}{1+\gamma^2} > \tau \geq 0$	3	$\tau = R_-$	2	$\frac{1}{1+\gamma^2} > \tau \geq 0$	1	$\frac{1}{1+\gamma^2} > \tau \geq 0$	1
		$R_- > \tau \geq 0$	1				
$0 > \tau > R_-$	2						
$\tau = R_-$	1	$0 > \tau$	0	$0 > \tau$	0	$0 > \tau$	0
$R_- > \tau$	0						

Here the notational device is

$$R_{\pm} = \frac{9}{8} \left(1 \pm \frac{\gamma}{\sqrt{3}} \right)$$

Knowledge of the location of stationary points, and the asymptotic forms of $w_{\pm}(\xi)$ can be combined. Figs. 27 and 28 show all the possible general forms of the zeroes of $Q(\xi)$ as functions of parameter w . In these, it is seen when a discontinuity in $\xi_0(w)$ exists. Fig. 29 shows the region of the $(\tau, \bar{\gamma})$ -plane in which it is possible. Below, there is an explicit presentation of this discontinuity.

D.2 SPECIAL CASES

Now examine some special cases in detail.

(i) CASE $\bar{\gamma} = 0$:

In understanding how the pattern of zeroes of $Q(\xi)$ changes, is easiest to consider special example with $\bar{\gamma} = 0$, i.e.

$$w(\xi) = \frac{\sqrt{\xi(1-\xi)}}{\xi|\xi-\tau|},$$

with

$$w'(\xi) = \text{sgn}(\xi - \tau) \frac{2\xi^2 - 3\xi + \tau}{2\xi^{\frac{3}{2}}(\xi - \tau)^2\sqrt{1-\xi}}$$

which gives stationary values at

$$\xi_{\pm} = \frac{3}{4} \left(1 \pm \sqrt{1 - \frac{8\tau}{9}} \right)$$

i.e. only if $\tau < 9/8$. If $\tau > 1$, then ξ_+ doesn't exist in the domain of interest; if $\tau < 0$, then ξ_- doesn't. Thus, at $\tau = \frac{9}{8}, 1, 0$, there are special transitions whose importance is best understood by considering a continuous variation of τ from infinity (see Fig. 27). The first is the value where the point of inflection occurs, i.e. the first appearance of a stationary value of $w(\xi)$; the second is when the τ -asymptote first appears in domain; the third is when this asymptote disappears.

For the smallest root of $Q(\xi)$, i.e. the function $\xi = \xi_0(w; \tau, 0)$, the important detail is that, for $\tau \in [0, 1.125]$, there is a discontinuity in ξ_0 at $w = w_D$. This is easily found to be

$$w_D = w(\xi_-) = \frac{2\sqrt{2}}{3\sqrt{3}} \left(\frac{4}{3}\tau - 1 - \frac{8}{27}\tau^2 + \left(1 - \frac{8}{9}\tau\right)^{\frac{3}{2}} \right)^{-\frac{1}{2}}.$$

The size of this discontinuity $\xi_J(\tau, 0)$ is given by

$$\xi_J = \frac{1}{w^2(\xi_-)\xi_-^2} - \xi_- = \frac{9}{4} \left(\sqrt{1 - \frac{8}{9}\tau} - 1 + \frac{8}{9}\tau \right).$$

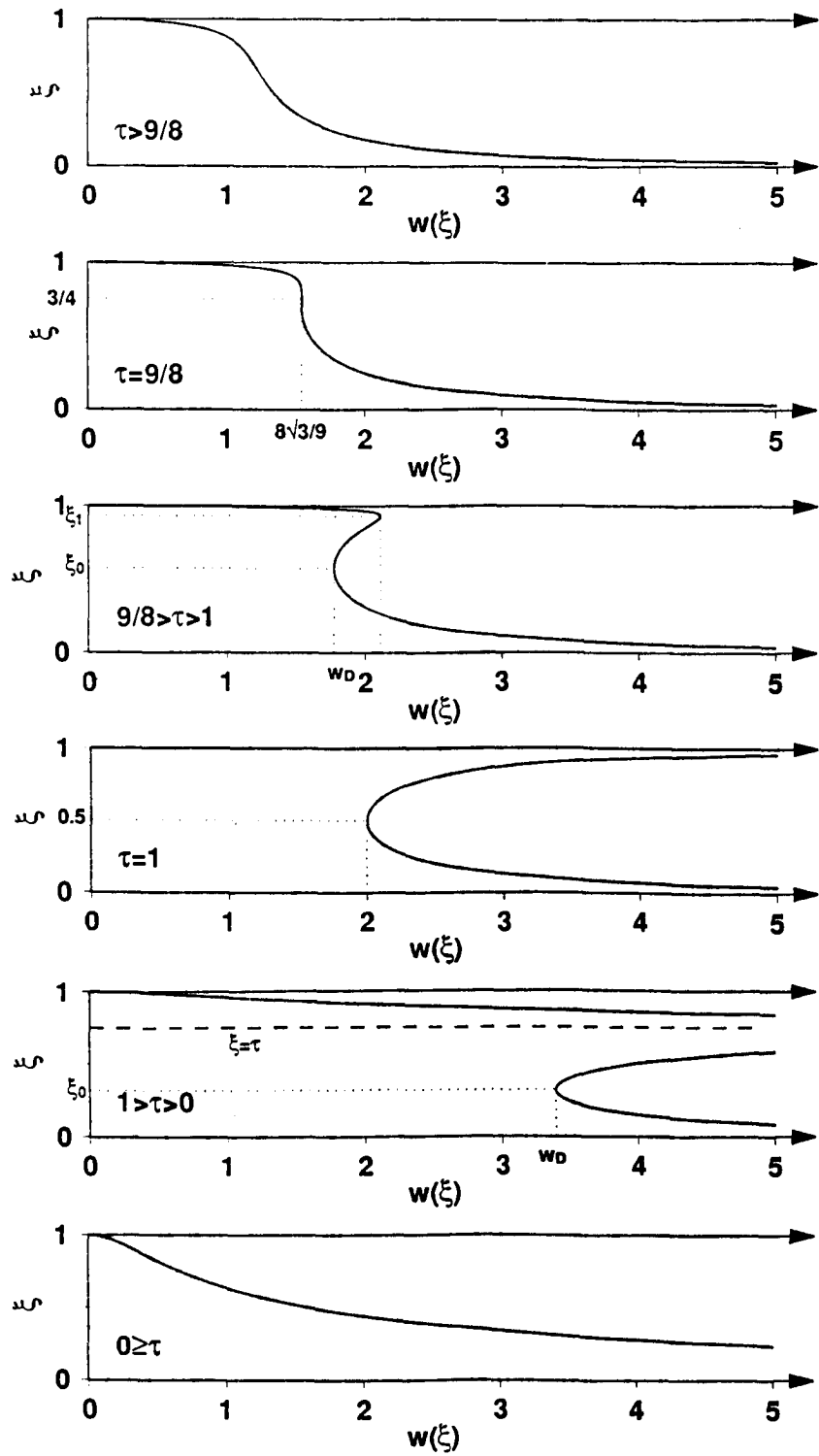


Figure 27: Pattern of zeroes $\bar{\gamma} = 0$

Functional dependence on w of the zeroes of the examined polynomial, defined by Eq. (D.1), for various choices of τ and with $\bar{\gamma} = 0$.

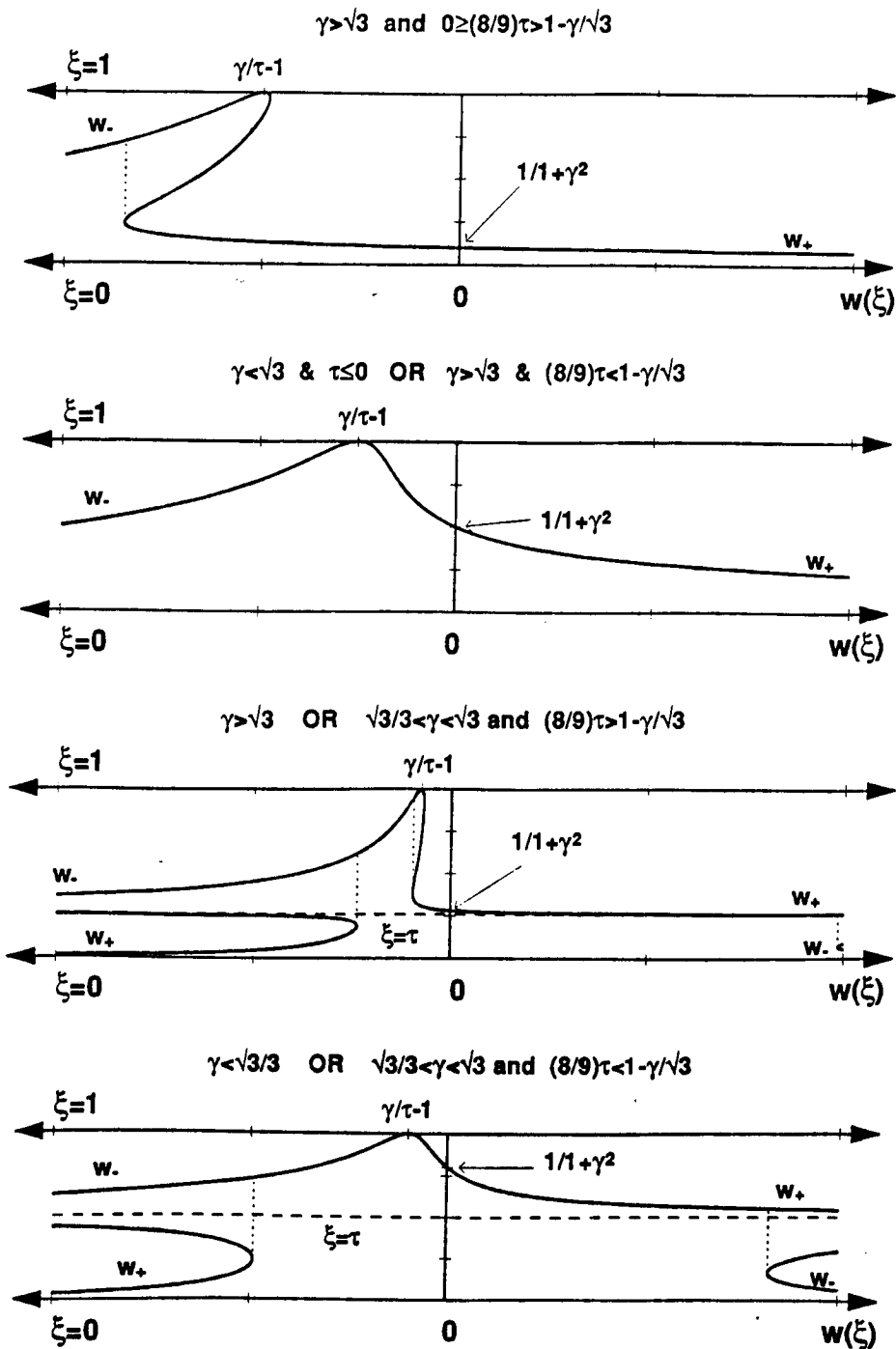
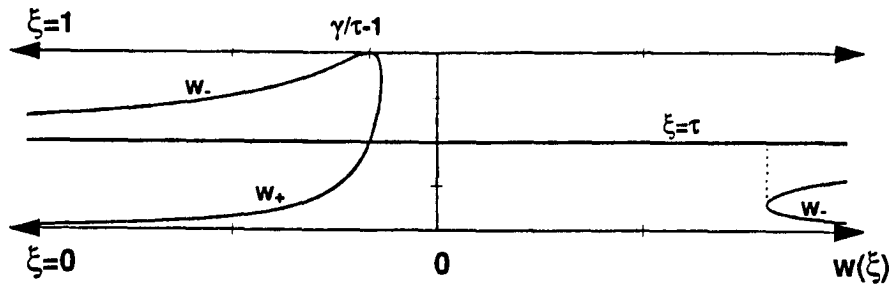
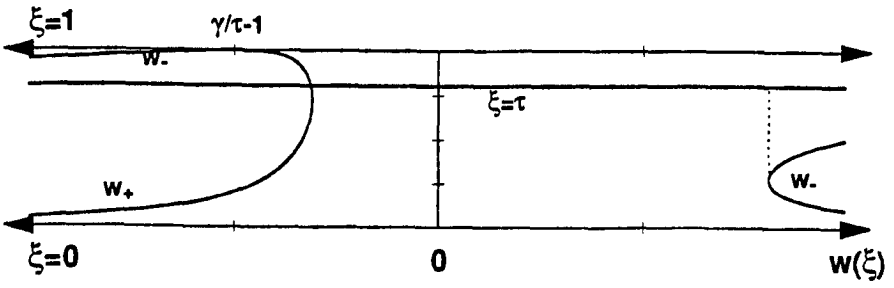


Figure 28: Examples of pattern of zeroes $\bar{\gamma} \neq 0$

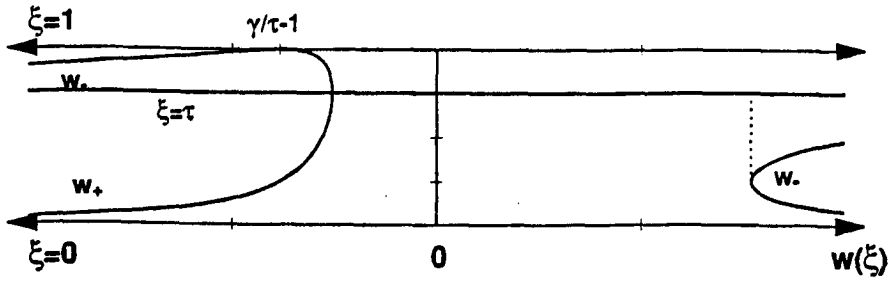
Functional dependence on w of the zeroes of the examined polynomial, defined by Eq. (D.1), for various choices of the parameter pair $(\tau, \bar{\gamma})$. Note that $w < 0$ is really $\bar{\gamma} < 0$, as explained in §D.1.



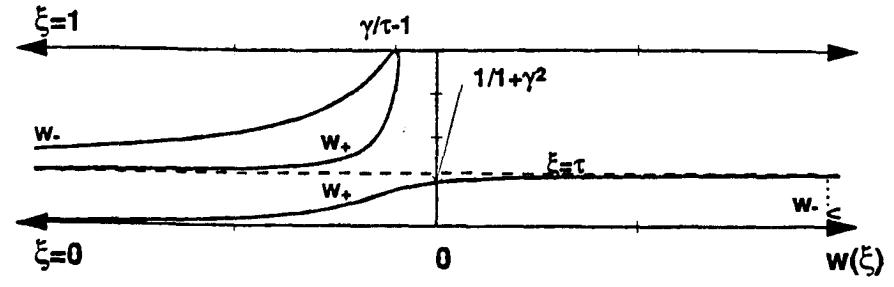
$\gamma > \sqrt{3}/3$ and $\tau = 1/1 + \gamma^2$



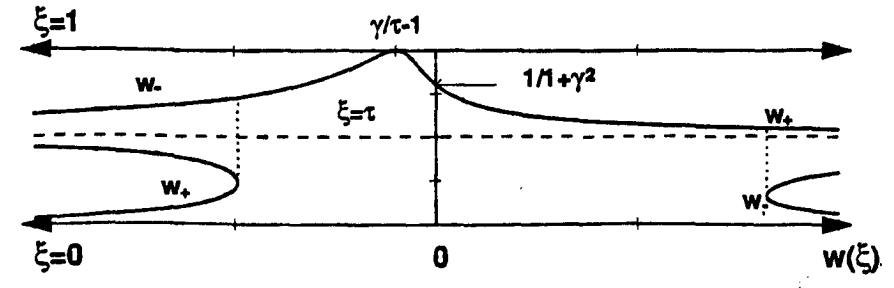
$\gamma < \sqrt{3}/3$ and $\tau = 1/1 + \gamma^2$



$\gamma = \sqrt{3}/3$ and $\tau = 1/1 + \gamma^2$



$\gamma > \sqrt{3}/3$ OR $1 - \gamma/\sqrt{3} < (8/9)\tau$
and $\sqrt{3}/3 > \gamma > \sqrt{3}/9$



$\gamma < \sqrt{3}/9$ OR $1 - \gamma/\sqrt{3} > (8/9)\tau$
and $\sqrt{3}/3 > \gamma > \sqrt{3}/9$

Figure 28: Continued

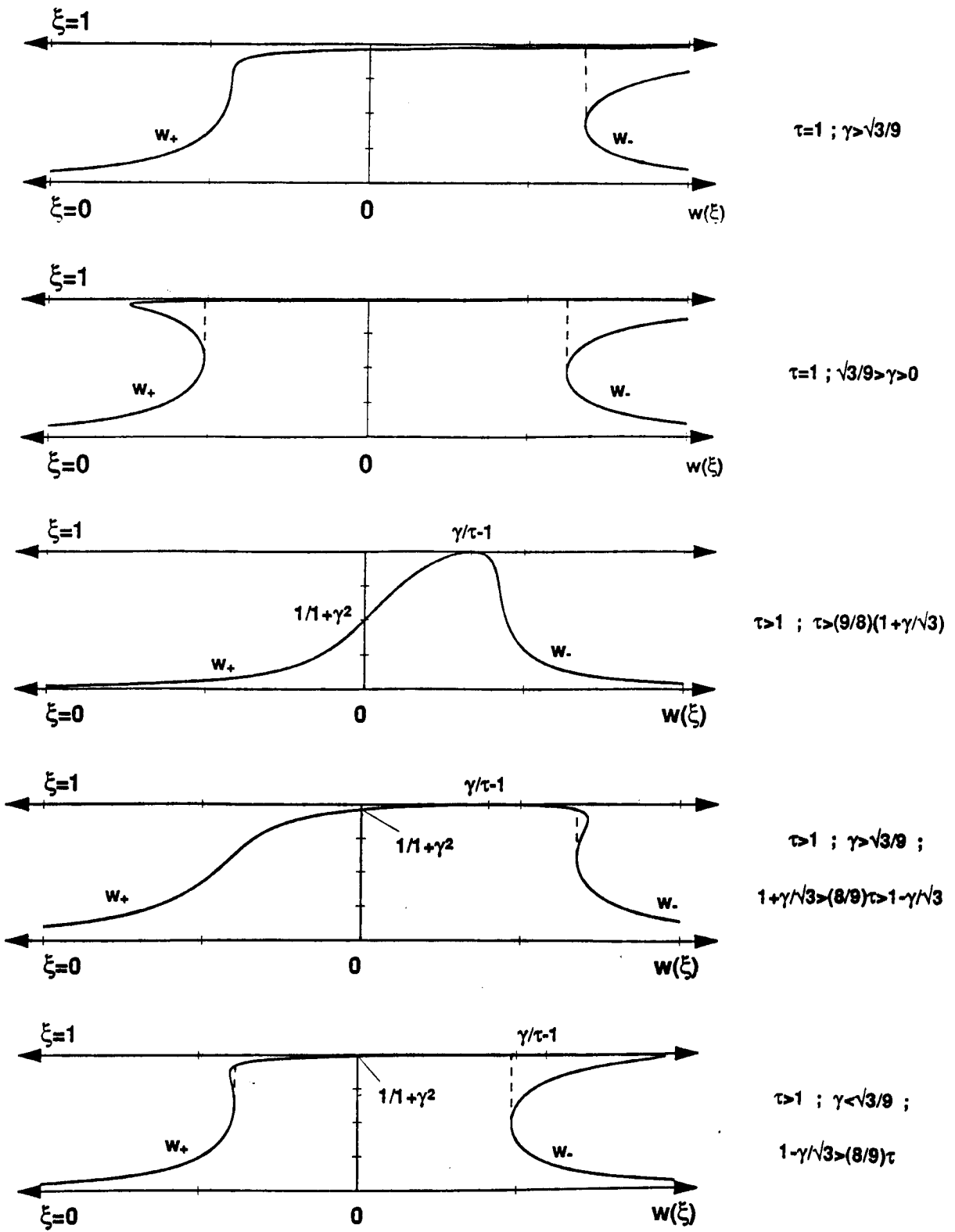


Figure 28: Continued

Its peak value is $9/16$, which occurs at $\tau = 27/32$ when $w_D = 32/3\sqrt{15}$. The accompanying two roots are $\xi_0 = 3/8$ and $\xi_1 = 15/16$.

(ii) CASE $\tau = \frac{1}{1+\bar{\gamma}^2}$:

In this case, $\tau = \frac{1}{1+\bar{\gamma}^2}$ is an asymptote. The value shown for $w = 0$ in the above analysis is no longer valid. However, it can be seen that $q(\frac{1}{1+\bar{\gamma}^2}) = 0$, independent of the choice of w . The other two roots are trivial as the solution of a quadratic:

$$\xi = \frac{-2\bar{\gamma}(1+\bar{\gamma}^2) + w \pm \sqrt{w^2 - 4\bar{\gamma}(1+\bar{\gamma}^2) - 4(1+\bar{\gamma}^2)^2}}{2w(1+\bar{\gamma}^2)}.$$

These two roots exist if

$$\begin{aligned} w^2 - 4(1+\bar{\gamma}^2)\bar{\gamma}w - 4(1+\bar{\gamma}^2)^2 &\geq 0 \\ \Rightarrow w &\geq 2(1+\bar{\gamma}^2)(\sqrt{\bar{\gamma}^2+1} + \bar{\gamma}). \end{aligned}$$

The critical value, at which the two roots are degenerate, gives

$$\xi = \frac{1}{2}\left(1 - \frac{\bar{\gamma}}{\sqrt{\bar{\gamma}^2+1}}\right).$$

Fig. 28 shows the curves $w(\xi)$ for representative values of $\bar{\gamma}$, and thus τ .

For $\bar{\gamma} < -1/\sqrt{3}$, the smallest root ξ_0 is always the value $\xi_0 = \frac{1}{1+\bar{\gamma}^2}$. For $\bar{\gamma} > -1/\sqrt{3}$, a discontinuity in ξ_0 occurs at

$$w_D = 2(1+\bar{\gamma}^2)(\sqrt{\bar{\gamma}^2+1} + \bar{\gamma}) = 2\frac{1 \pm \sqrt{1-\tau}}{\tau^{\frac{3}{2}}}$$

and the size of the discontinuity is

$$\xi_J = \frac{1 + \bar{\gamma}\sqrt{1+\bar{\gamma}^2} - \bar{\gamma}^2}{2(1+\bar{\gamma}^2)} = \frac{2\tau \pm \sqrt{1-\tau} - 1}{2},$$

since $\bar{\gamma} = \pm\sqrt{\frac{1-\tau}{\tau}}$. The peak value of this discontinuity is $9/16$, which occurs at $\tau = 15/16$, $\bar{\gamma} = 1/\sqrt{15}$ when $w_D = 32/3\sqrt{15}$. The value of the two roots are $\xi_0 = 3/8$ and $\xi_1 = 15/16$.

D.3 DISCONTINUITIES

It is easy to show that for a general $(\tau, \bar{\gamma})$ there is a discontinuity in $\xi_0(w; \tau, \bar{\gamma})$ in shaded region of Fig. 29. Further and more remarkably, an explicit solution for this discontinuity is possible.

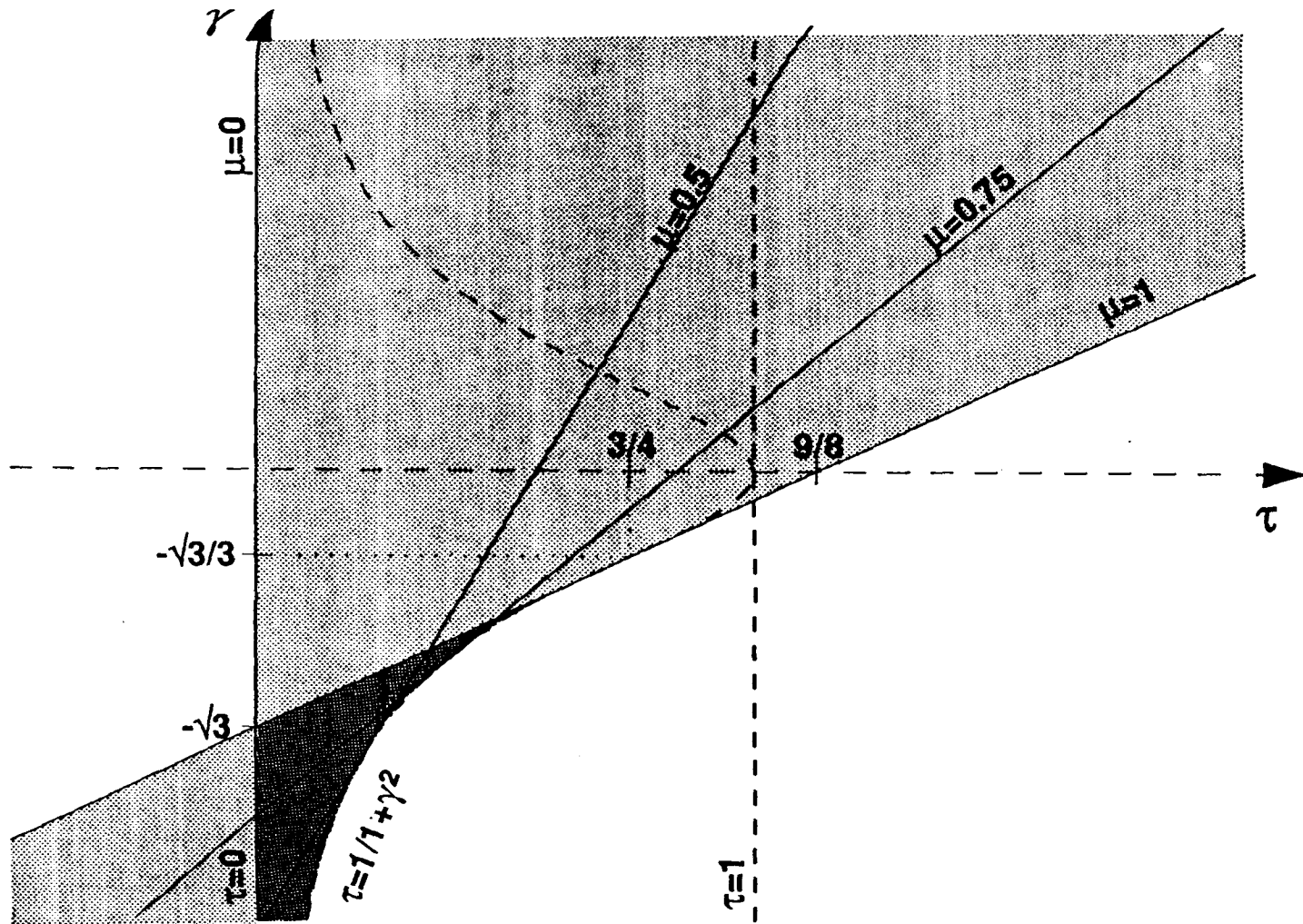


Figure 29: Region in which switching is possible

The shaded region is that portion of the $(\tau, \bar{\gamma})$ -plane in which a valid solution to Eq. (D.2) exists, i.e. parameters $(\tau, \bar{\gamma})$ for which a discontinuity exists in the function for the smallest zero of the polynomial defined by Eq. (D.1). The heavier shading indicates two solutions, i.e. two discontinuities, occur.

Suppose $(\tau, \bar{\gamma})$ satisfies

$$\tau - \frac{9}{8}\mu = \bar{\gamma} \frac{3\sqrt{3}}{2\sqrt{2}} \left(\frac{3}{2}\mu - 1 - \frac{3}{8}\mu^2 + (1 - \mu)^{\frac{3}{2}} \right)^{\frac{1}{2}} = \bar{\gamma}/w_D(\mu) \quad (\text{D.2})$$

for some $\mu \in [0, 1]$ (and $w_D(\mu)$ is defined below). Each such μ uniquely defines a straight line, cutting the τ -axis between 0 and 1.125. The value of the τ -intercept is $\frac{9}{8}\mu$. More usefully, given $(\tau, \bar{\gamma})$, it is possible to solve (D.2) for the appropriate μ and find on which such line, if any, $(\tau, \bar{\gamma})$ lies. A quartic polynomial in μ results. In general, there are 0, 1 or 2 valid solutions for μ . If there is no solution, then $(\tau, \bar{\gamma})$ lies outside the shaded region in Fig. 29.

If a valid solution for μ exists (As can be seen from some examples of Fig 28, there may be two solutions.), then for the pair $(\tau, \bar{\gamma})$, there is a discontinuity in ξ_0 when $w = w_D(\mu)$, given by

$$w_D(\mu) = \frac{2\sqrt{2}}{3\sqrt{3}} \left(\frac{3}{2}\mu - 1 - \frac{3}{8}\mu^2 + (1 - \mu)^{\frac{3}{2}} \right)^{-\frac{1}{2}}. \quad (\text{D.3})$$

The size of the discontinuity $\xi_J(\mu)$ and the value of the lesser root at the discontinuity $\xi_0(\mu)$ are given by

$$\xi_J(\mu) = \frac{9}{4}(\sqrt{1 - \mu} - 1 + \mu) \quad (\text{D.4})$$

$$\xi_0(\mu) = \frac{3}{4}(1 - \sqrt{1 - \mu}), \quad (\text{D.5})$$

respectively. Thus are given the constant values of these three functions whenever $(\tau, \bar{\gamma})$ lies on the straight lines defined as in (D.2) by a choice of $\mu \in [0, 1]$. As functions of μ , they are shown in Fig. 30. It is found that the maximum possible value of ξ_J is $\xi_J(\frac{3}{4}) = 9/16$, and that this always requires $w_D = 32/3\sqrt{15}$. Also, the two roots of $Q(\xi)$ are then $\xi_0(\frac{3}{4}) = \frac{3}{8}$ and $\xi_1 = 15/16$.

The design consideration for the optical switch is given simply. It is to maximize the value of $\xi_J(\mu)$, while minimizing the value of $w_D(\mu)$. It is apparent that the two cannot be achieved simultaneously.

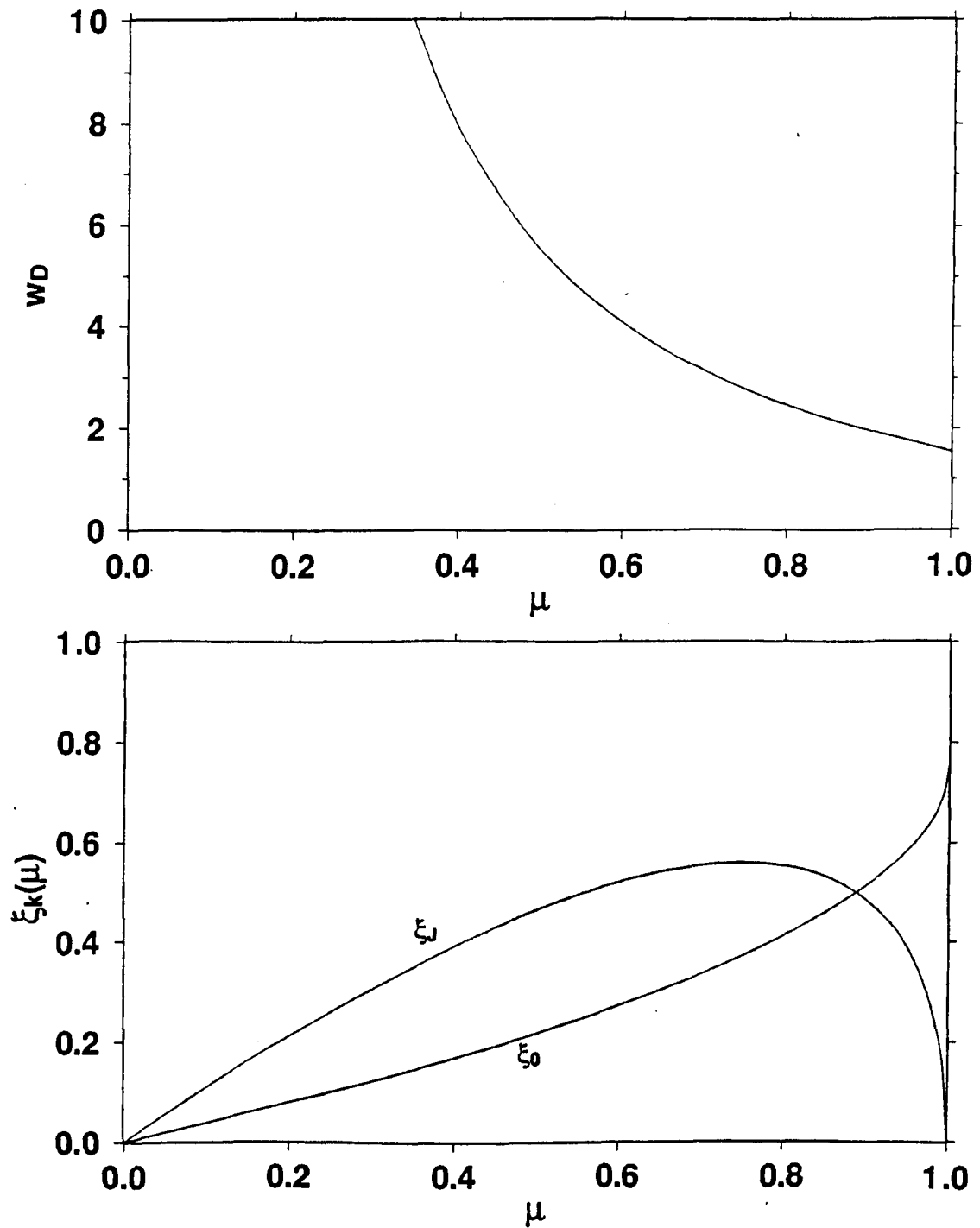


Figure 30: μ variation of discontinuity parameters

The variation of the three functions, given by Eqs (D.3), (D.4) and (D.5), of interest in seeking optimal solutions for all-optical switching.

APPENDIX E

Solution of Power Equation

The equation for the power propagating is given at (5.18). How does one explicitly solve for $y(t)$

$$y'(t)^2 = -yQ(y) \Rightarrow t = \int_0^{y(t)} d\xi \frac{1}{\sqrt{\xi Q(\xi)}} \quad (\text{E.1})$$

with the prescribed initial condition is $y(0) = 0$ and Q as defined at (D.1)? Put it into Legendre normal form [27: §13.5]. The transformation required for this depends on the roots of Q . There are various cases; all will be presented in detail. In all of them, remember $0 < y(t) < \xi_0$.

The case when Q has a triply degenerate root ξ_0 is the simplest. After rewriting (E.1), it follows that

$$\begin{aligned} wt &= \int_0^y d\xi \frac{1}{(\xi_0 - \xi)\sqrt{\xi(\xi_0 - \xi)}} = \int_{\xi_0 - y}^{\xi_0} dx \frac{1}{x\sqrt{\xi_0 x - x^2}} \\ &= \left[\frac{2\sqrt{x(\xi_0 - x)}}{\xi_0 x} \right]_{\xi_0}^{\xi_0 - y} \\ &= \frac{-2\sqrt{y(\xi_0 - y)}}{\xi_0(\xi_0 - y)}, \end{aligned}$$

from consultation of tables [28: #2.266]. This implicit definition of $y(t)$ can be inverted to give

$$y(t) = \xi_0 \frac{\frac{\xi_0^2 w^2 t^2}{4}}{1 + \frac{\xi_0^2 w^2 t^2}{4}} = \xi_0 \frac{1}{\frac{\xi_0^2 w^2 t^2}{4} + 1}. \quad (\text{E.2})$$

It is clear that $y(t) \rightarrow \xi_0$ monotonically at $t \rightarrow \infty$.

Next, consider the case when Q has a doubly degenerate root ξ_0 , less than the other

root ξ_1 . After rewriting (E.1), it follows that

$$\begin{aligned}
 wt &= \int_0^y d\xi \frac{1}{(\xi_0 - \xi)\sqrt{\xi(\xi_1 - \xi)}} = \int_{\xi_0 - y}^{\xi_0} dx \frac{1}{x\sqrt{(\xi_0 - x)(\xi_1 - \xi_0 + x)}} \\
 &= \left[\frac{1}{\sqrt{\xi_0(\xi_1 - \xi_0)}} \ln \frac{2\xi_0(\xi_1 - \xi_0) + (2\xi_0 - \xi_1)x + 2\sqrt{\xi_0(\xi_1 - \xi_0)(\xi_0 - x)(\xi_1 - \xi_0 + x)}}{x} \right]_{\xi_0 - y}^{\xi_0} \\
 &= \frac{1}{\sqrt{\xi_0(\xi_1 - \xi_0)}} \ln \left(\frac{\xi_0\xi_1 + (\xi_1 - 2\xi_0)y + 2\sqrt{(\xi_1 - \xi_0)y\xi_0(\xi_1 - y)}}{\xi_1(\xi_0 - y)} \right),
 \end{aligned}$$

from consultation of tables [28: #2.266]. This implicit definition of $y(t)$ can be inverted.

$$\begin{aligned}
 \exp(tw\sqrt{\xi_0(\xi_1 - \xi_0)}) &= \frac{(\sqrt{\xi_0(\xi_1 - y)} + \sqrt{(\xi_1 - \xi_0)y})^2}{\xi_1(\xi_0 - y)} \\
 \exp(-tw\sqrt{\xi_0(\xi_1 - \xi_0)}) &= \frac{\xi_1(\xi_0 - y)}{(\sqrt{\xi_0(\xi_1 - y)} + \sqrt{(\xi_1 - \xi_0)y})^2} \\
 &= \frac{(\sqrt{\xi_0(\xi_1 - y)} - \sqrt{(\xi_1 - \xi_0)y})^2}{\xi_1(\xi_0 - y)}.
 \end{aligned}$$

Hence,

$$\begin{aligned}
 \cosh(tw\sqrt{\xi_0(\xi_1 - \xi_0)}) &= \frac{\xi_0(\xi_1 - y) + (\xi_1 - \xi_0)y}{\xi_1(\xi_0 - y)} \\
 \Rightarrow y(t) &= \frac{\xi_0\xi_1(\cosh(tw\sqrt{\xi_0(\xi_1 - \xi_0)}) - 1)}{\xi_1(\cosh(tw\sqrt{\xi_0(\xi_1 - \xi_0)}) + 1) - 2\xi_0}. \tag{E.3}
 \end{aligned}$$

It is apparent that $y(t) \rightarrow \xi_0$ as $t \rightarrow \infty$.

Consider the case when Q has a doubly degenerate root ξ_1 , greater than the other root ξ_0 . After rewriting (E.1), it follows that

$$\begin{aligned}
 wt &= \int_0^y d\xi \frac{1}{(\xi_1 - \xi)\sqrt{\xi(\xi_0 - \xi)}} = \int_{\xi_1 - y}^{\xi_1} dx \frac{1}{x\sqrt{(\xi_1 - x)(\xi_0 - \xi_1 + x)}} \\
 &= \left[\frac{1}{\sqrt{\xi_1(\xi_1 - \xi_0)}} \arcsin\left(\frac{2\xi_1(\xi_0 - \xi_1) + (2\xi_1 - \xi_0)x}{x\xi_0}\right) \right]_{\xi_1 - y}^{\xi_1} \\
 &= \frac{1}{\sqrt{\xi_1(\xi_1 - \xi_0)}} \left(\frac{\pi}{2} - \arcsin\left(\frac{\xi_1\xi_0 + \xi_0y - 2\xi_1y}{\xi_0(\xi_1 - y)}\right) \right),
 \end{aligned}$$

from consultation of tables [28: #2.266]. The implicit definition of $y(t)$ can be inverted.

$$\frac{\xi_1\xi_0 + \xi_0y - 2\xi_1y}{\xi_0(\xi_1 - y)} = \sin\left(\frac{\pi}{2} - wt\sqrt{\xi_1(\xi_1 - \xi_0)}\right)$$

$$\Rightarrow y(t) = \frac{\xi_0 \xi_1 (1 - \cos(tw\sqrt{\xi_1(\xi_1 - \xi_0)}))}{2\xi_1 - \xi_0 (1 + \cos(tw\sqrt{\xi_1(\xi_1 - \xi_0)}))} \quad (\text{E.4})$$

In this case, $y(t)$ is a $\left(\frac{2\pi}{w\sqrt{\xi_1(\xi_1 - \xi_0)}}\right)$ -periodic function of amplitude ξ_0 .

Take the case of three real roots: $\xi_0 < \xi_1 < \xi_2$. After rewriting (E.1) and consultation of tables [28: #3.147(2)], it follows that

$$\begin{aligned} wt &= \int_0^y d\xi \frac{1}{\sqrt{\xi(\xi_0 - \xi)(\xi - \xi_1)(\xi - \xi_2)}} \\ &= \frac{2}{\sqrt{\xi_1(\xi_2 - \xi_0)}} F(\theta; \ell) \end{aligned}$$

where $F(\phi; \ell)$ is the elliptic integral of the first kind [14: ch16] and

$$\begin{aligned} \theta(y) &= \arcsin\left(\sqrt{\frac{(\xi_2 - \xi_0)y}{\xi_0(\xi_2 - y)}}\right) \Rightarrow y = \frac{\xi_0 \xi_2 \sin^2 \theta}{\xi_2 - \xi_0 + \xi_0 \sin^2 \theta}; \\ \ell^2 &= \frac{\xi_0(\xi_2 - \xi_1)}{\xi_1(\xi_2 - \xi_0)} = 1 - \frac{\xi_2(\xi_1 - \xi_0)}{\xi_1(\xi_2 - \xi_0)}. \end{aligned}$$

The implicit definition of $y(t)$ can be inverted in terms of the Jacobi elliptic functions [7: ch17] $\text{sn}(z; \ell)$, $\text{cn}(z; \ell)$, and $\text{dn}(z; \ell)$. This yields

$$\sin(\theta(y)) = \text{sn}\left(\frac{1}{2}tw\sqrt{\xi_1(\xi_2 - \xi_0)}; \ell\right)$$

and, thus, from the definition above of $\theta(y)$,

$$\begin{aligned} y(t) &= \frac{\xi_0 \xi_2 \text{sn}^2\left(\frac{1}{2}wt\sqrt{\xi_1(\xi_2 - \xi_0)}; \ell\right)}{\xi_2 - \xi_0 + \xi_0 \text{sn}^2\left(\frac{1}{2}wt\sqrt{\xi_1(\xi_2 - \xi_0)}; \ell\right)} \\ &= \frac{\xi_0 \xi_2 (1 - \text{cn}(tw\sqrt{\xi_1(\xi_2 - \xi_0)}; \ell))}{\xi_2 + (\xi_2 - \xi_0) \text{dn}(tw\sqrt{\xi_1(\xi_2 - \xi_0)}; \ell) - \xi_0 \text{cn}(tw\sqrt{\xi_1(\xi_2 - \xi_0)}; \ell)}. \end{aligned} \quad (\text{E.5})$$

Here, $y(t)$ is a $\left(\frac{4\mathbf{K}(\ell)}{w\sqrt{\xi_1(\xi_2 - \xi_0)}}\right)$ -periodic function with amplitude ξ_0 . $\mathbf{K}(\ell)$ is the complete elliptic integral of the first kind [7: ch16]. For the parameter, $0 < \ell < 1$, and $\ell \rightarrow 1$ as $\xi_1 \rightarrow \xi_0$, i.e. there is really a repeated root.

Finally, take the case of one real root ξ_0 and two complex roots $\xi_1 \pm i\xi_2$. It follows that

$$\xi_1 = \tau - \frac{\bar{\gamma}}{pq_0} - \frac{1}{2}\xi_0 \quad ; \quad \xi_1^2 + \xi_2^2 = 1/\xi_0 p^2 q_0^2.$$

After rewriting (E.1) and consultation of tables [28: #3.145(2)], it follows that

$$\begin{aligned} wt &= \int_0^y d\xi \frac{1}{\sqrt{\xi(\xi_0 - \xi)((\xi - \xi_1)^2 + \xi_2^2)}} \\ &= \frac{1}{\sqrt{rs}} F(\theta; \ell) \end{aligned}$$

where

$$\begin{aligned} \theta(y) &= 2\text{arccot}\left(\sqrt{\frac{s(\xi_0 - y)}{ry}}\right) \Rightarrow y = \frac{s\xi_0(1 - \cos\theta)}{r + s + (r - s)\cos\theta} \\ \ell^2 &= \frac{\xi_0^2 - (r - s)^2}{4rs} = \frac{1}{2} \left(1 - \frac{1 - (\tau pq_0 - \bar{\gamma})pq_0\xi_0^2 - \frac{1}{2}p^2q_0^2\xi^3}{pq_0r\xi_0^{\frac{1}{2}}}\right) \\ r^2 &= \xi_0^2 - 2\xi_0\xi_1 + \xi_1^2 + \xi_2^2 = -2\xi_0\left(\tau - \frac{\bar{\gamma}}{pq_0}\right) + \frac{1}{p^2q_0^2\eta_0} \\ s^2 &= \xi_1^2 + \xi_2^2 = 1/\xi_0q_0^2p^2. \end{aligned}$$

The implicit definition of $y(t)$ can be inverted in terms of Jacobi elliptic functions. This shows

$$\cos(\theta(y)) = \text{cn}(wt\sqrt{rs}; \ell)$$

and, thus, from the definition above of $\theta(y)$,

$$y(t) = \frac{s\xi_0(1 - \text{cn}(tw\sqrt{rs}; \ell))}{2r + (s - r)(1 - \text{cn}(tw\sqrt{rs}; \ell))}. \quad (\text{E.6})$$

The function $y(t)$ is a $\left(\frac{4K(\ell)}{w\sqrt{rs}}\right)$ -periodic function with amplitude ξ_0 . For the parameter, $0 < \ell < 1$, and $\ell \rightarrow 1$ only as $\xi_2 \rightarrow 0$ with $\xi_1 < \xi_0$, i.e. the two complex roots become a repeated real root.

DOCUMENT CONTROL DATA

(Security classification of title, body of abstract and indexing annotation must be entered when the overall document is classified)

1. ORIGINATOR (the name and address of the organization preparing the document. Organizations for whom the document was prepared, e.g. Establishment sponsoring a contractor's report, or tasking agency, are entered in section 8.) COMMUNICATIONS RESEARCH CENTRE, P.O. BOX 11490, STATION H, OTTAWA, ONTARIO, K2H 8S2		2. SECURITY CLASSIFICATION (overall security classification of the document including special warning terms if applicable) UNCLASSIFIED	
3. TITLE (the complete document title as indicated on the title page. Its classification should be indicated by the appropriate abbreviation (S,C or U) in parentheses after the title.) MODAL CONVERSION BY GRATINGS IN OPTICAL FIBRES: THE THEORY AND ITS APPLICATION TO ALL-OPTICAL SWITCHING (U)			
4. AUTHORS (Last name, first name, middle initial) SKINNER, IAIN M.			
5. DATE OF PUBLICATION (month and year of publication of document) OCTOBER, 1991		6a. NO. OF PAGES (total containing information. Include Annexes, Appendices, etc.) 129	6b. NO. OF REFS (total cited in document) 28
7. DESCRIPTIVE NOTES (the category of the document, e.g. technical report, technical note or memorandum. If appropriate, enter the type of report, e.g. interim, progress, summary, annual or final. Give the inclusive dates when a specific reporting period is covered.) TECHNICAL REPORT			
8. SPONSORING ACTIVITY (the name of the department project office or laboratory sponsoring the research and development. Include the address.) DEFENCE RESEARCH ESTABLISHMENT, OTTAWA, ONTARIO, K1A 0Z4			
9a. PROJECT OR GRANT NO. (if appropriate, the applicable research and development project or grant number under which the document was written. Please specify whether project or grant) 1410-041LP		9b. CONTRACT NO. (if appropriate, the applicable number under which the document was written)	
10a. ORIGINATOR'S DOCUMENT NUMBER (the official document number by which the document is identified by the originating activity. This number must be unique to this document.) CRC REPORT # CRC-RP-91-002		10b. OTHER DOCUMENT NOS. (Any other numbers which may be assigned this document either by the originator or by the sponsor) NONE	
11. DOCUMENT AVAILABILITY (any limitations on further dissemination of the document, other than those imposed by security classification) (<input checked="" type="checkbox"/>) Unlimited distribution () Distribution limited to defence departments and defence contractors; further distribution only as approved () Distribution limited to defence departments and Canadian defence contractors; further distribution only as approved () Distribution limited to government departments and agencies; further distribution only as approved () Distribution limited to defence departments; further distribution only as approved () Other (please specify):			
12. DOCUMENT ANNOUNCEMENT (any limitation to the bibliographic announcement of this document. This will normally correspond to the Document Availability (11). However, where further distribution (beyond the audience specified in 11) is possible, a wider announcement audience may be selected.) UNLIMITED			

13. ABSTRACT (a brief and factual summary of the document. It may also appear elsewhere in the body of the document itself. It is highly desirable that the abstract of classified documents be unclassified. Each paragraph of the abstract shall begin with an indication of the security classification of the information in the paragraph (unless the document itself is unclassified) represented as (S), (C), or (U). It is not necessary to include here abstracts in both official languages unless the text is bilingual).

(U) Using the formalism of coupled-mode theory, an improved description — allowing for a lack of axisymmetry in the waveguide — of the resonant transfer of power between modes propagating in a few-mode optical fibre is derived, and applied to both an axisymmetric $LP_{01} \leftrightarrow LP_{02}$ modal conversion grating and a non-axisymmetric $LP_{01} \leftrightarrow LP_{11}$ grating. The theory of the vector form of modes in a periodic, slightly non-axisymmetric structure is obtained, and applied to the $LP_{01} \leftrightarrow LP_{11}$ grating. For the $LP_{01} \leftrightarrow LP_{02}$ grating, the spectral region of appreciable resonant coupling, as measured by a linewidth, was found to be very narrow. The feasibility of exploiting this extreme sensitivity by using the grating as an all-optical switch was demonstrated.

14. KEYWORDS, DESCRIPTORS or IDENTIFIERS (technically meaningful terms or short phrases that characterize a document and could be helpful in cataloguing the document. They should be selected so that no security classification is required. Identifiers, such as equipment model designation, trade name, military project code name, geographic location may also be included. If possible keywords should be selected from a published thesaurus. e.g. Thesaurus of Engineering and Scientific Terms (TEST) and that thesaurus-identified. If it is not possible to select indexing terms which are Unclassified, the classification of each should be indicated as with the title.)

NONLINEAR OPTICAL EFFECTS
OPTICAL FIBRES
OPTICAL COMPUTING
OPTICAL SWITCHING

TK
5102.5
C673e
#91-002

Skinner, Iain M.
Modal conversion by...

DATE DUE